

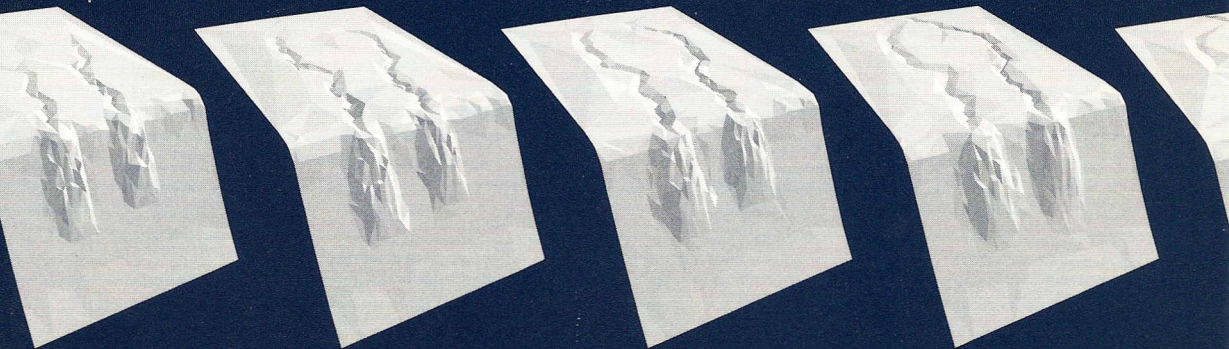
GEOLOGICA ULTRAIECTINA

Mededelingen van de
Faculteit Aardwetenschappen
Universiteit Utrecht

no. 221

Quantitative Three-dimensional Modelling of Quaternary Continental Passive Margins

*Forward modelling of the morphological evolution, sediment characteristics
and sequence stratigraphy of river - shelf sedimentary systems*



X. D. Meijer

GEOLOGICA ULTRAIECTINA

Mededelingen van de
Faculteit Aardwetenschappen
Universiteit Utrecht

no. 221

Quantitative Three-dimensional Modelling of Quaternary Passive Continental Margins

*Forward modelling of the morphological evolution, sediment characteristics
and sequence stratigraphy of river–shelf sedimentary systems*

X. D. Meijer

ISBN: 90-5744-078-4

Quantitative Three-dimensional Modelling of Quaternary Passive Continental Margins

*Forward modelling of the morphological evolution, sediment characteristics
and sequence stratigraphy of river–shelf sedimentary systems*

Kwantitatieve Driedimensionale Modelling van Kwartaire Passieve Continentale Marges

*Modelling van de morfologische ontwikkeling, sediment karakteristieken
en sequentie stratigrafie van rivier–shelf sedimentaire systemen*

(met een samenvatting in het Nederlands)

Proefschrift

ter verkrijging van de graad van doctor
aan de Universiteit Utrecht
op gezag van de Rector Magnificus, Prof. Dr. W.H. Gispen,
ingevolge het besluit van het College van Promoties
in het openbaar te verdedigen
op maandag 21 oktober 2002 des middags te 2.30 uur

door

Xander Dagmar Meijer

geboren op 22 september 1973 te Nijmegen

Promotores:

Prof. Dr. P.A. Burrough

Faculty of Geographical Sciences, Utrecht University

Prof. Dr. P.L. de Boer

Faculty of Earth Sciences, Utrecht University

Co-promotor:

Dr. G. Postma

Faculty of Earth Sciences, Utrecht University

The research in this thesis was supported by the Netherlands Council for Earth and Life Sciences (ALW) with financial aid from the Netherlands Organization for Scientific Research (NWO).

Contents

Chapter 1	Introduction	9
Chapter 2	Modelling the drainage evolution of a river–shelf system forced by Quaternary glacio-eustasy <i>(published in Basin Research)</i>	15
Chapter 3	Grain-size sorting of river–shelf–slope sediments during glacial–interglacial cycles: modelling grain-size distribution and interconnectedness	35
Chapter 4	Modelling the preservation of sedimentary deposits on passive continental margins during glacial–interglacial cycles <i>(co-authors G. Postma, P.L. de Boer, P.A. Burrough)</i>	53
Chapter 5	Conclusions	69
	References	73
	Samenvatting <i>(summary, based on Chapter 1)</i>	77
	Dankwoord <i>(acknowledgements)</i>	85
	Curriculum Vitae	87

Introduction

General introduction

As a result of continental plate motions, the world's oceans are fringed by a few types of continental margins with distinctly different crustal configurations. One type of ocean-basin margin is created after rifting of tectonic plates and sea-floor spreading. It gives rise to passive continental margins (Fig. 1.1), named after the fact that they are relatively devoid of earthquake and volcanic activity, as opposed to active continental margins adjacent to convergent plate boundaries. Passive margins are characterized by some initial uplift during rifting followed mainly by subsidence, increasing basinward from a hinge line and decelerating with time. Under these conditions, sediment successions with thicknesses of kilometres accumulate over periods of millions of years, increasing the extent of the continent.

The Quaternary is marked by the expansion of permanent continental ice sheets that already existed in the Tertiary. It witnessed great variations in the volume of polar ice and a series of major ice advances and retreats across Europe and North America, resulting in significant sea-level changes and in an alternation of intervals with glacial or interglacial conditions. The subdivision of Quaternary stratigraphy is based on these fluctuations. World-wide climate change and glacio-eustasy, the change of global sea level as a consequence of the change in volume of continental ice masses and the mean sea-water temperature, are intricately linked and have been related to Milankovitch insolation cycles (e.g. Berger *et al.*, 1994). Sea-level oscillations occurred at a high frequency, initially with a period of ~41 kyr associated with the rhythm of orbital obliquity, until the mid-Pleistocene

when the ~100 kyr cycle of orbital eccentricity became dominant. The course of sea-level change is typically asymmetric with a slow fall during the growth of ice caps and a fast rise during melting. The amplitude of change is high, ranging up to ~120 m between highstands and lowstands. Such glacial episodes forced by Milankovitch cycles are thought to have also taken place earlier in the Phanerozoic, like in the Permo-Carboniferous (e.g. Heckel, 1986; Maynard & Leeder, 1992) and the Neogene (e.g. Hodell *et al.*, 1986; Pillans *et al.*, 1998).

The effects of glacial–interglacial sea-level and climate change on the morphology of passive continental margins result in a dynamic sedimentary system in terms of accommodation space. In response to sea-level change, lowlands known as continental shelves repeatedly emerge and submerge, and concomitant regressions and transgressions of coastlines occur over great distances across these shelves, involving shifts in the location of deposition of river-borne sediment. The evolution of a passive margin system undergoing sea-level change is roughly characterized by the transition from a highstand situation where deposition is restricted to up-dip areas and where the submerged continental shelf and slope are largely starved of sediments, to a situation around lowstand that allows shelfal erosion and sediment bypass to the shelf edge — and back. These are the basics of the concept of sequence stratigraphy (Posamentier *et al.*, 1988; Galloway, 1989), which need to be adapted for the specific conditions of the glacio-eustatic cycles of the Quaternary.

One of the aims of Sedimentology is to gain understanding of the role of sedimentary processes in the development of stratigraphic

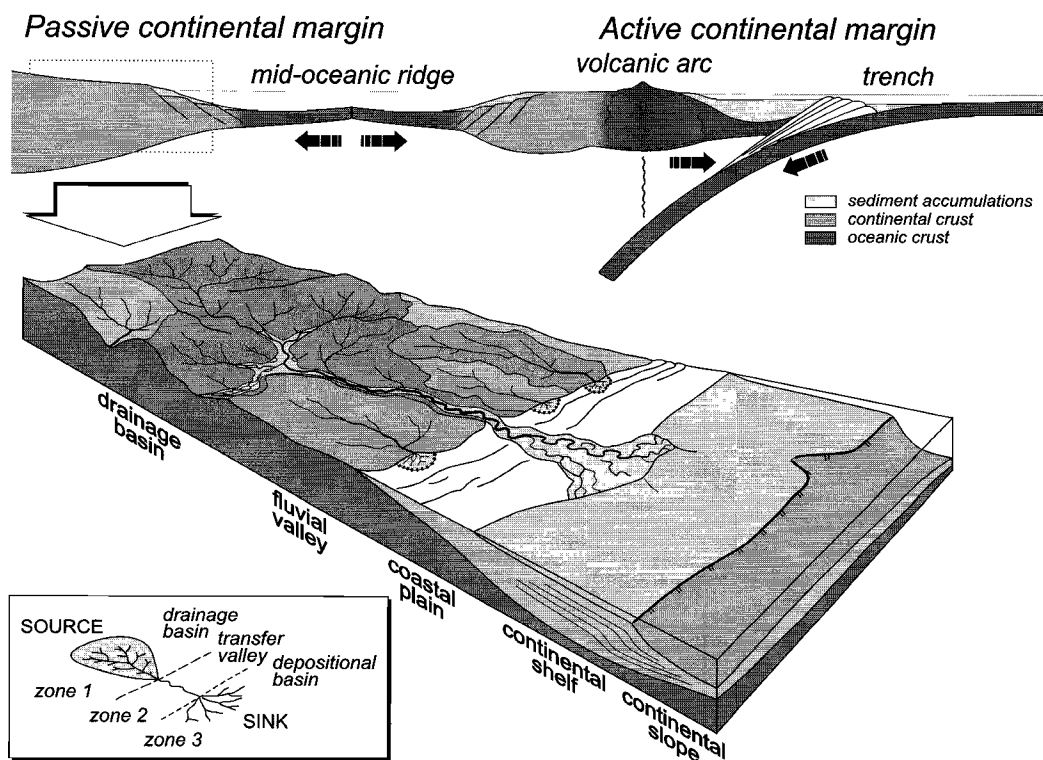


Fig. 1.1 — At the top, an overview of divergent and convergent plate boundaries and the passive and active continental margins, respectively, that are adjacent to them. In broad outline, in a passive margin setting, a generally major river carries sediment from the often distant drainage basin down to the coast, eroding or depositing sediment en route. The position of the shoreline is affected by sea level changes. Depicted here is an interglacial situation with a sea level highstand, where a delta is built on a submerged continental shelf (after Van Heijst *et al.*, 2001). During glacial times with a lower sea level, the shoreline is located more basinward or even at the shelf edge. The inset on the bottom left shows a simplified sketch of a system of sediment production, transport and deposition (after Schumm, 1977). In this thesis, only zones 2 and particularly 3 are covered.

successions. The two complementary aspects of sedimentation, process and product, are important. The object of sequence stratigraphy is to unravel the causal relations between the evolution of a sedimentary system and the driving forces, such as sea-level change, basin subsidence and sediment supply, and thus to interpret the geologic record of facies (process-related assemblages of sedimentologic features) and sequences (repetitive depositional packages). Despite the problems we are faced with in trying to accomplish this task for Quaternary passive continental margins, a great deal of progress has been made in the past few decades (Emery

& Myers, 1996, ch. 1; Miall, 1995). The obstacles to be overcome can be categorized into two main aspects.

Firstly, compiling a complete and detailed image of the stratigraphic architecture of an empirical basin margin is difficult owing to the large areal extent and lateral variability of the study area. Moreover, in the present-day sea-level highstand situation, the area of interest is almost entirely submerged, making gathering of field data extremely costly and thus placing restrictions on the amount and type of collected information. At present, comprehensive, three-dimensional stratigraphic data sets with good

age-constraints are largely lacking. In addition, process intensities in the past are likely to be different from those measured today and certain geomorphic thresholds are not crossed under present conditions. Holocene fluxes are not representative for an entire glacial–interglacial cycle, let alone the entire Quaternary. Since glacial cycles are global events, space–time substitution does not apply and contemporary analogues are hard to find, if at all.

The second complication is the incomplete understanding of the mechanisms of sediment erosion, transport and deposition, and the inability to scale them up to large time and spatial scales. The complexity is overwhelming due to the sheer number of variables involved, including physical, chemical and biological elements, in a wide range of different depositional environments. Furthermore, equifinality, the notion that different processes can produce similar results (Schumm, 1998, p. 58; Heller *et al.*, 1993), hinders the identification of causal correlations. Finally, sedimentary system evolution involves phenomena that display chaotic, non-linear behaviour, in other words exhibit sensitive dependence on initial conditions, so that minute discrepancies in initial conditions can produce large differences in outcome (Lorenz, 1993b; Smith, 1998). The interaction between forcing and dissipative constituent processes is so complex and riddled with feedbacks that the distinction between cause and effect is lost (Slingerland, 1990; Smith, 1994) and emerging developments are only predictable within certain limits. Such chaotic processes are abundant in nature (Tetzlaff, 1990; Lorenz, 1993a), certainly in sedimentary systems.

To advance the research, modelling of the sedimentary system of passive continental margins has proven to be a useful aid (Emery & Myers, 1996, ch. 12; Paola, 2000). Initially, the nature of Sedimentology was largely descriptive. As in every natural science, the first priority of Sedimentologists was to make a

thorough inventory and catalogue of the world. However, since then the emphasis has steadily shifted from qualitative to quantitative research, a trend that will continue in the future. Models are an additional tool next to empirical studies, offering a quantitative coupling between established, individual sedimentologic and stratigraphic principles. They can test the validity of hypotheses emanating from field research by evaluating whether the hypotheses are feasible, internally consistent and probable. Methodical investigation over a complete range of variables can identify the gaps in knowledge and may guide further gathering of data. The predictive merit of large-scale and long-term models, such as models of passive-margin sequence stratigraphy, is principally the interpretation of present lithology and stratigraphic architecture (Posamentier & James, 1993), which is the product of past evolution, and not any future development. For instance, a forecast of what will happen to the continental shelves in the coming 100 000 years has no priority, in contrast to predictions by short-term (river, coastal, or delta) models.

In the first place, scientific research is done to pursue a complete understanding of nature, in other words, to satisfy our ‘scientific curiosity’. In this case, we want to know how a particular sedimentary system works, and thus explain the observations made in the field and predict them where they are lacking. However, this academic approach by no means excludes any practical applications of the research. For instance, there is a considerable economic interest in the subject because of the presence of hydrocarbon (oil and gas) reservoirs and fresh water reserves in deposits on passive continental margins. The purpose of the studies of basin margin development presented in this thesis is to appeal to both the pure and the applied aspects of research. Recently, related topics have been addressed in experimental flume studies (Wood *et al.*, 1993; Koss *et al.*, 1994; Van Heijst *et al.*, 2001; Van Heijst & Postma, 2001) and numerical modelling work (e.g. Syvitski & Daughney,

1992; Burgess & Allen, 1996; Ritchie *et al.*, 1999; Granjeon & Joseph, 1999; Ainsworth *et al.*, 2000; Tebbens *et al.*, 2000; Syvitski & Hutton, 2001).

The subject of this thesis is a study of the sedimentary development of passive continental margins. The results are based on a newly developed numerical model. It is three-dimensional, dynamic and applies to large time (several 100s kyr) and spatial ($\sim 100 \times 300$ km) scales. The model set-up is deliberately straightforward to promote computation speed. This allows a statistically significant number of model runs to be made in

a reasonable space of time and a short cycle of drafting and testing hypotheses. Time-averaged sediment fluxes in the model are based on a formulation of a set of rules of material (sediment and water) transport over a cellular (grid) representation of a passive basin margin. Interaction between neighbouring grid cells described by these relatively simple rules results in a complex, non-linear process-response system. The explicit flow of sediment from cell to cell enables monitoring of its properties, such as grain size, provenance and age. This information can subsequently be recorded in the model stratigraphy upon deposition and remains available when the

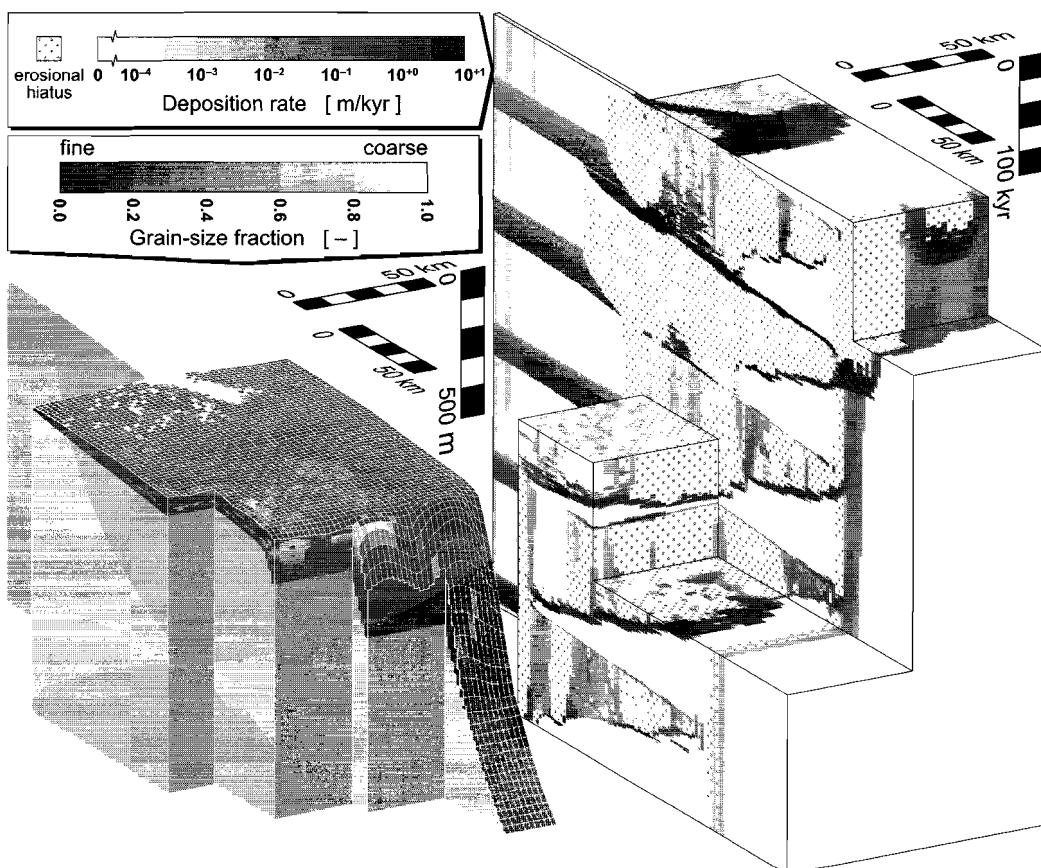


Fig. 1.2— An example lithostratigraphy and corresponding chronostratigraphy produced with the model presented in this thesis. The lithostratigraphy (left) shows the grain size fraction (relative abundance of the coarse grain size class; see Chapter 3) of sediment, and the chronostratigraphy (right) displays the rate of deposition.

sediment is remobilized after erosion. In short, the model presented here is capable of representing the evolution of the geomorphology as well as the lithostratigraphy and chronostratigraphy of a basin margin setting (Fig. 1.2).

Because of the tremendous natural variation between passive continental margins around the world, this study has been restricted to systems with only siliciclastic sediment, i.e. no biogenic sediments (carbonates), and which are well away from regions with glacier activity. Standard for all model runs is a basic system configuration consisting of a river originating from the hills of the hinterland, a delta coast, a continental shelf and upper continental slope on a mature passive margin. The boundary conditions are eustatic sea level and the influence of hinterland climate expressed in the yield from the drainage basin, i.e., the water discharge and supply of sediment. Tectonic subsidence is less significant relative to typical rates of Quaternary sea-level change and therefore receives little attention.

The model is used here as a heuristic tool to test the responses of alternative driving-force scenarios, and is therefore generic rather than tailored to a specific field case. The aim is to derive general statements of the sedimentary system evolution and to identify first-order trends that emerge. Furthermore, certain sequence-stratigraphic terminology, such as sequence boundary and systems tracts, is avoided where possible, as there is no consensus on the application of alternative sequence stratigraphic paradigms like the use of 'depositional' (Posamentier *et al.*, 1988; Posamentier & James, 1993) or 'genetic' (Galloway, 1989) sequences and, for example, the incorporation of a falling stage systems tract into the concept (e.g. Plint & Nummedal, 2000).

Three facets of passive continental margin evolution during Quaternary glacial–interglacial cycles are investigated. First, the development of palaeogeography and

drainage pattern is examined, followed by an analysis of the stratigraphic architecture and basin-scale grain-size sorting, and finally the stratigraphic development is discussed from the perspective of preservation.

Synopsis

Chapter 2 — Modelling the drainage evolution of a river–shelf system forced by Quaternary glacio-eustasy

In Chapter 2, the model is introduced. The set-up, the underlying assumptions and the algorithms of the model are explained. Subsequently, an extensive description is made of the model evolution of the accommodation space, depocentre shift, palaeogeography and drainage pattern on a passive continental margin during a single glacio-eustatic cycle. River avulsion, delta-lobe switching, incision and knickpoint migration are shown to be important processes in the system development. Particularly significant is 'drainage connection', an event whereby a direct and inextricable link between the drainage basin and the depocentre on the shelf edge is established, thereby bypassing the exposed shelf. The experiment is repeated many times with different random noise on the initial topography, which leads to different model realizations every time. It demonstrates that in non-linear systems initial conditions can have a great influence. By accumulating a great number of model runs, an image of the drainage evolution emerges that remains hidden in single runs. This argues for a more extensive use of statistics in model studies to improve the insight into system behaviour.

Chapter 3 — Grain-size sorting of river–shelf–slope sediments during glacial–interglacial cycles: modelling grain-size distribution and interconnectedness

Chapter 3 deals with grain-size sorting on

a basin-margin scale. During sea-level highstand and falling stage, progradational coarsening-upward paralic successions are deposited on the continental shelf, as coarse material settles proximal to the river mouth and fine material builds the prodelta. The coarse topset-strata are more likely to be eroded than the fine sediment in the foresets when the shelf is exposed. This chapter describes how this difference in preservation potential of deposits on the shelf results in enrichment of the river load with coarse material during the formation of a subaerial erosional unconformity, which reduces the coarse sediment content on the shelf and enriches shelf-edge deposits. The distribution of sediment volume and grain size in the stratigraphy after several glacial–interglacial cycles is discussed, as well as the occurrence of coarse-grained bodies in the stratigraphic architecture. Major coarse bodies are found in shelf-edge deltas formed during times of low sea level and at the base of transgressive, incised valley fills. The interconnectedness of such bodies appears to depend strongly on the palaeogeographic development of the depositional system.

Chapter 4 — Modelling the preservation of sedimentary deposits on passive continental margins during glacial–interglacial cycles

The preservation of deposits, their lateral and temporal variation, and the relation to the development of the palaeogeography is

investigated in Chapter 4. The coastal wedge and inner shelf, and the shelf edge, which are convex morphologies on passive continental margins, are most affected by river incision and gradient-dependent transport processes. Strata that are deposited on the shelf have a greater chance of being reworked than those on the upper continental slope. Hence, deposits of roughly the first half of a glacial–interglacial cycle are badly preserved compared with the second half. Furthermore, various scenarios of sea-level change, water discharge and sediment supply are compared, and the preservation of highstand topographies is examined as a function of the difference in gradient between the coastal wedge and the shelf, and the sediment supply.

Chapter 5 — Conclusions

A synthesis of the results of Chapters 2, 3 and 4 is presented in Chapter 5. The roles of relative sea-level change and climate-related palaeohydrology in the evolution of passive margin systems are discussed. The relative importance of these main driving forces is dependent on the location, time-interval and scale of interest. Furthermore, the relationships between palaeogeographic development, stratigraphic architecture, grain-size distribution and preservation potential are recapitulated. Finally, it is argued that a statistical approach is required for the three-dimensional dynamic modelling of sedimentary systems.

Modelling the drainage evolution of a river–shelf system forced by Quaternary glacio-eustasy

Abstract

The Quaternary glaciations had a profound impact on the geomorphology and stratigraphy of passive continental margins. The challenge is to resolve the contributions of the main forcing controls relative sea-level change and sediment flux. Key to answering this question is understanding the interaction between the marine and terrestrial environments, where river dynamics play an essential role. A comprehensible three-dimensional numerical model is presented to investigate quantitatively the behaviour of river–shelf sedimentary systems under glacio-eustatic conditions. Distinctive features observed in the model results include river avulsion, delta-lobe switching, incision and knickpoint migration. An important event in the development of the modelled river–shelf system is the establishment of a direct and inextricable link between the drainage basin and the depocentre on the shelf edge, thereby bypassing the exposed shelf. This is termed ‘drainage connection’. In the model, the timing of drainage connection occurs over a broad interval when the model run is repeated many times with small differences in the initial topography, reflecting the sensitivity of the system to its initial state. It demonstrates the inherent variability in the evolution of a sedimentary system as a consequence of non-linear behaviour. A statistical approach to modelling is suggested to deal with this problem.

Introduction

A salient characteristic of the Quaternary is the high-frequency waxing and waning of continental ice sheets resulting in a succession of ice ages. The alternations of interglacial and glacial conditions had a profound impact on the development of sedimentary systems adjacent to depositional basins. One of these sedimentary systems is situated along passive continental margins. Present morphologies and architectures of passive margins are the result of a multitude of glacial–interglacial cycles.

Many researchers have studied cyclicity in the stratigraphic record and have attempted to link it to the possible driving forces. Relative sea level and palaeohydrology, as a derivative of climate change, are the allocyclic forcing controls in the evolution of stratigraphic sequences. In the Quaternary, glacio-eustatic sea-level change and climate change are in many cases interlocked. The relative contributions of climate and sea-level changes

in the development of basin-margin architecture are not easily unravelled from the stratigraphic record alone because of equifinality (Schumm, 1998 p. 58; Heller *et al.*, 1993). Data sets of alluvial and shelfal sediment budgets with good age constraints are a prerequisite for resolving the individual contributions of the two controls, but are not available at present. Modelling can aid in placing quantitative constraints on the effect of changes in climate and sea level on basin margin architecture.

Here, a generic three-dimensional numerical model of passive margins encompassing the lower reaches of a river, a delta, a shelf and upper continental slope is introduced, and used to forward model the geomorphologic evolution of such a system. The focus of this chapter is the evolution of drainage networks (i.e., the dynamics of the fluvial and deltaic environments) during Quaternary glacial cycles. Developments in this setting profoundly affect the stratigraphy

along the entire transport route by influencing sediment flux, the distribution of subaerial erosion and deposition, the location of marine depocentres and the timing of coastal retreat and advance. In addition, in order to gain insight into the system's sensitivity to initial conditions and the solution space it creates, this chapter takes a statistical approach to describe drainage network development.

Method

Premise of the model

Spatial variations of erosion and sedimentation make sequence stratigraphy an inherently three-dimensional problem. However, until recently, computational limitations effectively confined numerical research to two-dimensional models (Paola, 2000), which were unable to incorporate processes and features that extend outside the two-dimensional profile, such as river avulsion and delta-lobe switching, the formation of incised river valleys and unconformities, and the related connectivity of sand bodies.

In order to produce a significant number of model runs, necessary for a statistical approach to modelling stratigraphy, in a reasonable amount of time, the model is

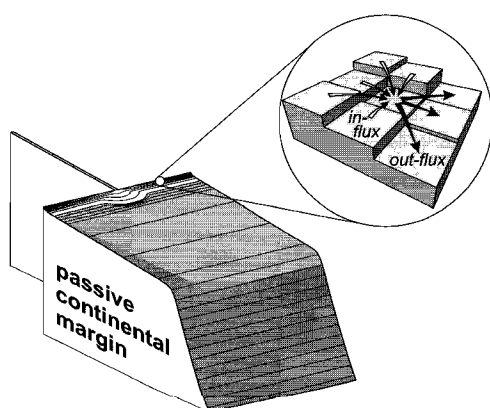


Fig. 2.1 — A schematic portrayal of a portion of the model grid illustrating the fundamentals of the model algorithms.

designed to be straightforward. Furthermore, a comprehensible model benefits interaction between modellers and field workers.

An important aspect of the three-dimensional cellular model methodology presented here is that properties of the sediment can be monitored through time as it is being transported. The method is based on a grid of cells interacting with each other on the basis of a number of rules for sediment transport. From this small set of relatively simple algorithms, an intricate process-response system arises which exhibits dynamic, non-linear behaviour, resembling that of a natural system.

Description of the model

In Fig. 2.1, a portion of a grid of square cells is depicted that, by having various elevations, shape a landscape. The total grid outlines a system with closed boundaries. Sediment and water enter the system at an inlet grid cell (Fig. 2.1). Within the system, sediment and water can move between adjacent grid cells according to a few simple rules. Each grid cell is evaluated in the order of its elevation, starting with the highest one. The volume of sediment moving out of a grid cell (the 'out-flux' Ψ^{OUT} [m^3yr^{-1}]) is determined by the combined action of two transport algorithms – 'diffusive transport' and 'stream transport'. Distribution of this volume of sediment yields the 'in-flux' (Ψ^{IN} [m^3yr^{-1}]) of the neighbouring grid cells.

Diffusive transport

Diffusive transport is a *short-range* mechanism for interfluvial, delta-plain, coastal and marine transport processes. The total out-flux as a result of diffusive transport is the sum of the out-fluxes in all available 'grid directions' (Eq. 2.1). Available grid directions are all directions with down-slope grid cells; no transport can occur to up-slope grid cells and over the boundaries of the grid. Diffusive transport only applies to grid cells where a constant 'threshold discharge' value Q_{thr} [m^3yr^{-1}] is not exceeded.

$$\Psi_D^{OUT} = \sum_{dir} \Psi_{D\ dir}^{OUT} \quad (2.1)$$

The out-flux in a particular grid direction (dir) is proportional to a ‘resulting slope’ S_{dir}^* [–] to a given power U , provided a certain threshold slope S_{thr}^* [–] is exceeded (Eq. 2.2). The sedimentary system includes a number of depositional environments (env) from terrestrial to deep-sea. Their boundaries are determined by transitions, such as sea level and wave base. For each of these environments, a threshold slope and a ‘transport-efficiency constant’ K_D [m^3yr^{-1}] is defined.

$$\Psi_{D\ dir}^{OUT} = K_D(env) \cdot \left[(S_{dir}^* - S_{thr}^*(env)) \cdot H(S_{dir}^* - S_{thr}^*(env)) \right]^U \quad (2.2)$$

where $H(x)$ [–] is the Heaviside-function (“on-off switch”; $H(x)$ is zero when arbitrary variable $x < 0$, and unity for $x \geq 0$). The resulting slope equals the ‘initial slope’ S_{dir} [–] plus the balance of in-flux and total out-flux, i.e., erosion or deposition (Eq. 2.3).

$$S_{dir}^* = S_{dir} + \frac{\Psi^{IN} - \Psi_D^{OUT}}{grid\ cell\ area} \cdot \frac{time\ step}{distance_{dir}} \quad (2.3)$$

However, grid directions that are initially up-slope remain excluded from transport even if the resulting slope would exceed the threshold value. The total diffusive out-flux can be formulated as follows (Eq. 2.4).

$$\Psi_D^{OUT} = K_D(env) \cdot \sum_{dir} \left[\left(\frac{\Psi^{IN} - \Psi_D^{OUT}}{grid\ cell\ area} \cdot \frac{time\ step}{distance_{dir}} + S_{dir} - S_{thr}^*(env) \right) \cdot H(S_{dir}^* - S_{thr}^*(env)) \right]^U \quad (2.4)$$

Stream transport

Stream transport represents *long-range* transport by rivers and river-plumes. The total out-flux owing to stream transport is the sum of all contributions in the down-slope grid directions (Eq. 2.5). Stream transport only

applies to terrestrial grid cells where the threshold discharge is exceeded.

$$\Psi_S^{OUT} = \sum_{dir} \Psi_{S\ dir}^{OUT} \quad (2.5)$$

In geomorphological modelling, it is common practice to transfer material in the direction of steepest descent (Schoorl *et al.*, 2000). This means that only convergent stream networks can evolve. This may be applicable in mountainous drainage basins where streams are restricted by topography, but it is not realistic in depositional basins where river belts are laterally unconfined. In delta-plains or fans, river discharge tends to diverge. In the model, sediment and discharge are therefore distributed relative to the initial slopes in the respective grid directions (Eq. 2.6). In view of the size of the grid cells, slopes should be considered valley gradients rather than river gradients. A threshold on the available grid directions fixes a possible position between the steepest descent and sheet-flow end-members (cf. Freeman, 1991; Schoorl *et al.*, 2000), producing channelisation with an opportunity to avulse and bifurcate.

$$p_{dir} = \frac{S_{dir} \cdot H(S_{dir} - k \cdot S_{max})}{\sum_{dir} [S_{dir} \cdot H(S_{dir} - k \cdot S_{max})]} \quad (2.6)$$

The stream transport algorithm requires an amount of river water ‘discharge’ Q [m^3yr^{-1}] to be present in the grid cell in order to be effective. The transport equation is based on the common formulation of stream power. The stream in a given grid direction has a ‘carrying capacity’

$$K_S \cdot [Q \cdot p_{dir} \cdot H(Q \cdot p_{dir} - Q_{thr})]^W \cdot S_{dir}^V \quad [m^3yr^{-1}].$$

The carrying capacity entails the sediment load that the stream is able to carry for the present conditions. The current sediment load is subtracted from it in order to get — after division by a value L_S [–] — the volume that is eroded or deposited by the river.

$$\Psi_S^{OUT} = \left[\Psi^{IN} \cdot P_{dir} \right] - \frac{\left[\Psi^{IN} \cdot P_{dir} \right]}{L_S(capacity)} + \frac{K_S \cdot \left[Q \cdot P_{dir} \cdot H(Q \cdot P_{dir} - Q_{thr}) \right]^W \cdot S_{dir}^V}{L_S(capacity)} \quad (2.7)$$

When the carrying capacity exceeds the sediment load, erosion will occur. On the other hand, a sediment load greater than the carrying capacity will result in deposition. The value of L_S depends on whether the river is at a condition of overcapacity or undercapacity. In case of erosion, it is a measure of the detachability or erodibility (Kooi & Beaumont, 1996; Crave & Davy, 2001). It is affected by characteristics like substrate material and vegetation. When deposition occurs, L_S reflects how well sediment is able to settle from the flowing water.

Similar to before, the resulting slope equals the 'initial slope' S_{dir} plus the balance of in-flux and total out-flux, i.e., erosion or deposition (Eq. 2.8).

$$S_{dir}^* = S_{dir} + \frac{\Psi^{IN} - \Psi_S^{OUT}}{grid\ cell\ area} \cdot \frac{time\ step}{distance_{dir}} \quad (2.8)$$

Substitution of Eqs 2.7 and 2.8 in 2.5 yields the composite equation of the stream out-flux (Eq. 2.9a).

$$\Psi_S^{OUT} = \Psi^{IN} - \frac{\Psi^{IN}}{L_S(capacity)} + \frac{K_S}{L_S(capacity)} \cdot \sum_{dir} \left[\left[Q \cdot P_{dir} \cdot H(Q \cdot P_{dir} - Q_{thr}) \right]^W \cdot \left(\frac{\Psi^{IN} - \Psi_D^{OUT}}{grid\ cell\ area} \cdot \frac{time\ step}{distance_{dir}} + S_{dir} \right)^V \right] \quad (2.9a)$$

Apart from erosion or deposition, a river is also able to respond to changing conditions by adapting its characteristics, such as pattern, shape and bed roughness (e.g. Schumm, 1993; Wescott, 1993; Leeder & Stewart, 1996).

Hence, in order to account for river dynamics in the model the assumption is made that when the river in the model is at undercapacity it will respond preferably by changing its properties, effectively constituting a threshold on incision. One river characteristic that has been suggested to play a role as a constraint on incision is sinuosity. A meandering river's response to increasing gradient is to become more sinuous unless the gradient is too steep, whereupon the river will incise and braid (Schumm, 1981; Schumm *et al.*, 1987; Schumm, 1993). It is not implied here that the incision-threshold is equivalent to the transition from a meandering to a braided river-pattern (Bridge, 1993), but in the model a similar expression is used to prescribe the geomorphic threshold to initiate erosion (Bledsoe & Watson, 2001). The tentative formulation implies that a river below incision-threshold does not incise (Eq. 2.9b). On the other hand, aggradation is allowed in streams above as well as below threshold.

$$\Psi_S^{OUT} = \Psi^{IN} \quad \text{if } capacity = undercapacity \quad \text{and} \quad \sum_{dir} \left[\left[Q \cdot P_{dir} \cdot H(Q \cdot P_{dir} - Q_{thr}) \right]^W \cdot S_{dir}^V \right] < P_{thr} \quad (2.9b)$$

When a river discharges into the sea, sediment is carried away from the river mouth in a plume. The algorithm for river-plume transport is an adaptation of that of stream transport. Thus, underwater relief (e.g. estuaries or submarine canyons) is taken into account when distributing the sediment. The difference is that within the plume the carrying capacity equals zero (Eq. 2.10; i.e., exponential decrease of transport) and that diffusive transport can occur as well.

$$\Psi_P^{OUT} = \Psi^{IN} - \frac{\Psi^{IN}}{L_S(capacity = overcapacity)} \quad (2.10)$$

Wave and current transport apart from diffusive transport are not incorporated into the model.

Model procedure

The parameters incorporated into this model have been calibrated by using general values that have been chosen from geologically realistic ranges derived by reference to data on actual passive margins. Model process rates and morphologic attributes that have been used for calibration by comparison with empirical data are knickpoint migration rates, maximum extent of fluvial onlap, rates of erosion and deposition, river avulsion behaviour, and final stratigraphical architecture geometry. These features and their calibration are discussed further on.

The values of the parameters in the above equations are listed in Table 2.1. The model is furnished with a scenario, i.e., a history of imposed variables such as sea-level change and hydrology. The most significant variables of the applied scenario are constant discharge and

sediment supply, and a sinusoidally, slowly falling and rapidly rising sea level. These were applied to a generalized configuration of passive margins characteristic for the Quaternary, with a wide shelf that is somewhat steeper than the river profile (Butcher, 1990; Miall, 1991; Nummedal *et al.*, 1993). No precipitation is applied in the scenario used here. The details of this scenario are listed in Table 2.2 and illustrated in Fig. 2.2. The initial landscape topography (Fig. 2.2) is roughened with white-noise from a uniform distribution within a range of ± 0.025 m. The model experiment is repeated many times; each time with the same scenario but with different white-noise so that 1000 realizations of the scenario are created. From the model output, maps and profiles are extracted, as well as more abstract scalar quantities describing drainage evolution.

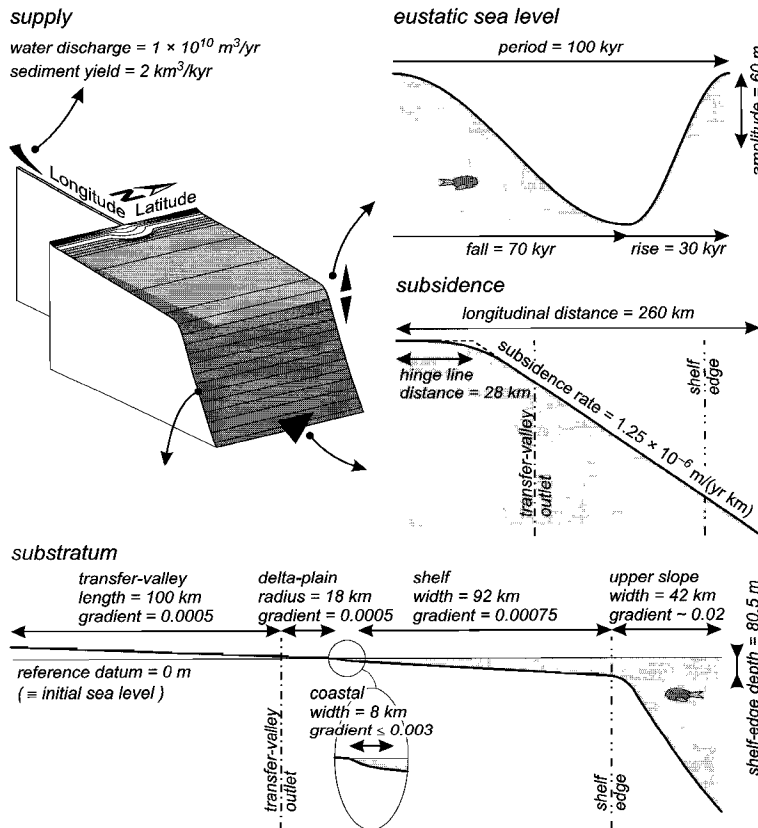


Fig. 2.2 — Diagram outlining the initial morphology and the scenario of forcing variables (i.e., the boundary conditions) of the model experiments. The landscape consists of a transfer-valley, a delta-plain, a coastal zone, a continental shelf and an upper continental slope. The variables are constant supply, sinusoidal sea-level change and subsidence basinward of a hinge line. The horizontal reference datum is the inlet of the transfer-valley. The vertical reference datum is initial sea level.

Table 2.1 — Values of parameters applied in the model runs.

<i>Parameter</i>	<i>Value</i>	<i>Unit</i>	<i>Equation</i>
<i>Environment</i>			
U	1.0	–	Eq. 2.2
K_D			Eq. 2.2
terrestrial	0.30	km ³ kyr ⁻¹	
coastal	0.40	km ³ kyr ⁻¹	
marine	0.40	km ³ kyr ⁻¹	
deep marine	0.32	km ³ kyr ⁻¹	
S_{thr}^*			Eq. 2.2
terrestrial	0.0005	–	
coastal	0.0040	–	
marine	0.0200	–	
deep marine	0.0200	–	
transition depth			
terrestrial – coastal	0	m	
coastal – marine	25	m	
marine – deep marine	100	m	
k			Eq. 2.6
terrestrial	0.75	–	
non-terrestrial	0.00	–	
V	1.0	–	Eq. 2.7
W	1.0	–	Eq. 2.7
Q_{thr}	2.0×10^8	m ³ yr ⁻¹	Eq. 2.7
K_S	0.4	–	Eq. 2.7
L_S			Eq. 2.7
at overcapacity	10	–	
at undercapacity	50	–	
v	1.00	–	Eq. 2.9b
ω	0.25	–	Eq. 2.9b
P_{thr}	0.224	(m ³ yr ⁻¹) ^{0.25}	Eq. 2.9b
grid cell size	2000	m	
time step	10	yr	
white-noise range	0.05	m	

Table 2.2 — Values of variables applied in the model runs.

<i>Variable</i>	<i>Value</i>	<i>Unit</i>
<i>Component</i>		
supply		
water discharge	1.0×10^{10}	m ³ yr ⁻¹
sediment yield	2.0	km ³ kyr ⁻¹
sea level		
period	100	kyr
duration of fall	70	kyr
amplitude	60	m
substratum		
transfer-valley length	100	km
delta-plain radius	18	km
coastal width	8	km
shelf width	92	km
upper slope width	42	km
fluvial-valley gradient	0.00050	–
delta-plain gradient	0.00050	–
coastal gradient	< 0.00300	–
shelf gradient	0.00075	–
upper slope gradient	~ 0.02000	–
subsidence		
hinge line distance	28	km
subsidence rate	1.25×10^{-6}	myr ⁻¹ km ⁻¹

Results and Discussion

A large number of model runs was performed. In this section, two examples of such model realizations are described qualitatively.

At initial sea-level highstand, the shelf is flooded and the river and the delta plain are at grade. The avulsion rate is high; avulsion points, both divergent and convergent (*sensu* Jones & Schumm, 1999), are numerous. Virtually the entire delta plain is covered by channel belts of varying size, most of which are

short-lived. As a result, the sediment that reaches the coast is distributed evenly over the entire delta rim. Delta progradation is accompanied by subaerial aggradation on the delta and in the transfer-valley (Fig. 2.3a).

Some time later, avulsions continue to take place but patches of interfluvium develop between the active distributaries (Fig. 2.3b). As the length of the delta coastline increases, the sediment sources into the sea become more dispersed. With aggradation decreasing overall (Fig. 2.3c), avulsion rate declines. As sea level falls, the delta increases in area and develops

into two isolated lobes. The distributaries on these active lobes are sites of channel extension and channel switching (*sensu* Coleman, 1976).

The lower reaches of the distributaries are adapting to relatively steep gradients that have developed owing to the increasing rate of sea-level fall (Fig. 2.3d). The rivers largely manage to remain below the incision-threshold and need only minor incision. The two active delta parts are extending but the accelerating sea-level fall makes it increasingly difficult for the supply to keep up. As a consequence, the delta front becomes exposed rather than covered with sediment and is eroding. The area of fluvial aggradation has been retreating towards the delta apex and into the transfer-valley for some time but has finally ceased there altogether (Fig. 2.3e).

The activity of the river mouths of the southern delta lobe shifts sideways from the forced regressive extensions of the old highstand delta to a new delta-plain lower on the shelf floor. A very distinct step in the topography (*cf.* Posamentier & Morris, 2000) is present in the section normal to the basin axis, whereas the river profile has only a slight increase in gradient where the river crosses the front of the abandoned delta lobe. Similar steps occur during the time that the coastline migrates across the shelf, resulting in a succession of delta lobes that are imbricately and obliquely stacked. However, since the rate of regression increases they tend not to be as pronounced as the one in front of the highstand delta.

As sea level continues to fall, the upstream position of the channel belts is stabilized (Fig. 2.3f). The forced regressive

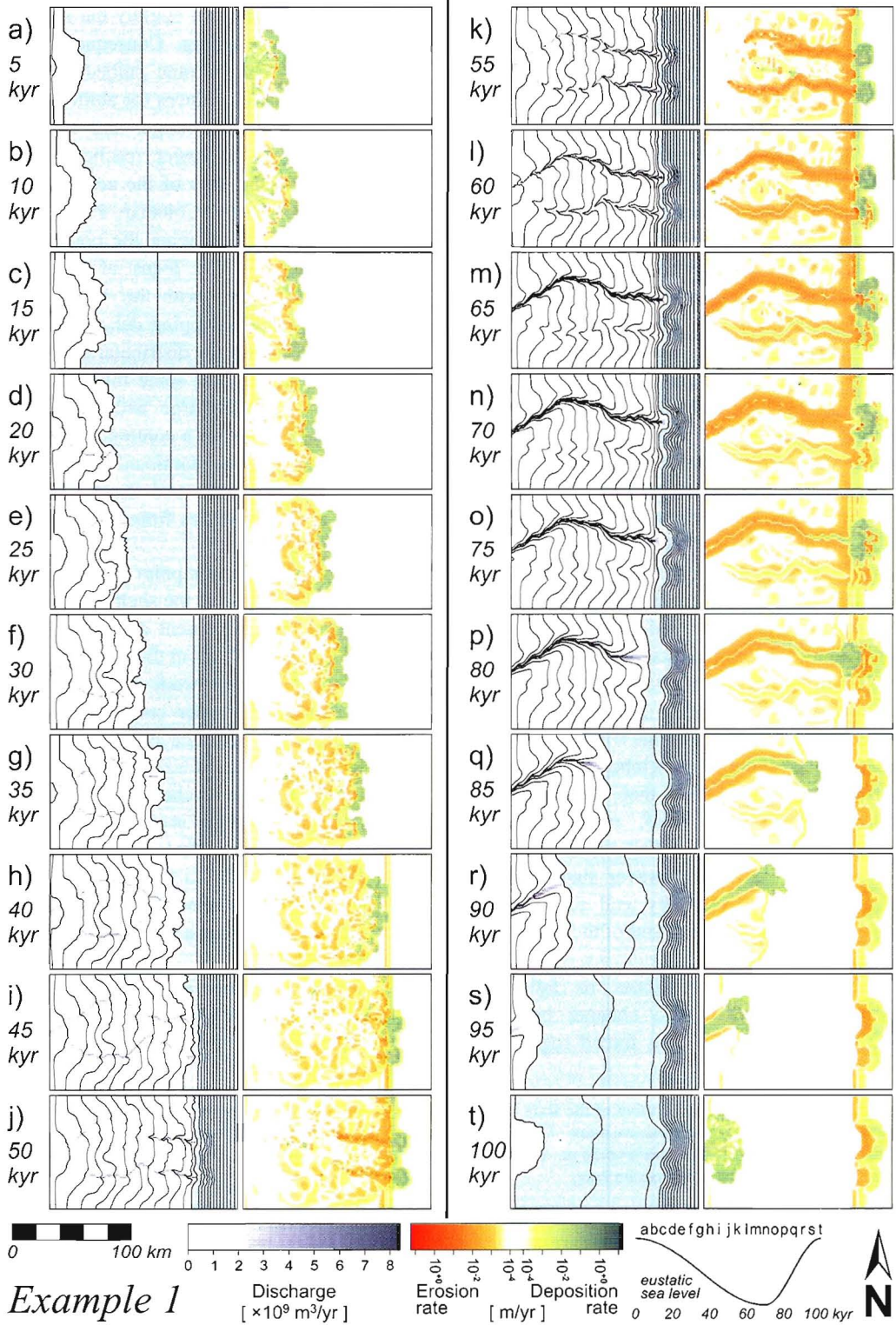
deposits are being incised slightly but steadily while sea level is dropping. Consequently, the larger channel belts become embedded in a shallow valley, which reduces the ability of the river to avulse in this range, and avulsion occurs mainly in the lower reaches of the channel belts, at the sites of the active lobes. Branch switching (*sensu* Coleman, 1976) is the main mechanism of changing the position of the river mouths. The locus of diversion corresponds commonly with the “apex” of a newly forming down-stepping delta lobe (Fig. 2.3g). From this point the distributaries spread. The branches coexist for some time until the weaker one loses discharge and disappears. The avulsions are part of a continuous process of development of the dominant branch, the decline of smaller ones, and the subsequent formation of new branches from the dominant one.

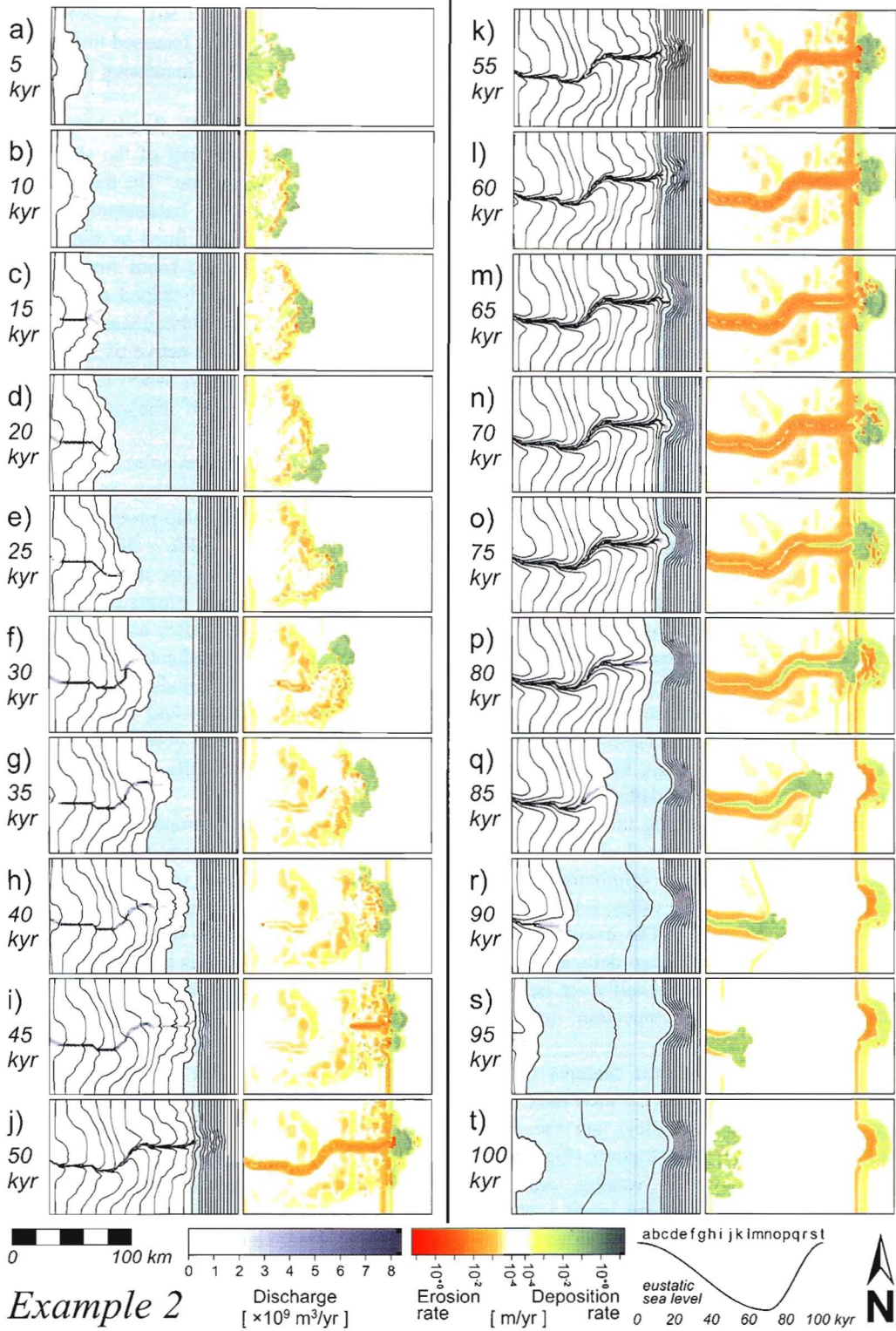
As the fall inflection point on the eustatic sea-level curve is passed, the shelf edge comes into the coastal environment and starts to be eroded (Fig. 2.3h). At about the same time, the first sediment derived from proximal river sources reaches the upper continental slope. Up until this point, the delta system’s response to sea-level fall has been a rapid progradation over the shelf, but as it reaches the deeper water beyond the shelf edge this is no longer feasible. Hereafter, the river mouths respond vertically rather than horizontally to sea-level fall. The first shelf-edge deltas arise (Fig. 2.3i) and the coastline straightens over a wide distance along the shelf edge.

After the coastline has reached the shelf edge, incision into the shelf itself commences, through the deposits that have been laid down

Fig. 2.3 (next page) — The evolution of the state of the system of example 1. The transfer-valley is omitted to save space. On the left of each column are maps of the discharge rate and the topography. Topographic contour interval above sea level is 10 m; below sea level 50 m. The coastline is indicated by a thick line. On the right of each column, the instantaneous erosion/deposition rate.

Fig. 2.4 (opposite next page) — The evolution of the state of the system of example 2. The transfer-valley is omitted to save space. On the left of each column are maps of the discharge rate and the topography. Topographic contour interval above sea level is 10 m; below sea level 50 m. The coastline is indicated by a thick line. On the right of each column, the instantaneous erosion/deposition rate.





since the start of this sea-level cycle (Fig. 2.3j). The zone along the river profile where erosion takes place extends headward by the process of knickpoint migration (Butcher, 1990). Deep incision into the shelf gives rise to steep, eroding valley walls (Fig. 2.3k). Minor branches near the coast are soon cut off as the front of the erosional zone passes their bifurcation site. The incised valley shallows landward. Pulses of erosion by smaller knickpoints migrating upstream follow under the continuous driving force of falling base level, alternating with episodes of relative rest with only sediment bypass. Thus, the river reach consists at any given time of different domains of activity.

Deposition at the shelf edge occurs in two distinct deltas. The exposed shelf edge itself is eroding, and, combined with the area of incised valleys, forms a large area of erosion (Fig. 2.3l).

The knickpoint of the northern channel belt accelerates upstream as it approaches the transfer-valley and captures more discharge from the other belt (i.e., positive feedback). The moment it cuts off the southern channel belt, a single bypass valley arises that connects the transfer-valley emerging from the hills of the hinterland with the delta on the upper continental slope, bypassing the shelf entirely (Fig. 2.3m). The abandoned channel belt is filled with sediment originating from continuing erosion of the valley walls, and its delta starts to degrade. The event whereby transfer-valley and shelf-edge delta are linked directly by a single cross-shelf river belt has been named 'drainage connection' (cf. Van Heijst & Postma, 2001).

Towards lowstand, the features of the forced regressive wedge on the shelf have been smoothed; the incised valleys are the most striking palaeogeographic features (Fig. 2.3n). The rate of incision is waning, and the segments of the river where erosion occurs decrease in size and number. Following first signs of onlap at relative sea-level lowstand at the mouth, proper onlap into the incised river

valley takes place (Fig. 2.3o). Accumulation on the shelf-edge delta is focussed towards the river mouth, resulting in increasing submarine aggradation.

The shelf is gradually flooded by the sea (Fig. 2.3p) and aggradation of the shelf-edge delta turns to retrogradation. The transgressive deposits are delta lobes backstepping into a relatively narrow area defined by the incised valley, with only limited room for avulsion. This results in an funnel-shaped river mouth (Fig. 2.3q). Note that subaqueous deposition fills up the estuary of the active river resulting in a convex topography, whereas the shelf inherits a flooded shelf canyon from the abandoned valley.

As the rise inflection point is passed, the shelf edge is still adjusting to the new conditions and fluvial onlap proceeds into the transfer-valley (Fig. 2.3r). Retrogradation slows down as sea-level rise decelerates (Fig. 2.3s) and passes into progradation. The remains of the incised valley are infilled (Fig. 2.3t) and the low gradient of the young highstand delta and the newly acquired spatial freedom allows avulsion and lobe switching (*sensu* Coleman, 1976) to occur again, as it did on the initial highstand delta.

In the second example (Fig. 2.4), the system's development is similar to that of the first example for some time (Figs 2.4a, b). However, in this model realization, one of the distributaries on the delta captures most of the discharge early on towards late highstand (Fig. 2.4c). The channel belt rests in a shallow valley incised in the highstand delta, and only the lower reaches of the river are prone to avulsion. There, the river branches at the apex of the active delta lobe, and the position of this branching point repeatedly jumps basinwards (Figs 2.4c-h) along with the location of the active delta during continued fall. In contrast to the first example, branches do not coexist for a long time; a stretch is appended regularly to the trunk river that lies upstream. Because sediment enters the sea along a relatively

limited part of the coastline the delta protrudes clearly basinward (e.g. Fig. 2.4f).

A significant avulsion event diverts in the channel belt (between Figs 2.4e and f) to the north owing to a gradient advantage (Jones & Schumm, 1999). The new active system causes a relatively deep incision into the convex edge of the exposed highstand-delta front (Fig. 2.4f), while downstream, the delta is aggrading. Under the conditions of forced regression, the increase in sediment load brought on by cannibalization is usually not enough for the river to switch to deposition further downstream. Rather, it moderates erosion downstream or prevents the system from crossing the incision-threshold.

Eventually, sediment reaches the shelf edge (Fig. 2.4h). Several distributaries incise into the shelf edge, although one remains dominant (Fig. 2.4i). Headward erosion proceeds with a distinct knickpoint marking the upstream limit of erosion (Figs 2.4i, j). This happens at a greater pace than in the first example as the single channel belt has greater erosive power, and already accomplished a substantial amount of ‘preparatory work’ during the previous expansion of the river over the shelf. As a consequence, drainage connection occurs much earlier than in the first example (at 49 kyr as opposed to 60.5 kyr).

The overall picture of erosion of the river floor and the valley walls persists until lowstand (Figs 2.4k–n). A single delta has accumulated on the upper continental slope, much larger than either delta in the first example. Developments during the subsequent sea-level rise are very similar to those in the first example (Figs 2.4o–t).

Drainage evolution

Comparison of model results with empirical stratigraphic data remains problematic. Large-scale three-dimensional field studies of continental shelf and slope are scarce (e.g. Anderson *et al.*, 1996; Hernández-Molina *et al.*, 2000) and lack sufficient age constraints (Gensous & Tesson,

1996; Van Heijst *et al.*, 2001). Moreover, very few complete data sets exist that cover both marine and correlative alluvial strata (Shanley & McCabe, 1994). A crucial development in a forced regressive system is incision and the formation of a subaerial erosive unconformity, during which much of the preceding morphology is removed. Field observations of shelf incisions are not detailed enough to determine spatial patterns (Talling, 1998; Wescott, 1993) or distinguish them from river scours (Salter, 1993), let alone to provide evidence of the palaeohydrology. Ravinement reduces the preservation of diagnostic features, such as valley-fills and palaeosols. In spite of the difficulties, three-dimensional, regional studies of outcrop or seismic and well data are essential to understand how incised valleys evolve (Leeder & Stewart, 1996).

In anticipation of future field studies, experimental (flume) modelling studies (e.g. Schumm *et al.*, 1987; Koss *et al.*, 1994; Van Heijst & Postma, 2001; Paola, 2000) are a useful complementary comparison to numerical models. Although they have different methodologies, both numerical and experimental modelling efforts aim to test how natural sedimentary systems work. The evolution of the shelf in the model of this thesis has many similarities with that displayed in various flume studies (Wood *et al.*, 1993; Koss *et al.*, 1994; Van Heijst & Postma, 2001), such as initial formation of incipient shelf-edge deltas, subsequent headward erosion of competing valleys, and infill of the remaining active incised valley by backstepping lobes during transgression.

The frequency of avulsion in the model shows a relation to aggradation rate as has been suggested for fans by Bryant *et al.* (1995). The three consecutive phases of development of fans in their experiments, viz. from no clear channels to distinct but unstable channels to a single channel, are remarkably similar to the evolution of the drainage pattern up to late highstand in the model examples (see Figs 2.3

and 2.4). The style of drainage during falling stage is less dynamic as incision, to greater or lesser extent, makes the upstream river course less susceptible to diversion (cf. Posamentier *et al.*, 1992). Avulsion can be “instantaneous” or may span several millennia (cf. Jones & Schumm, 1999). Fluvial activity during sea-level rise is constrained by a valley that limits lateral avulsion, until aggradation brings the river profile above the valley sides (Quirk, 1996; Aslan & Blum, 1999).

The model has incorporated a geomorphic threshold on incision by assuming a coupling between erosion and a river-pattern criterion. This is not to suggest that in nature this threshold is identical to the crossover between channel forms from meandering to braided. There is an abundance of alternative formulations that describe the conditions under which a transition between channel forms occurs (see Bridge, 1993 for overview), but none of them does so unambiguously (Van den Berg, 1995). Moreover, the presumed existence of a discrete boundary is a mathematical simplification of a gradual transition in natural systems (Van den Berg, 1995; Bledsoe & Watson, 2001). However, since an incision-threshold criterion is to be quantified (Leeder & Stewart, 1996; Bledsoe & Watson, 2001), it is necessary to use a simple assumption pending a better expression for the threshold. Model results highlight the importance of this threshold, as it enables the river to extend across the shelf without major erosion during a large part of sea-level fall by absorbing most of the valley gradient changes, thereby postponing widespread incision until after sea level has dropped below the shelf edge.

Minor incisions into shelf deposits during rapid forced progradation, however, do occur in the model. This behaviour has been expected (Wescott, 1993) and observed in experimental studies (Koss *et al.*, 1994; Van Heijst *et al.*, 2001) and in the field (Posamentier *et al.*, 1992; Törnqvist *et al.*, 2000). Talling (1998) and Törnqvist *et al.* (2000) emphasize that incision

prior to shelf-edge exposure will primarily take place in the convex topography (‘coastal prism’) that has formed at sea-level highstand. Indeed, this happened in the second model example (Fig. 2.4f).

The area of shelf erosion after emergence grows landward (e.g. Butcher, 1990; Posamentier *et al.*, 1992; Wescott, 1993), partly due to the exposure of a relatively steep continental slope, but mainly due to river-valley entrenchment and widening. The river reacts to a lowered base level by developing knickpoints that migrate headward (Butcher, 1990). Sea-level fall provides a persistent driving force, which is modified by delta activity, and knickpoint activity in the model occurs in successive surges. An initial main knickpoint is followed by smaller ones, which was observed by Koss *et al.* (1994) in their flume experiments. Knickpoint migration proceeds at different rates in individual channels, depending on discharge and proximity to incision-threshold conditions. A river branch captures the discharge of a competing branch when its headward migrating knickpoint reaches the trunk stream first, leaving the other abandoned.

The lag time between sea-level forcing and the upstream response results in a fluvial system that is increasingly out of phase further inland with events at the coast (e.g. Shanley & McCabe, 1994; Ethridge *et al.*, 1998). There is a delay between the time when first incisions develop at the shelf edge and the time when the headward erosion reaches the transfer-valley. This delay is also seen in flume experiments (Van Heijst & Postma, 2001). The delay is far too great to be considered instantaneous at the scale of a glacial cycle. Even during transgression, incised valley walls on the inner shelf continue to be eroded while downstream they are already being buried by coastal onlap. This implies a large diachroneity of the subaerial erosion surface.

When the knickpoint in a river course finally reaches the transfer-valley, the river performs the ultimate capture and focusses

deposition. Afterwards, river diversion landward of the shelf edge is impossible. In the model, the event whereby transfer-valley and shelf-edge delta are directly linked by a single cross-shelf river is termed ‘drainage connection’. This is significant because after connection only a single depocentre remains and sediment supply to the upper continental

slope becomes a point source. Drainage connection affects subsequent developments, such as the evolution of river gradient, and the timing and upstream extent of knickpoint migration. Also, there are important implications for the size and composition (e.g. grain size, sediment provenance) of sediment in the active shelf-edge delta, and the mass flow

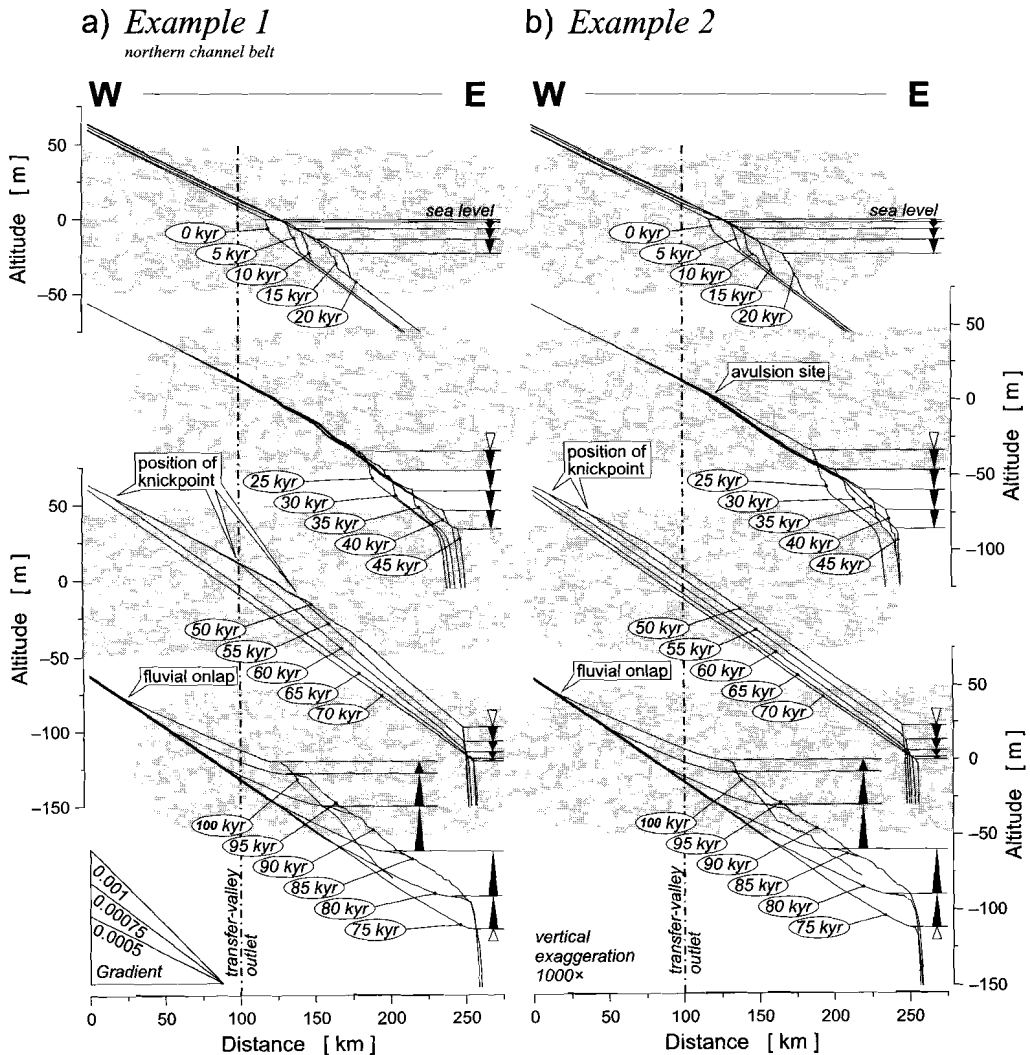


Fig. 2.5 — Longitudinal profiles of the main river channel belts. a) Profile evolution of the main northern channel belt of example 1. b) Profile evolution of the main channel belt of example 2. The site of the major avulsion occurring in example 2 between 25 and 30 kyr, discussed in the text, is indicated.

deposits that derive from there (Wood *et al.*, 1993; Van Heijst & Postma, 2001). Experimental (Koss *et al.*, 1994; Van Heijst & Postma, 2001) and numerical (Ritchie *et al.*, 1999) model studies, as well as theoretical work (Butcher, 1990; Posamentier & Morris, 2000), all underline the importance of drainage connection and the developments that lead up to it.

River profile development

Many authors (e.g. Miall, 1991; Posamentier *et al.*, 1992; Schumm, 1993; Wescott, 1993) have stressed the importance of contrasting gradients between fluvial and shelf profiles in the fluvial response following inner shelf emergence. When the river extends over an exposed shelf that is steeper, incision is expected (when adaptation of river characteristics is insufficient to compensate), while a lower shelf gradient produces aggradation. However, only in the absence of sediment supply, the path of coastal retreat will be defined simply by the intersection of sea level and the shelf profile. Through paralic sedimentation, river mouths actively influence the location of the coastline, and thus the location to which rivers grade (Fig. 2.5). The influence of gradient contrast on fluvial response is therefore indirect, depending on the amount and distribution of sediment supply (Nummedal *et al.*, 1993). In the configuration of the model, these circumstances postpone incision into the coastal prism by some 20 kyr (Fig. 2.5). Around that time, sea level is falling too fast for sediment supply to keep up. Relatively minor incisions can occur and paralic successions become thinner. Large-scale rejuvenation (i.e., crossing the incision-threshold) of the drainage network begins when sea level falls below the shelf edge (Fig. 2.6), resulting in steepening of cross-shelf valley gradients (Blum & Price, 1998).

The progress of knickpoint migration after the shelf edge has emerged above sea level is shown in Fig. 2.7 for the two model examples. Note that the knickpoint migration

accelerates in the second example when it passes the domain of the river that has incised the former highstand delta and which has been just under incision-threshold conditions since. In the first example, erosion initially propagates rapidly up the southern channel belt. Incision initiates fluvial-valley wall steepening and erosion. This increases the river's sediment load, which decreases the downstream disequilibrium. In the southern belt this feedback mechanism brought advancement of the knickpoint to a halt. As sea level continues to fall, a new knickpoint subsequently appears further downstream. This is repeated several times, resulting in pulses of incision activity and a train of knickpoints. A similar fluvial response to base-level lowering of alternating degradational and aggradational stages has been described for the lower regions of a drainage basin by Schumm and Parker (1973), and is likely to be modified by climate-forced sediment supply (Blum & Törnqvist, 2000). Remarkably, despite the southern channel belt's early rapid migration, it is the more steadily incising northern channel that is able to achieve drainage connection. Likewise, Koss *et al.* (1994) remark that they were unable to predict which of the incised valleys in their flume experiments would eventually link up with the drainage basin outlet. The rate of knickpoint migration averages about 10–20 myr⁻¹ with peaks of up to ~100 myr⁻¹. This is in accordance with observed values of knickpoint migration rates in unconsolidated sediments that are inferred to be representative of Quaternary shelves (Van Heijst & Postma, 2001, their Fig. 18).

During sea-level rise, coastal and fluvial onlap takes place (Fig. 2.5, bottom). Transgressive lobes fill the valley and as sea-level rise decelerates a new coastal prism is built (cf. Talling, 1998). In the real world, this may involve a complex history of valley filling with terrace formation and shifting avulsion style, depending on climate-controlled river supply signals (Blum & Price, 1998; Blum &

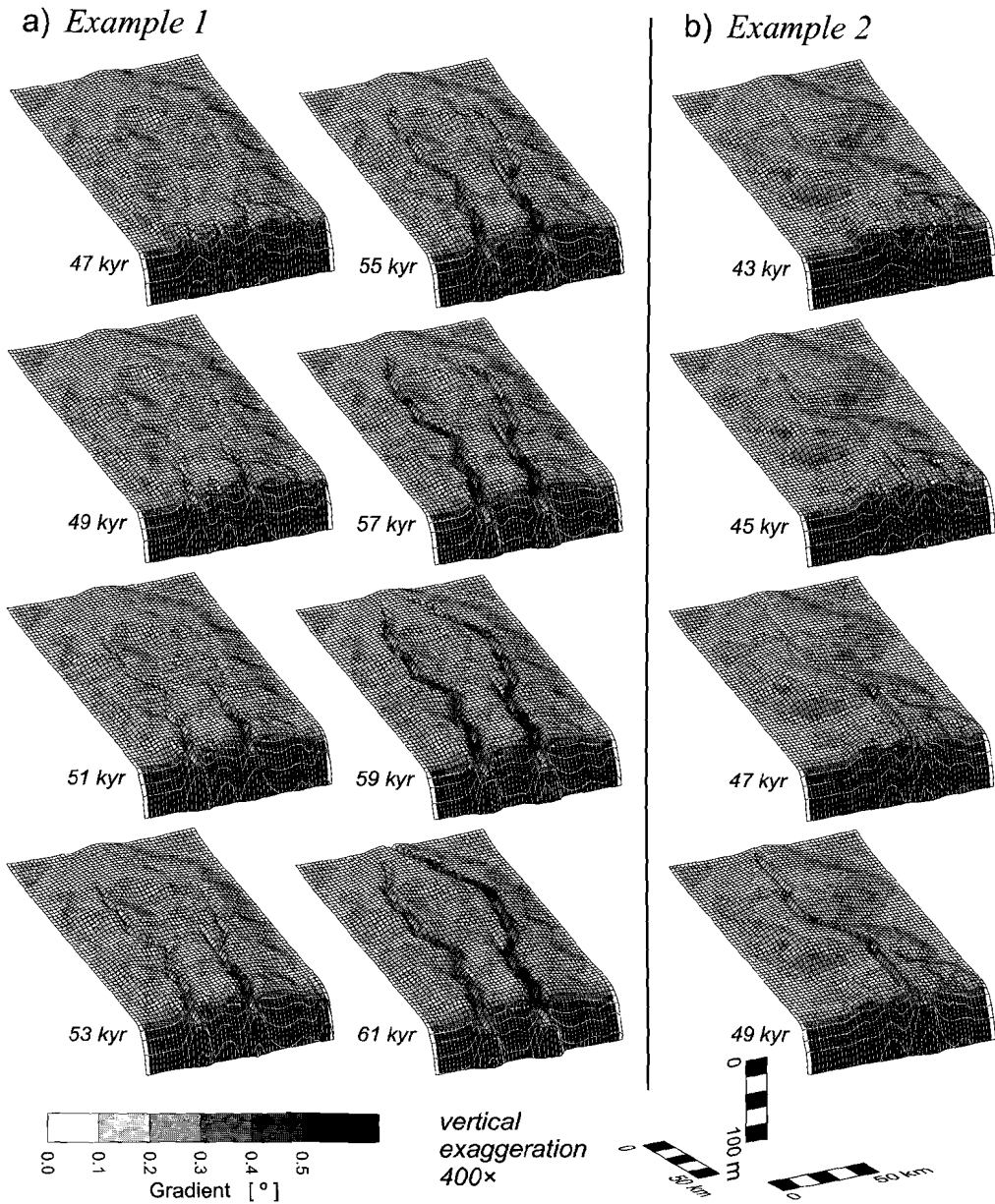


Fig. 2.6 — The development of the topography from first incision at the shelf edge until drainage connection. a) Example 1. b) Example 2.

Törnqvist, 2000) and the amount of sediment supply (Aslan & Blum, 1999).

Since in the lowermost reaches of major rivers, the amount of added rainwater is small in relation to the accumulated hinterland water

discharge, no precipitation was applied in the model scenario. As a result, the ‘equilibrium’ river profiles on the shelf are straight. However, during transgression, two sites of downstream decreasing gradient are discernible

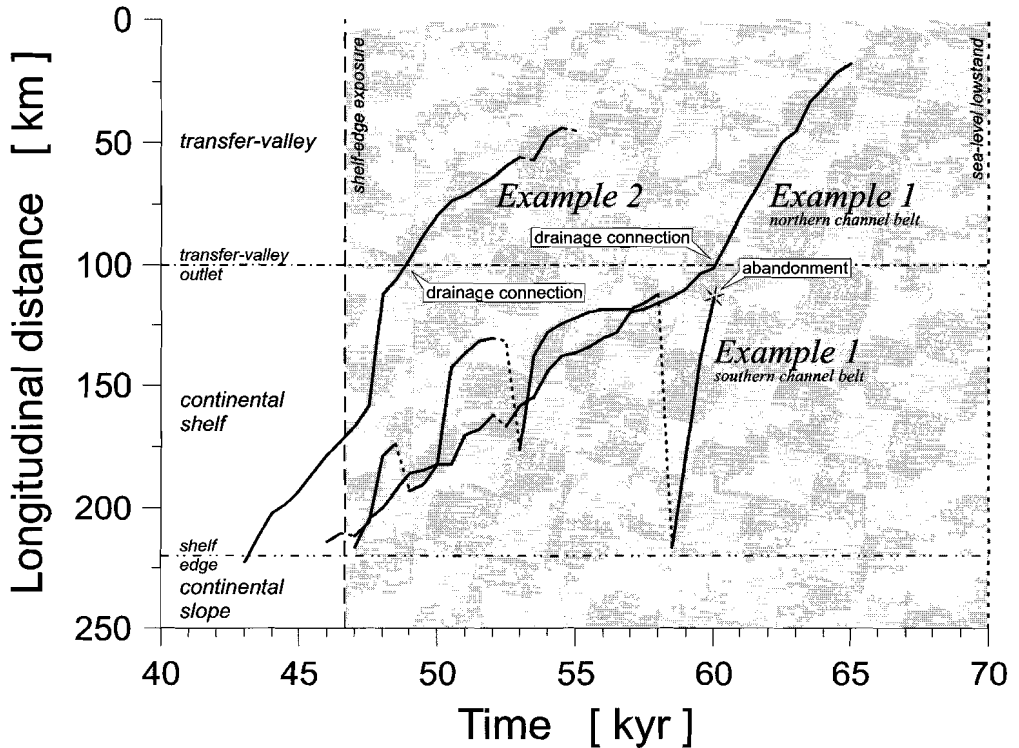


Fig. 2.7 — The progress of headward fluvial erosion when sea level falls below the shelf edge. The positions of the upstream limit of fluvial erosion (most inland knickpoint) of example 1 (northern and southern channel belts) and example 2 are plotted against time. The diagram illustrates incision that is progressing landward from the shelf edge, resulting in a diachronous onset of erosion of shelf strata.

in the model river profile (Fig. 2.5, bottom). The distinct, most inland one corresponds with the upstream limit of fluvial onlap, i.e., the boundary between bypass and aggradation (cf. Talling & Sowter, 1998). The more gradual basinward site of fluvial gradient change is associated with the most upstream location of branching. Throughout the cycle of coastal regression and transgression, the most basinward point to which the rivers grade has been the river mouth. There is no indication of the presence of “an inland location where fluvial processes cease to be dominant”, as defined by the term ‘bayline’ (Posamentier & Vail, 1988; Posamentier *et al.*, 1992; cf. Miall, 1991).

Statistical approach to modelling drainage evolution

The two examples shown are from a set of 1000 model runs. Each model realization in this collection has been created with the same scenario of controlling variables (i.e., sea-level change, hydrology and subsidence). The only distinction is the white-noise on the otherwise equal initial topography. The two examples that were highlighted have not been selected arbitrarily. They are used in order to demonstrate that a seemingly trifling difference in model input can steer the system on dissimilar paths, and lead to an entirely different outcome owing to non-linear behaviour. In this case, the time of drainage connection is dispersed over a broad range. Below this subject will be discussed quantitatively in more detail.

Firstly, a quantity termed ‘discharge density’ is defined as the number of grid cells where the amount of discharge is non-zero divided by the number of grid cells above sea level (Eq. 2.11a). Similarly, ‘river density’ can be defined as the number of grid cells where the amount of discharge is above threshold, divided by the number of grid cells above sea level (Eq. 2.11b).

$$\text{discharge density} = \frac{\sum_{\text{grid cells}} H(Q | Q \neq 0)}{\sum_{\text{grid cells}} H(-\text{bathymetry})} \quad (2.11a)$$

$$\text{river density} = \frac{\sum_{\text{grid cells}} H(Q - Q_{thr})}{\sum_{\text{grid cells}} H(-\text{bathymetry})} \quad (2.11b)$$

where $H(x)$ is the Heaviside-function.

In Fig. 2.8 the discharge and river densities are plotted against time for the two model examples. Initially, the density is relatively high, reflecting a network of many channel belts on the highstand delta. As the number of distributaries decreases and their courses stabilize, the curves of both examples fall drastically. In contrast to the first example (Fig. 2.8a), the river density drop (at ~15 kyr) is larger in the second example (Fig. 2.8b) because only one channel belt becomes dominant (see Fig. 2.4c). The abandonment of one of the two branches upon drainage connection at 60.5 kyr is reflected clearly in the graph of the first example by an abrupt plunge of the river density (Fig. 2.8a). A similar drop in river density is visible in the graph of the second example at 45.5 kyr (Fig. 2.8b), but this must be attributed to the headward migrating knickpoint passing the mid-shelf branching point (Fig. 2.4i). The fact that a connected drainage network has not yet been established at this point is demonstrated by the short-lived avulsion (the discharge-density peak at 48.5 kyr) that occurs upstream of the knickpoint. At 49 kyr this upstream limit of erosion finally reaches the transfer-valley, so that drainage connection occurs (Fig. 2.8b). In

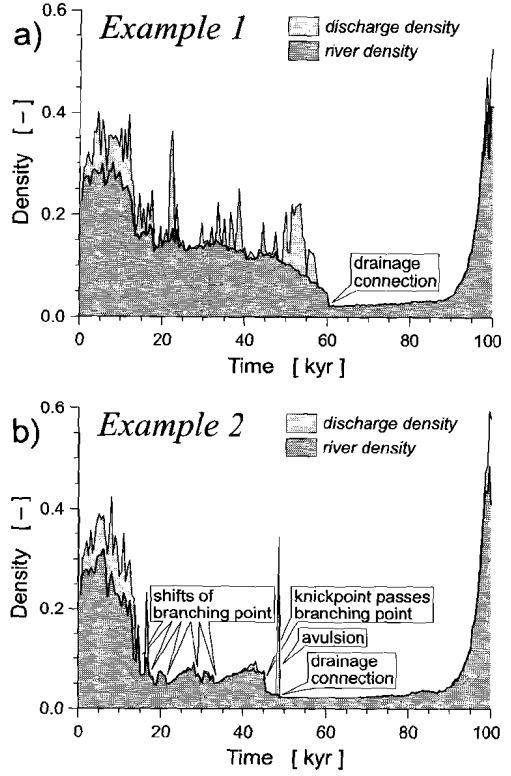


Fig. 2.8 — The development of the discharge and river density (Eq. 2.11) through time. a) Example 1. b) Example 2.

both examples, the confinement of the fluvial system in the depression of an incised valley hardly allows any change in density until sea-level rise decelerates sufficiently for the coastal-plain to build up above the valley walls.

Next, a quantity ‘river weight’ is defined as the sum of the amount of discharge in grid cells where the discharge is above threshold divided by the amount of discharge in the transfer-valley, divided by number of grid cells where the discharge is above threshold (Eq. 2.12).

$$\text{river weight} = \frac{\sum_{\text{grid cells}} \left[\frac{Q}{Q_{t-v}} \cdot H(Q - Q_{thr}) \right]}{\sum_{\text{grid cells}} H(-\text{bathymetry})} \quad (2.12)$$

where Q_{t-v} [m^3yr^{-1}] is the discharge at the outlet

of the transfer-valley. For example, when a river bifurcates due to avulsion (and the discharges of the branches remain above threshold), the numerator of the river weight fraction will decrease or remain unaltered, whereas the denominator will increase in any case. Therefore, branching will decrease the value of river weight, whereas capture will increase it. Thus, river density and river weight are inversely related. The closer the river weight is to unity, the more the drainage network resembles a single chain of grid cells from the transfer-valley to the coastline.

The river weight of the two model examples is plotted against time in Fig. 2.9. The progress prior to shelf-edge exposure is steady in the first example (Fig. 2.9a). The creation of new channel belts and the disappearance of others are reasonably

balanced. The plot of the second example exhibits a more dynamic development (Fig. 2.9b). The succession of peaks and troughs occurring between ~15 and ~45 kyr is related to the basinward shifts of the point of branching in the main channel as described earlier. In the first example, headward fluvial erosion beginning from ~47 kyr and the subsequent capture of smaller branches makes the river weight climb steadily, until drainage connection at 60.5 kyr brings on an abrupt jump. The fact that the river weight in either example does not reach a value of one can be attributed to the small-scale branching on the shelf-edge delta. The limited opportunity for branching during sea-level rise is expressed by a gradually decreasing river weight. In both examples, decline increases when the new highstand delta is formed (~90 kyr; Fig. 2.9).

There appears to be a good correlation in all 1000 model runs between attaining a river-weight value of 0.8 and the instant of drainage connection. Therefore, this value is used to define the time of drainage connection quantitatively. The connection times of all of the 1000 model realizations are shown in Fig. 2.10. The only difference between the model realizations is the white-noise on the initial topography. Nevertheless, the range of outcomes, spanning 30 kyr from just before shelf-edge exposure to shortly after the lowstand maximum, is considerable. This illustrates the system's sensitivity to initial conditions.

In the model, drainage evolution shows two separate end-member modes. In the first mode, practically no entrenchment takes place prior to the time of emergence of the shelf edge. Drainage connection is achieved primarily by subsequent incision and associated knickpoints that migrate upstream (landward-shifting fixation of drainage network). In the second mode, drainage connection is initiated by incision of the convex topography of the highstand delta and regressive wedge during coastline regression (basinward-shifting fixation of drainage network). The following

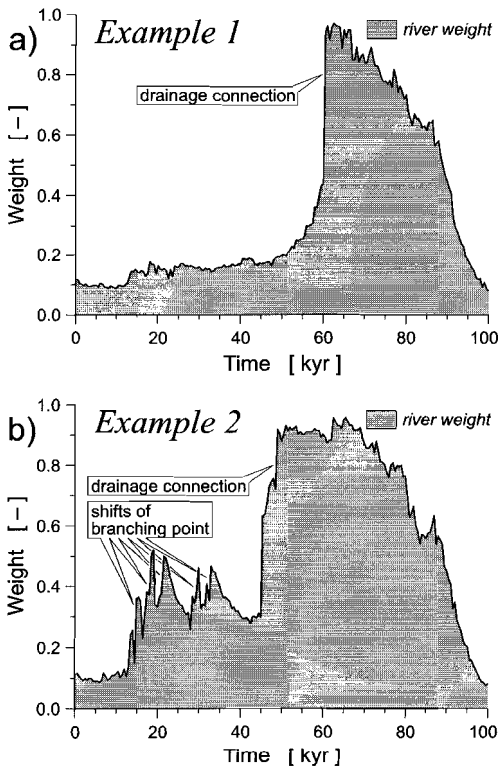


Fig. 2.9 — The development of the river weight (Eq. 2.12) through time. **a)** Example 1. **b)** Example 2.

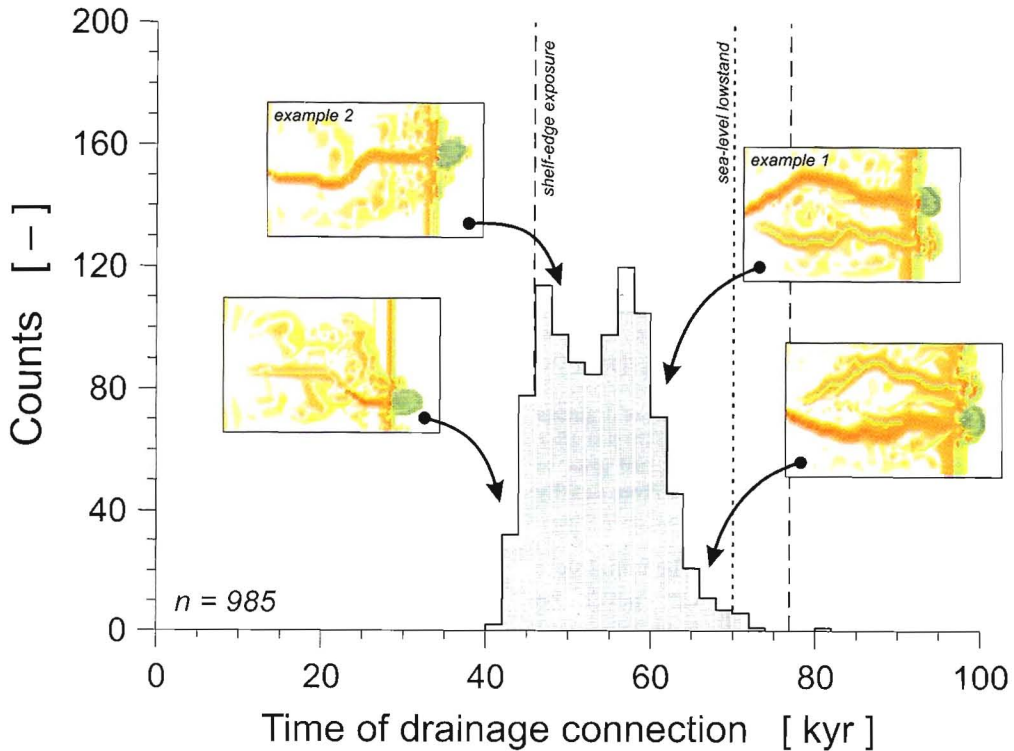


Fig. 2.10 — Histogram of the times of drainage connection of the 1000 model realizations. Fifteen model realizations did not achieve drainage connection. The bimodal distribution reflects the presence of two end-member modes of drainage evolution in the model. Note that this histogram can be interpreted as a probability function. Maps of erosion/deposition rate (see Fig. 2.3 for scale) just after drainage connection of examples 1 and 2, as well as two additional examples, are added to illustrate the relation between landscape development and the timing of drainage connection.

knickpoint migration that starts at the shelf edge is then very rapid as quite some preparatory work has already been done. Since the drainage network has a “headstart” at the time of shelf-edge exposure, the drainage connection time generally occurs earlier than under the conditions of the first mode. The bimodal distribution displayed in the histogram of drainage connection moment (Fig. 2.10) is in fact an amalgamation of the distributions of the two modes. The earlier peak (at 46–48 kyr) represents the second mode and the later peak (at 56–58 kyr) the first.

Out of the 1000 model runs, 15 did not achieve drainage connection. The erosive capability of multiple coexisting channels in these runs was low, incision was sluggish and

the driving force weakened during decelerating sea-level fall. Hence, the domain of erosion was not able to move upstream up to the transfer-valley before fluvial onlap instigated by sea-level rise caught up. More generally, there is a correlation between river density (related to the number of channel belts) and connection time (Fig. 2.11).

Deterministic, non-linear systems can exhibit sensitive dependence on initial conditions. Small discrepancies in initial conditions can produce large differences in outcome. Here, topography has been chosen as the initial condition to illustrate the sensitivity of a sedimentary system, although vegetation, lithology, permeability and probably many

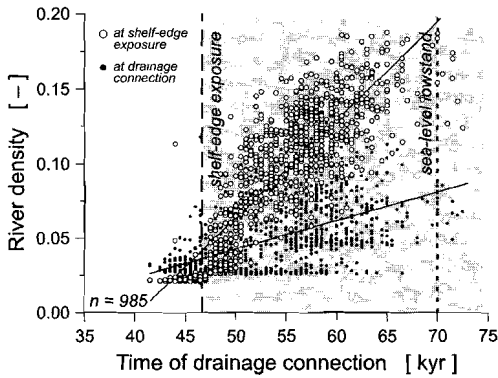


Fig. 2.11 — The relation between the time of drainage connection and the river density (Eq. 2.11b) just after shelf-edge exposure (open circles) and just prior to achievement of drainage connection river density (closed circles).

others can have similar effects. The initial state of a sedimentary system can never be determined entirely. This has to be taken into consideration before concluding that two dissimilar morphologies or stratigraphies have evolved under different circumstances with different forcing factors. These restrictions have been overcome by describing the evolution of a model system in statistical terms. Analysis of the sensitivity of the system to initial and boundary conditions gives a sense of the likeliness, improbability or impossibility of model paths and outcomes (Heller *et al.*, 1993; Burgess & Allen, 1996). Thus, a solution space recording the statistical relation between cause (e.g., sea-level or climate change) and effect (e.g., geomorphology or stratigraphy) can be assessed.

Conclusions

The model presented here, although straightforward, unites many aspects of the geomorphologic development included in the sequence stratigraphic concept for passive continental margins under glacio-eustatic conditions. The model represents important developments in basin margin evolution, such as: 1) the transition of normal regression to forced regression; 2) the basinward decrease in thickness of forced regressive deposits related to an increasing rate of sea-level fall; 3) river avulsion and delta-lobe switching; 4) river incision accompanied by knickpoint migration and the diachronous formation of a subaerial erosional unconformity after shelf emergence; 5) progradation of shelf-edge deltas during lowstand; 6) the infill of incised valleys during transgression; and 7) the construction of a highstand coastal prism. The terrestrial environment plays an important role in the development of the entire system. A particularly significant event is drainage connection, the timing of which is mainly prompted by the rate of knickpoint migration under influence of falling base level. By varying the pattern of white-noise on the initial topography, the specific realization of the system evolution has been shown to be dependent on the initial conditions. However, statistical analysis of model results, supported by statistical field data, provides generic knowledge on how a glacio-eustatic controlled sedimentary system works. This general framework can then be applied to specific field situations by taking local factors into account.

Grain-size sorting of river–shelf–slope sediments during glacial–interglacial cycles:

modelling grain size distribution and interconnectedness

Abstract

Changing conditions during glacial and interglacial of the Quaternary have had a great influence on the location and amount of sedimentation, and also the grain size of deposits has been significantly affected. In this modelling study, the volume and grain-size distribution in passive continental margin strata is investigated. A principal aspect of the basin-scale grain-size sorting process is the formation of a subaerial erosional unconformity. During forced regression, deltaic coarsening-up sequences were deposited on the shelf. The relatively coarse-grained topsets of these successions have a lower preservation potential than the finer prodelta deposits. Therefore, erosion on the exposed shelf results in enrichment of river-transported sediments with coarse material during sea-level lowstand. Thus, shelfal strata are depleted of coarse material, increasing the coarse content of deposits on the upper continental slope. In contrast, in the absence of an erosional unconformity, the composition of sediments on the shelf is relatively coarse. The extent to which sediment within a stratigraphic column has been separated into coarse strata, as opposed to mixed compositions, is expressed as a 'differentiation ratio'. Interconnectedness of coarse-grained sediment bodies in the stratigraphy of the continental shelf and slope is closely related to the palaeogeographic evolution, and is consequently a highly variable property.

Introduction

In the stratigraphy of clastic sedimentary rocks, grain size is without a doubt the most prominent characteristic. However, in stratigraphic modelling it has proved to be a very elusive one.

Sediment grain size is an important aspect in facies classification. Sediments reflect the conditions of their origin and, consequently, sedimentary facies are often accorded an environmental significance. A facies model associates lithology and sedimentary structures, amongst others, with transporting agents and consequent depositional and erosional processes. However, since an unknown portion of the supplied sediment is passed on, it is unclear how the grain-size distribution of the deposited material relates to the composition of the original sediment. Dispersal not only depends

on process intensity but also on sediment calibre and availability. Furthermore, facies models are mostly qualitative in nature and controlling conditions are poorly constrained. The process activity that leads to sediment sorting is therefore rather intangible for a stratigraphic basin modeller.

In spite of the complexity of the problem, various models have been developed that incorporate dynamic grain transport in one way or another (hydraulic approach, e.g. Bitzer & Harbaugh, 1987; Tetzlaff & Harbaugh, 1989; Syvitski & Hutton, 2001; and rule-based approach, e.g. Angevine *et al.*, 1990; Rivenæs, 1992; Granjeon & Joseph, 1999). Much is to be gained by understanding the development of the petrologic characteristics of sedimentary units. For instance, the location and the architecture of coarse-grained bodies are important constituents in determining the reservoir potential for hydrocarbons and

aquifers. Furthermore, such modelling studies will advance the extension of the sequence stratigraphic concept with sediment calibre.

Here, a three-dimensional numerical model is used to examine the grain-size distribution of sediments on a passive continental margin under Quaternary glacio-eustatic conditions. The occurrence of coarse-grained units on continental shelf and slope and their interconnectedness are investigated for several scenarios of boundary conditions.

Method

The following is a brief description of the conceptual model. For a more comprehensive explanation of the model scheme, see Chapter 2.

The model used in this study is a cellular representation of a landscape and subsurface in which the relation between adjacent grid cells are laid down in a number of rules of sediment transport, distribution and grain-size sorting. The set of rules constitutes a three-dimensional process-response system prompted by boundary conditions (e.g. sea level, subsidence), which is capable of complex behaviour (Ch. 2). Elevation changes in grid cells are evaluated in order of their altitude, starting with the highest. The elevation change due to sediment transport is derived by balancing deposition (or erosion) and sediment out-flux on the basis of the 'resulting' gradient (Fig. 3.1a). The amount of sediment (if available) that is deposited is such that a gradient will arise that is exactly competent to transport any remaining (i.e., bypassing) sediment downslope. Similarly, erosion produces a gradient that is exactly capable of transporting the amount of in-fluxed plus denudated sediment downslope. Sediment out-flux to all (up to eight) downward grid cells is determined concurrently. However, these gradients may subsequently be altered in response to elevation changes that can occur in

downslope grid cells. They may be further modified by tectonic movements (and other processes not included in the model used here, such as sediment compaction and isostasy). Short-range, diffusive transport is related to gradient, whereas long-range, stream transport is governed by the degree of undercapacity or overcapacity of the river related to water discharge as well as slope. Transport parameters depend on the depositional environment related to bathymetry (named 'terrestrial', 'coastal', 'marine' and 'deep marine'; see Table 3.1). River sediment and water discharge enter the model landscape at an inlet grid cell, mimicking the outflow of a drainage basin (Fig. 3.2a). Rainwater is distributed evenly over the entire landscape. To minimize edge effects, the grid boundaries perpendicular to the basin axis are joined.

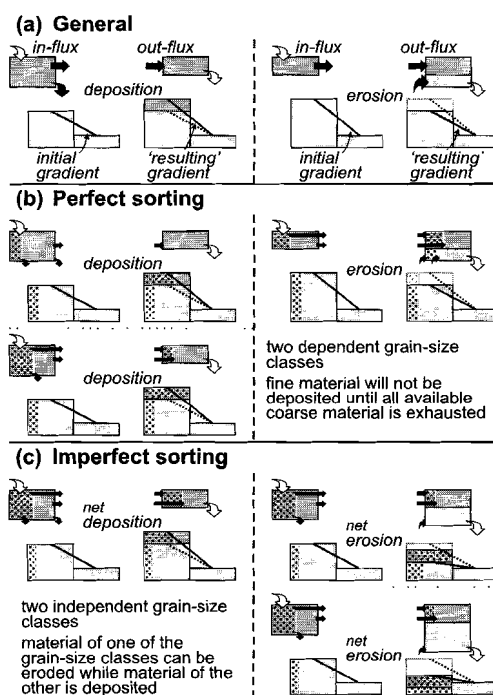


Fig. 3.1 — A schematic portrayal of a portion of the model grid explaining the fundamentals of the model. a) General sediment transport algorithms. b) The perfect sorting sediment transport algorithm. c) The imperfect sorting sediment transport algorithm.

Table 3.1: Values of parameters applied in the model runs. See Chapter 2 for an explanation of the parameters and the accompanying equations.

Parameter	Symbol	Environment	Value			Unit	
			General	Perfect sorting	Imperfect sorting Fine fraction Coarse fraction		
diffusive transport power	U		1.0			–	
diffusive transport coefficient	K_D	terrestrial		0.30	0.24	0.06	km ³ kyr ⁻¹
		coastal		0.40	0.32	0.08	km ³ kyr ⁻¹
		marine		0.40	0.32	0.08	km ³ kyr ⁻¹
		deep marine		0.32	0.26	0.06	km ³ kyr ⁻¹
threshold slope	S_{thr}^*	terrestrial		0.0005	0.0005	0.0005	–
		coastal		0.0040	0.0030	0.0050	–
		marine		0.0200	0.0200	0.0250	–
		deep marine		0.0200	0.0200	0.0250	–
transition depth w.r.t. sea level		terrestrial – coastal	0				m
		coastal – marine	25				m
		marine – deep marine	100				m
discharge distribution threshold	k	terrestrial	0.75				–
		non-terrestrial	0.00				–
stream transport power	V		1.0				–
stream transport power	W		1.0				–
discharge threshold	Q_{thr}		2.0×10^8				m ³ yr ⁻¹
stream transport coefficient	K_S			0.40	0.36	0.04	–
stream attenuation constant	L_S	at overcapacity		10	20	5	–
		at undercapacity		50	50	50	–
incision criterion power	ν		1.00				–
incision criterion power	ω		0.25				–
incision threshold	P_{thr}		0.224				(m ³ yr ⁻¹) ^{0.25}
grid cell size			2000				m
time step			10				yr
white-noise range			0.05				m

Modelling grain-size sorting

Whereas the general model treats sediment size as constant, real world processes sort fine and coarse materials, leading to deposits that may be dominantly coarse textured (gravel, sand) or fine (clay). Because the distribution of coarse and fine stratigraphic units is important for predicting storage of water or hydrocarbons, it is interesting to include grain-size sorting in the model.

Most modelling approaches proceed by representing a grain-size distribution by a finite number of classes rather than by a continuous population. Such subdivision enables conservation of mass of each class. The divisions may correspond to classes of the grain-size scale (gravel, granule, sand, silt and clay) or are left unresolved.

There are two prevalent process-based sorting algorithms (Den Bezemer *et al.*, 2000): ‘perfect’ and ‘imperfect’ sorting.

Perfect sorting

Perfect sorting (Angevine *et al.*, 1990; Paola *et al.*, 1992) is the more transparent

method of the two. This sorting algorithm breaks sediment down into a coarse and a fine class, although it can be extended to more than two classes. The relative abundance of the two classes is expressed as the ‘grain-size fraction’ (with zero signifying solely fine material and unity only coarse). The underlying assumption of perfect sorting is that the coarser class takes precedence over the finer one at sedimentation (Fig. 3.1b). When the situation requires sediment entering the grid cell to be deposited, the perfect sorting algorithm will first draw upon the supplied coarse-grained portion. Fine sediment will not be deployed until all available coarse material is exhausted. No such grain-size preference exists when material is eroded.

Imperfect sorting

Imperfect sorting was introduced by Rivenaes (1992) and involves two (or possibly more) independent grain-size classes. The above-mentioned balancing of elevation change and sediment out-flux by means of the gradient is done simultaneously for all

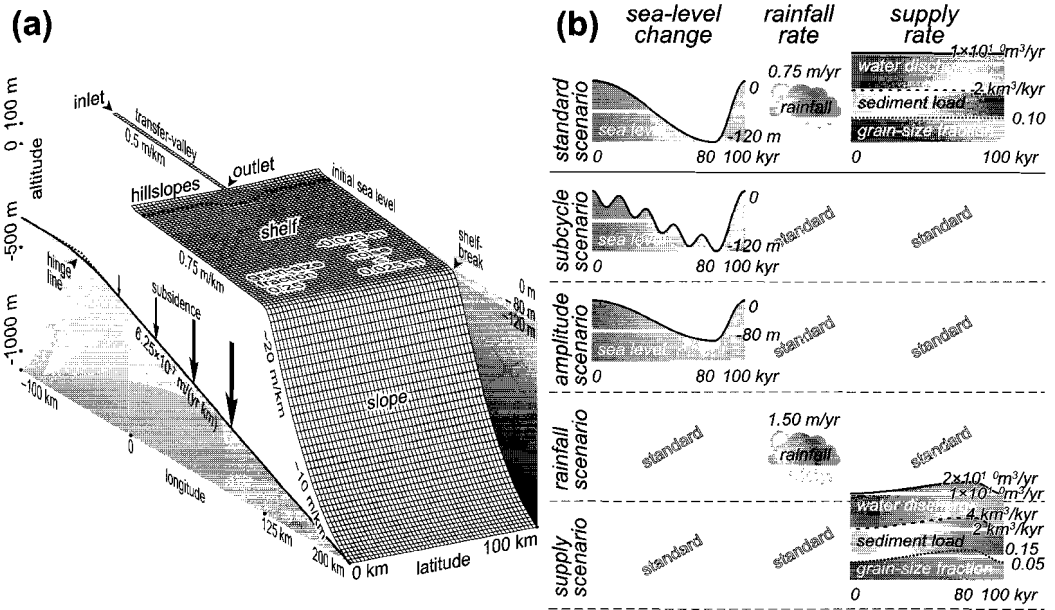


Fig. 3.2 — Overview of the model. a) Model grid set-up. b) Model variables of the various scenarios. Scenarios 2–5 are variants of the standard scenario 1. One glacial–interglacial cycle is depicted. Model runs typically cover five cycles.

grain-size classes. This comprises the only coupling between sediments of the individual classes. As in perfect sorting, net erosion is limited by relief (i.e., the relative altitude of the downslope grid cells). However, because the two classes are independent, sediment of one of the classes can be taken away from strata below the level of downslope grid cells as long as material of the other is deposited concurrently on-site (Fig. 3.1c, bottom right). A depth to which this sediment extraction can occur needs to be defined. This depth is attuned to the thickness of the ‘surface transport layer’ which is thought to represent a cover containing all activity of transport and sorting processes (Rivenæs, 1992; Den Bezemer *et al.*, 2000). For convenience, it is assumed to be constant over the entire area of interest.

Model procedure

For this chapter, the standard model setting is a passive continental margin with a major river and a wide shelf (a ‘river–shelf system’). The applied forcing variables, such

as high-amplitude eustatic sea-level change and sediment supply signals, are characteristic of late Quaternary glacial–interglacial cycles, each spanning 100 kyr. Every model run completes five of such cycles. Various scenarios of allogenic forcing have been examined (Fig. 3.2b). For the benefit of statistical analysis, each model scenario was run 50 times, each time with different a white-noise pattern superimposed on the initial topographic surface. This enables results of different scenarios to be compared (Ch. 2).

Values of model parameters are listed in Table 3.1. In the interest of data reduction, new strata are compiled by joining a number of layers (each spanning one model time step) in a column and taking the weighted average of their properties. These compiled strata are used for calculations on stratigraphy and are depicted in the stratigraphic sections. For the benefit of explanation, the terms inner and outer shelf are used as geographical designations related to the interglacial (highstand) situation, rather than

physiographical definitions. Furthermore, in this chapter, depositional environments correspond to bathymetric zones (Table 3.1).

The objective of this study is not to replicate any specific geological history. Instead, the experiments explore model solution space and the system’s sensitivity in order to draw general conclusions for a set of geologically realistic conditions.

Results and Discussion

In order to evaluate the effects of different approaches to grain-size sorting, the two sorting algorithms are compared. Next, the results are considered in terms of sediment distribution, grain-size distribution, and stratigraphic architecture for a standard scenario. In addition, the effects of different boundary conditions are examined using various scenarios with sea-level change, increased precipitation, and increased sediment supply during glacial periods.

The choice of sorting algorithm

Figure 3.3 (on the next page) shows examples of grain-size distributions produced by the model with the perfect (top) and imperfect (bottom) sorting algorithms incorporated. By and large, both sorting algorithms generate comparable distribution patterns. However, deposits brought about by imperfect sorting display a more gradual transition between coarse and fine sediments. Perfect sorting gives rise to a more differentiated grain-size stratigraphy.

Perfect sorting is a more elementary representation of sorting processes than imperfect sorting. However, the resulting large-scale stratigraphy does measure up to that of imperfect sorting (Fig. 3.3c). In addition, the perfect sorting algorithm is considerably less time-consuming. Since the requirements of the model are to be able to recognize diagnostic first-order trends, perfect sorting was considered to be adequate for our present purposes and has been used for the model experiments in the remainder of this chapter.

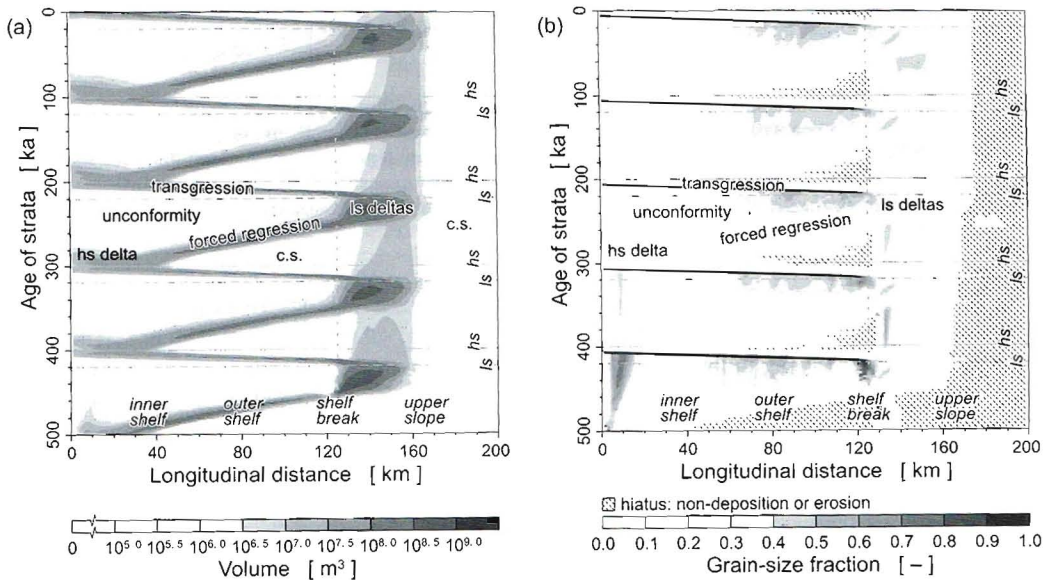


Fig. 3.4 — Chronostratigraphy displaying sediment properties of strata of a given age, at a given longitudinal distance. Average of 50 similar model runs with the standard scenario. a) Total volume of sediment. b) Mean grain-size fraction (relative abundance of the coarse grain-size class) of the sediment. *hs* = highstand, *ls* = lowstand, *c.s.* = condensed section.

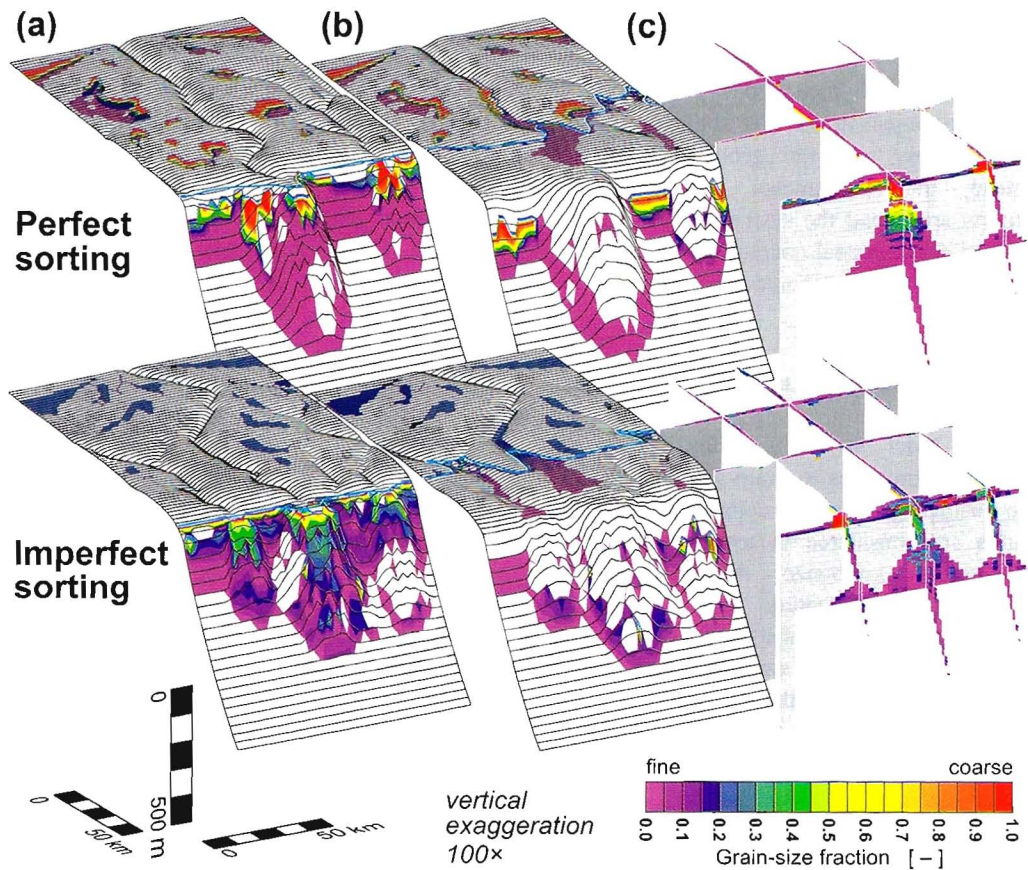


Fig. 3.3 — Illustration of the performance of the perfect sorting algorithm (top) and imperfect sorting algorithm (bottom). The model is run with the standard scenario. Strata represent intervals of 200 yr. a) Topography with grain-size fraction (relative abundance of the coarse grain-size class) of deposits at sea-level lowstand (80 kyr). The blue line is the coastline. b) Topography with grain-size fraction of deposits at the sea-level rise inflection-point (90 kyr). c) Lithostratigraphy after one 100-kyr cycle with the sediment grain-size fraction.

Sediment distribution

The standard model scenario was applied to the passive margin system in order to examine patterns emerging in the stratigraphy. The diagrams in Fig. 3.4 outline the chronostratigraphy created after five glacial–interglacial cycles. The total sediment volume in the system between consecutive 1-kyr spaced isochrons (i.e., strata between particular age limits) is summarized in Fig. 3.5a. A volume of sediment of 2 km^3 enters the system every 1 kyr. Wherever in the stratigraphy there is less than this amount preserved, net erosion has occurred. Any

volume exceeding this value represents remobilized material from earlier strata or from the initial substratum. It is evident that deposits from roughly the first half of the cycle have a lower preservation potential than those from the second half (Fig. 3.5a).

A detailed description of the river-shelf system development during a Quaternary glacio-eustatic cycle emphasizing the landscape and drainage evolution is presented in Chapter 2. Here, I concentrate on stratigraphic characteristics, and sketch the stages of deposition only briefly, starting at

sea-level highstand. In Fig. 3.5b, highstand-delta aggradational and progradational units reveal themselves in the considerable volume of terrestrial sediments from the earliest phase (~20 kyr) of every new cycle. Gradually, normal regression turned into forced regression (Posamentier *et al.*, 1992). Terrestrial deposits from this time dwindle because aggradation diminished under the influence of falling base-level and sediment was removed during subsequent subaerial erosion. Instability along the shelf edge induced by basin subsidence and sea-level fall resulted in marine re-deposition (Posamentier & Allen, 1993). Later, about halfway through the cycle, sediments were no longer laid down on the gentle shelf that supports a wide prodelta. On the relatively steep continental slope, there was less room for shallow deposits, and they were more readily eroded. This led to a decline in coastal deposition (Fig. 3.5b). River sediment was subsequently supplied directly to deeper water, bypassing the shelf.

At that time, formation of an unconformity had already begun. The few terrestrial deposits that date back from falling sea-level stage originated primarily from the degradation of topography on the exposed shelf (i.e., delta lobes). Note that the volume of these sediments (Fig. 3.4a) corresponds to a mean thickness of less than 5×10^{-3} m or a mean deposition rate of 5×10^{-6} myr⁻¹. At such low deposition rates, processes like aeolian transport, bioturbation, soil formation and vegetation growth are likely to play an important role locally (Galloway, 1989). Erosion concentrated mainly around incising rivers of the main, hinterland-fed and the

secondary drainage systems. The inner shelf in particular was subject to erosion since it was exposed longer and because the higher gradient

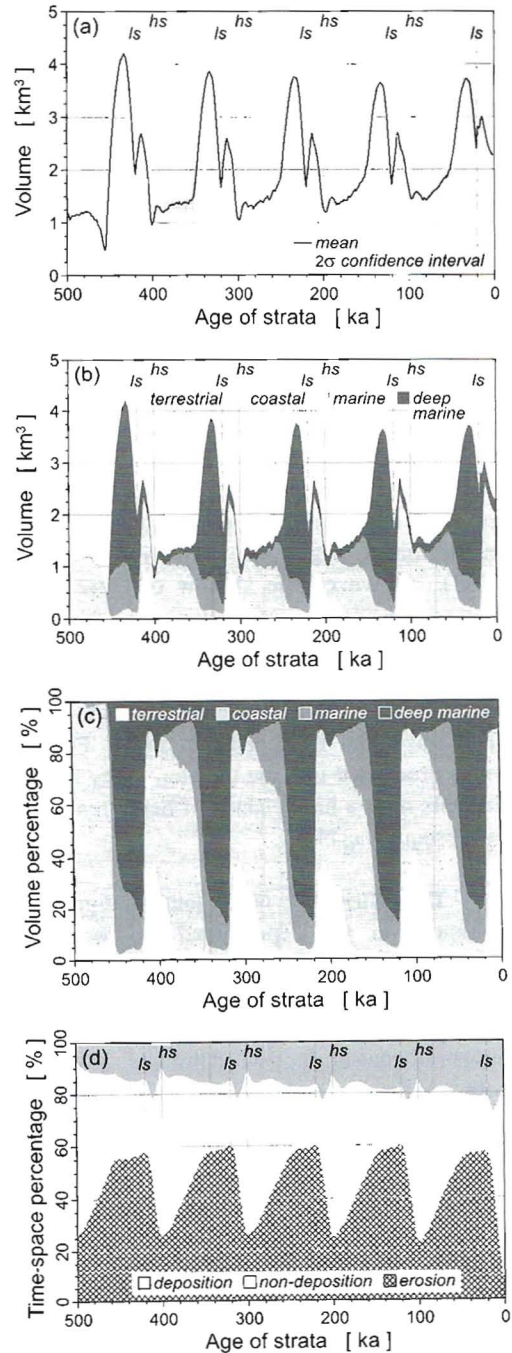


Fig. 3.5 — Sediment properties as a function of stratal age. Average of 50 similar model runs with the standard scenario. Strata represent intervals of 1 kyr. a) Volume of sediment preserved in the stratigraphy. b) Volume of sediment subdivided by depositional environment. c) Volume percentage subdivided by depositional environment. d) Percentage of stratigraphy taken up by deposition or hiatus owing to non-deposition or erosion. *hs* = highstand, *ls* = lowstand.

of the shelf with respect to the transfer-valley promoted incision (e.g. Miall, 1991; Posamentier *et al.*, 1992; Schumm, 1993; Wescott, 1993).

As the incising river system eventually neared equilibrium, supply decreased. Shortly before eustatic lowstand, relative sea-level started to rise owing to subsidence, resulting in transgression and a depocentre shift from deep, upper continental slope waters to the outer shelf. The low preservation potential of (shallow) shelf-edge deposits manifests itself in a depression in stratigraphic volume around lowstand (Fig. 3.5a, b). Back-filling of fluvial valleys accompanied by coastal onlap explains the large amount of terrestrial and coastal sediments dating from the period of sea-level rise. At the same time, the submerged shelf-edge deltas acted as a source for deposits on the upper continental slope. Degradation of the shelf edge continued throughout the cycle in the model (Fig. 3.4a) (Vanney & Stanley, 1983). However, the volume of these deep marine deposits, consisting entirely of remobilized sediment, is relatively low (cf. Fig. 3.5b, c). As sea-level rise decelerated, a coastal prism (Talling, 1998) was built up on the inner shelf and in the drainage basin outlet. Fluvial onlap proceeded into the transfer-valley where deposits have a high chance of being removed in subsequent cycles.

The distribution of the total stratigraphic volume over the depositional environments (Fig. 3.5c) reflects the dichotomy typical of Quaternary passive margins: highstand depositional systems on the inner shelf where terrestrial/coastal deposits dominate, alternate both temporally and laterally with lowstand upper-slope depocentres with mainly marine sediments. If we envisage the stratigraphic record as a three-dimensional Wheeler-diagram (with units 'time-space'), it can be broken down into the categories: preserved deposition, hiatus owing to non-deposition and hiatus owing to erosion (Fig. 3.5d). Preserved strata do not occupy more than a fifth of the

chronostratigraphic record; the decrease with age indicates the role of remobilization of sediment during subsequent cycles. The bulk is taken up by non-deposition, corresponding to the formation of condensed sections in the real world, and hiatuses owing to unconformity formation and degradation of the shelf edge.

Grain-size distribution

The grain-size evolution through the stratigraphy fluctuates around the composition of 10% coarse sediment (i.e., a grain-size fraction of 0.10) that enters the system (cf. Burgess & Hovius, 1998) (Fig. 3.6a). During the first halves of each cycle, deposits are finer than average owing to erosion of coarse topsets of highstand and forced-regressive units. These intervals are followed by periods with strata that are coarser than average owing to the supply of sediment enriched with coarse material to the oceanic basin where preservation potential is higher. The trend is similar to that of volume (cf. Fig. 3.5a) because the stratigraphic properties grain size and preservation potential are correlated. For instance, since deltaic sequences tend to be coarsening up, coarse sediments are more likely to be removed upon erosion. Therefore, differential preservation during large sea-level oscillations in a situation with practically disjointed depositional systems on shelf and slope is the main mechanism for basin-scale grain-size sorting.

In Fig. 3.6b, the grain-size fraction is depicted per depositional environment. Initially, at the start of every glacial cycle the mean grain size of preserved terrestrial sediments is relatively fine. This value is dictated by the few hillslope sediments (Fig. 3.4a, b), because concurrent highstand (and preceding transgressive) coarse material in the transfer-valley was largely flushed out by river incisions during subsequent falling stage and lowstand. In reality, terrace formation could preserve some of the latter deposits (Blum & Price, 1998); that process, however, is below

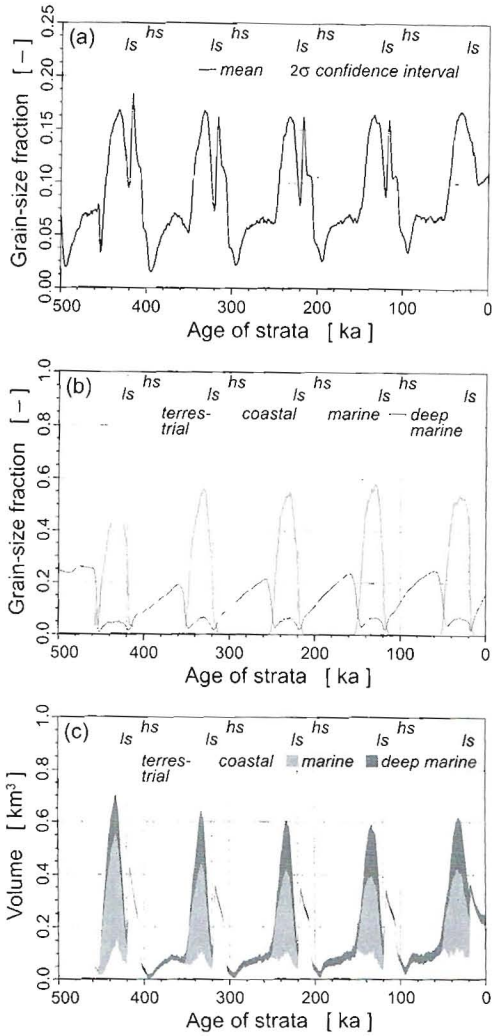


Fig. 3.6— Sediment properties as a function of stratal age. Average of 50 similar model runs with the standard scenario. Strata represent intervals of 1 kyr. a) Grain-size fraction (relative abundance of the coarse grain-size class) of sediment in the stratigraphy. b) Grain-size fraction of sediment of each depositional environment. c) Volume of coarse sediment fraction subdivided by depositional environment (volume (Fig. 3.5b) multiplied by grain-size fraction (Fig. 3.6b)). *hs* = highstand, *ls* = lowstand.

the resolution of the model. Aggradational and progradational paralic successions on the shelf were responsible for high terrestrial grain-size values at times of falling sea level. Coarse deposits found in deep water environments

dating back from the same periods are due to instabilities on the upper continental slope, i.e., the initial substratum and the front of drowned shelf-edge deltas.

From halfway through to the cycle, the river system delivered directly to the shelf edge. Fine river-plume sediment preceded deposits of the advancing coastline. The river load then became enriched with coarse material originating from shelf erosion (Posamentier & Allen, 1993). Most of the coarse fraction in the supplied sediment has been incorporated in coastal and marine deposits; mainly fines went through to deeper water. Although coarse sediment was delivered to the basin edge during lowstand delta-construction, it is striking that in the model, transport of relatively coarse material further into the basin occurred during periods of falling sea-level (Fig. 3.4b).

As relative sea-level began to rise, the proximal parts of the shelf-edge deltas were covered with relatively fine-grained transgressive strata. Transgressive fill of incised river valleys trapped almost all available coarse material from the hinterland (Posamentier & Allen, 1993) (Fig. 3.6c). ‘Estuarine’ deposits are fine, overlaying the coarse fills at the base of the valley. The transition from coarse to fine fluvial deposition was upstream from the delta plain during early highstand, leaving the delta starved of coarse material until late highstand. This would be similar to many Holocene coasts and estuaries that are withheld coarse sediment from a fluvial source.

Figure 3.7a recapitulates the stratigraphy by plotting mean grain-size of the five cycles against distance along the river–shelf system. The high values on the most landward part of the profile reflect highstand-delta topsets, mostly originating from the late sea-level highstand. Directly basinward of this, fine sediments of the highstand prodelta occur, which were rapidly crossed and bypassed after the transition from normal to forced regression. On the shelf, substrate cannibalization has

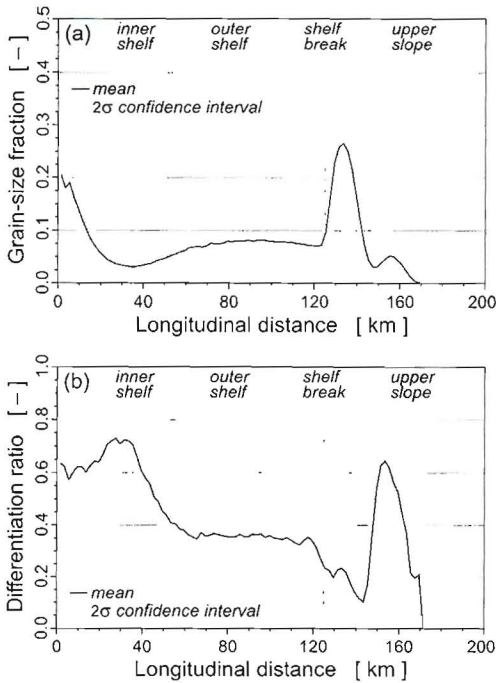


Fig. 3.7 — Sediment properties as a function of longitudinal distance. Average of 50 similar model runs with the standard scenario. **a)** Grain-size fraction (relative abundance of the coarse grain-size class) of sediment in the stratigraphy of five cycles. **b)** Differentiation of coarse material into coarse bodies within the stratigraphy.

resulted in a mean grain-size below the hinterland supply value, increasing basinward (Posamentier & Morris, 2000). Delta sorting-processes have created coarsening up sequences during sea-level fall, and subsequent unconformity formation has removed their top. Shelf-edge deltas are responsible for the coarse composition beyond the shelf-break. There is a second, smaller peak (Fig. 3.7a) where slope-dependent flows, as opposed to more proximal river-plume transported sediments, come to a rest. In reality, these deposits can also be transported to greater depths, for instance by turbidite systems depending on the ratio of coarse to fine material (Posamentier & Allen, 1993). Turbidite current processes, however, are not part of the model.

Although the increase of sediment flux

and sand-to-mud ratio during forced regression has been recognized (Posamentier & Morris, 2000), some researchers (e.g. Galloway, 1989; Burgess & Hovius, 1998; Blum & Törnqvist, 2000) argue that delivery of sediment to the shelf edge at times of sea-level lowstand is not altered significantly relative to hinterland yield in terms of volume and grain size. However, a river can adjust to changing base level in ways other than incision by adapting its channel characteristics (Schumm, 1993; Wescott, 1993; Leeder & Stewart, 1996). Thus, because widespread incision into the exposed shelf does not occur during a large part of sea-level fall (Van Heijst & Postma, 2001; this thesis, Ch. 2), the generated additional supply will be a surge during a limited period of the interglacial–glacial cycle, rather than a sustained, gradual one. Therefore, the consequences of valley formation for the grain-size distribution and stratigraphic architecture can still be substantial.

Stratigraphic architecture

In Chapter 2, it was demonstrated that the landscape evolution of river–shelf systems is sensitive to initial conditions. Seemingly insignificant random noise on the initial morphology leads to a great variation in development. Similarly, the spatial distribution of stratigraphic characteristics can vary considerably under identical forcing conditions owing to non-linear behaviour. For instance, both stratigraphies depicted in Fig. 3.8 have developed under exactly the same standard scenario, but with different distributions of white-noise superimposed on the initial topography. Even though the details of the stratigraphic architecture in the individual model runs deviate, the stratigraphies exhibit comparable coarse-calibre features. The most prominent are the voluminous delta-front deposits located on the upper continental slope. Secondly, the shelf is criss-crossed with elongated bodies at the base of incised valleys deposited during transgression and covered by fine material, which makes them potential

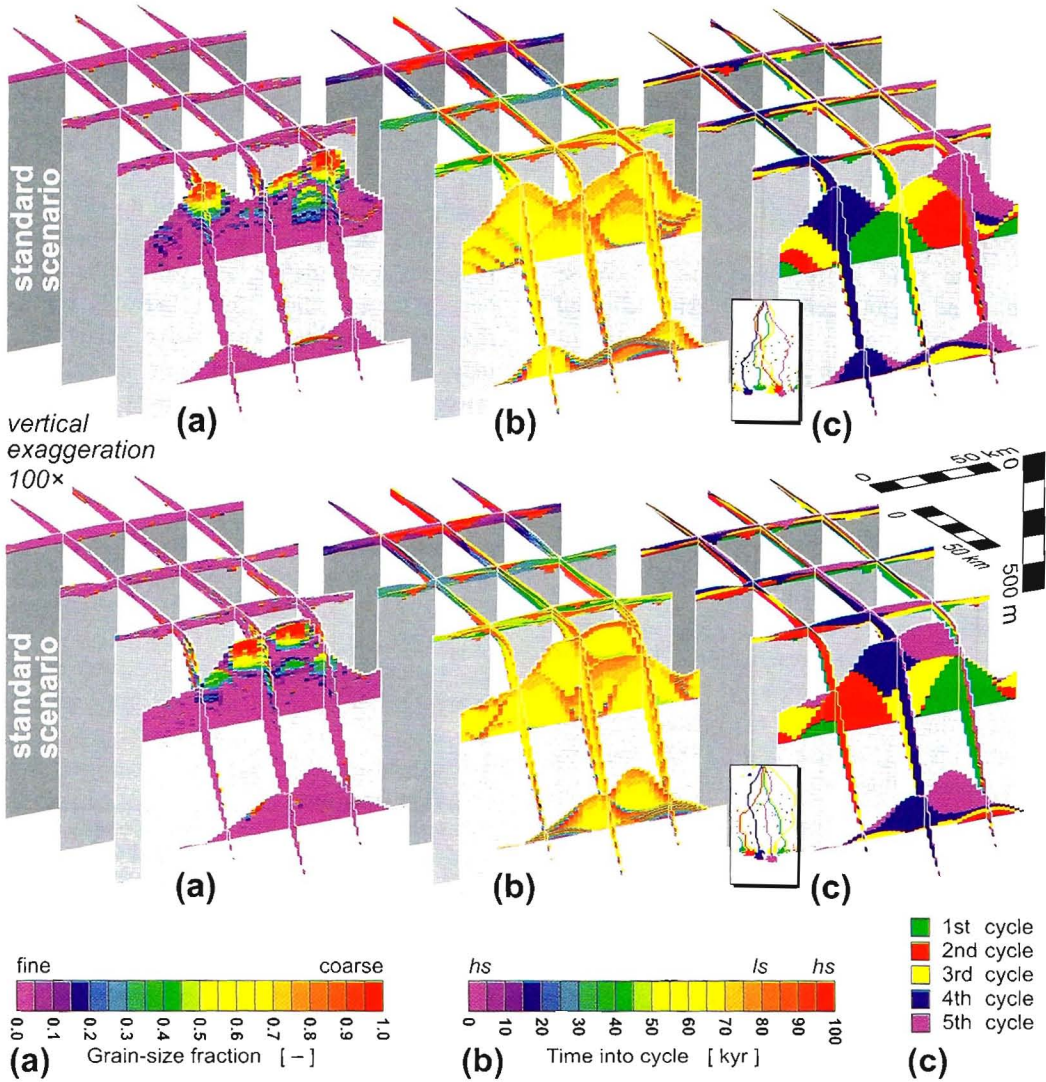


Fig. 3.8 — Lithostratigraphies of two examples of similar model experiments run with the standard scenario. a) Grain-size fraction (relative abundance of the coarse grain-size class) of sediment. b) Time of deposition within a 100-kyr cycle. c) Glacial–interglacial cycle in which deposition occurred. Inset: map view of coarse bodies thicker than 1 m.

hydrocarbon reservoirs (Posamentier & James, 1993). Finally, coarse sediments derived from the degradation of shelf-edge deltas occur, enveloped in fine material, at relatively great depths.

An aggregate of connected sequences in a model stratigraphy with grain-size fraction ≥ 0.95 (i.e., coarse-grained blocks in adjacent

grid columns that share part of a side or an edge) is defined here as a ‘coarse body’. The criterion threshold is set rather high, since the perfect sorting algorithm is predisposed to unmixing, and thus to the formation of coarse bodies. These coarse bodies can be determined in two different ways. The first method is to define them solely based on lithostratigraphy,

whereas the second is more restrictive as it also takes chronostratigraphy into account: coarse sediment successions that are spatially connected but are divided by a hiatus, either erosional or non-depositional, are considered to be separate units. The presence of coarse bodies is an indication of potential resource reservoirs.

The ratio of the thickness of coarse bodies and the total sediment thickness divided by the mean grain size is a measure of separation of the two grain-size classes. This 'differentiation ratio' is plotted in Fig. 3.7b as a function of longitudinal distance. On the inner shelf, for example, roughly 60% of the total amount of coarse grains is part of a coarse body. In contrast, outer shelf successions are less differentiated owing to the relative scarcity of aggradational deposits, both at the time of deposition owing to the rapidly retreating coastline, and after preservation. Prolonged dumping of river sediment on the continental slope during lowstand led to oversteepening of the delta front (Coleman *et al.*, 1983), and thus to a greater influence of mass transport relative to river-plume transport. Consequently, deposits exhibit a greater range of blends of coarse and fine grains (Fig. 3.8), resulting in a low differentiation ratio despite a high mean grain-size value. More distal sediments become more differentiated owing to continuous sorting that took place under less turbulent circumstances when the depocentre was removed from the shelf edge. The variation, however, is great (Fig. 3.7b).

The probability of finding coarse bodies in the stratigraphy of a given volume and average thickness based on 50 model runs is plotted in Fig. 3.9. Figure 3.9a considers aggregates of strictly genetically-related strata. Most of these bodies are small. Exceptions are the bases of major incised-valley fills, large clusters of coarse material on the continental slope, and sheet-like highstand deposits. However, the coarse valley fills and the shelf-edge bodies can connect with each other in various combinations, resulting in a wide

band of possible connected coarse bodies (Fig. 3.9b). The fills of cross-shelf river belts are usually joined at or near the transfer-valley outlet to form large basinward dipping bodies. Although their winding paths often intersect in map-view on the shelf (Fig. 3.8), incisions during successive glacial cycles do not reach the same depth owing to subsidence and sediment accumulation, and valley fills rarely connect there (Talling, 1998). In reality, shelfal deposits, including transgressive valley fills, may be removed partially or entirely, or reworked into coarse-grained sheets, depending on the effectiveness of wave or tidal ravinement during sea-level rise (Zaitlin *et al.*, 1994). On the other hand, the coarse bodies in

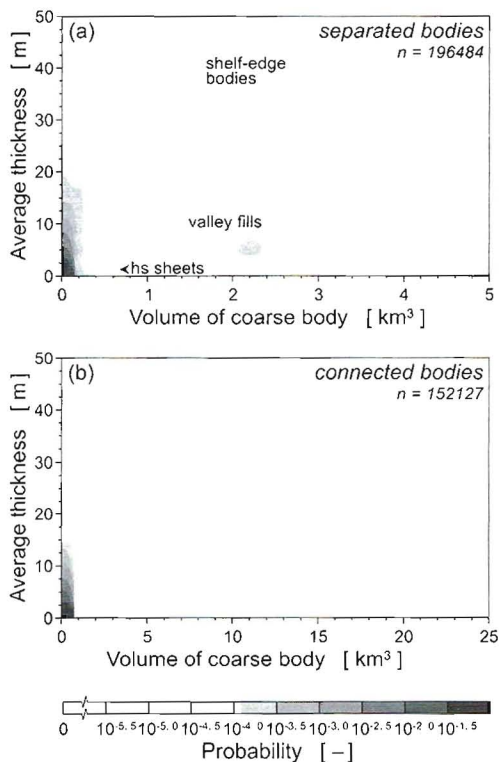


Fig. 3.9 — Probability of the occurrence in the stratigraphy of coarse bodies of a given volume and average thickness. Total of 50 similar model runs with the standard scenario. Strata represent intervals of 1 kyr. a) Coarse bodies that are separated by non-depositional or erosional hiatuses. b) Connected coarse bodies.

the model occur at the base of incised valleys, which has a relatively high preservation potential. Similarly, when subaerial accommodation is reduced, for instance during highstand, fluvial deposits are prone to floodplain reworking (Wright & Marriott, 1993). These effects may significantly alter the interconnectedness on the shelf. The large shelf-edge bodies are blanketed with early transgressive sediment (with a low preservation potential) and, more importantly, they may have been covered by prodelta fines of subsequent cycles (see also Fig. 3.4b). Whether these bodies are connected with each other or to transgressive bodies is highly variable. That makes the interconnectedness of individual passive margin coarse bodies extremely unpredictable, but statistically fair prediction may be possible.

Other scenarios

Scenario with sea-level change including subcycles

The first variant of the standard scenario (Fig. 3.2b) is one with five additional sea-level ‘subcycles’ to each glacial–interglacial cycle. These higher order oscillations are clearly expressed in the record of preserved volume and grain-size fraction (Fig. 3.10a, b). Similarly to the case of a single cycle, sub-lowstand sediments have a greater preservation potential than sub-highstand strata, and transgressive valley fills that are particularly vulnerable during the subsequent sea-level falls. However, sub-lowstand deposits on the shelf, in contrast to the upper continental slope, are in reality likely to be

reworked by waves during transgression, promoting the formation of coarse bodies. Note that, because of this differential

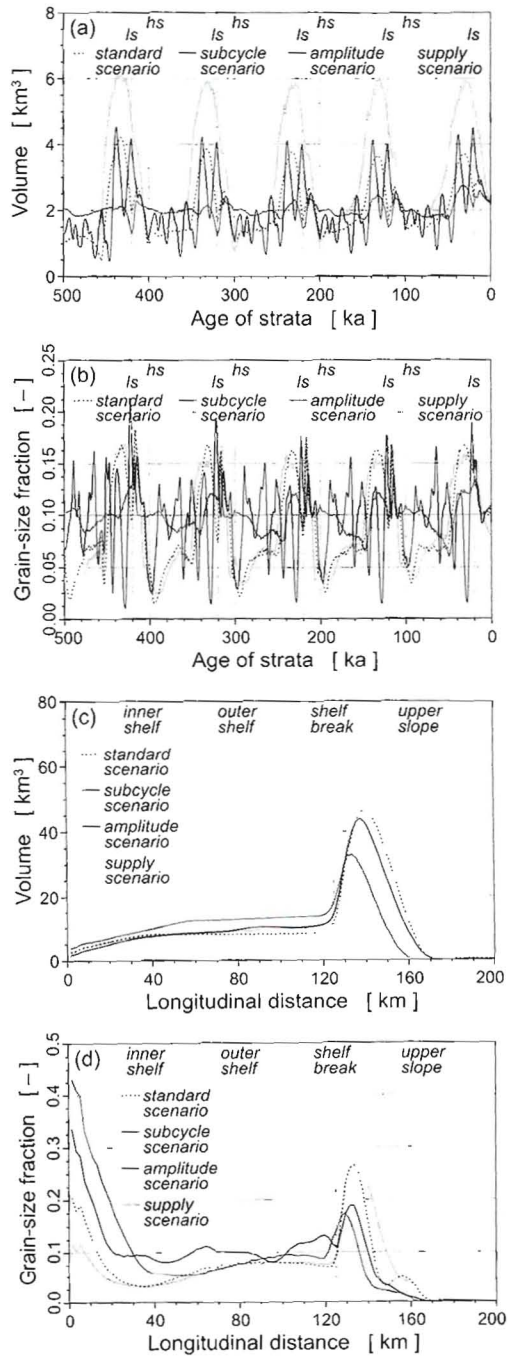


Fig. 3.10 — Sediment properties as a function of stratal age or longitudinal distance for various model scenarios. Average of 50 similar model runs. Strata represent intervals of 1 kyr. a) Volume of sediment preserved in the stratigraphy versus stratal age. b) Grain-size fraction (relative abundance of the coarse grain-size class) versus stratal age. c) Volume versus longitudinal distance. d) Grain-size fraction versus longitudinal distance. *hs* = highstand, *ls* = lowstand.

preservation of deposits from periods within the subcycles, there are more 'subsequences' in the volume record than there are sea-level forced subcycles. In the standard scenario, relative sea-level change was stagnant before lowstand, allowing the river system to achieve a near-equilibrium profile, and resulting in early transgressive strata with low preservation potential on the shelf edge. However, with the subcycles superimposed, major river-incision, that had been temporarily interrupted during the preceding sub-highstand, was still going on at ultimate lowstand under the influence of the much higher rate of sea-level fall. Moreover, knickpoint migration continued upstream during the rapid relative sea-level rise that immediately followed. Consequently, deposition on the continental slope occurred later than in the standard scenario. Since the coastline resided on the shelf for a longer period of time, more sediment as well as more coarse material remains on the shelf (Fig. 3.10c, d). Coarse sheet-like bodies deposited during subcycle transgression and highstand are found there (Fig. 3.11). The succession of relative sea-level rises and falls resulted in different levels of incision on the shelf (cf. Thomas & Anderson, 1994) and in a stepped topography on the exposed shelf (cf. Posamentier & Morris, 2000), although large-scale delta lobe switching leads to very similar configurations (Ch. 2).

Scenario with lower amplitude sea-level change

The second variation on the standard scenario has a lower amplitude of eustatic sea-level change: 40 m instead of 60 m (Fig. 3.2b). Initially, sea level remained above the level of the shelf-break throughout the cycle. Many river belts distributed sediment over the shelf. Avulsions were frequent, but their number decreased as sea-level fall progressed. Regressive delta build-up resulted in numerous thin sheets of coarse-grained bodies (Fig. 3.11). Incisions away from the shelf edge only occurred very locally in convex topographic

features and were never deeper than roughly 2 m. Several hinterland-fed river sources supplied sediment to the shelf edge, approximating a line source. During transgression, there was no fluvial onlap, except near the river mouth. Marine onlap occurred by widespread coastal deposits, rather than in the form of valley fills like in the standard scenario. However, by filling much of the accommodation space on the shelf, the sedimentary system evolved toward a situation where the level of the shelf-break matched the sea-level lowpoint. Major erosion was initially restricted to the rim of the shelf. In the last two to three cycles, incision increasingly took place over the entire shelf and eventually as far back as halfway into the transfer-valley. Excavation limited itself to recent falling stage deposits, playing a relatively small role in the formation of an unconformity. Nevertheless, the pattern of preserved sediment in the stratigraphy becomes more similar to the standard scenario in the latest cycles (Fig. 3.10a). In the present scenario, there is ~30% less hiatus owing to erosion in the final stratigraphy after five glacial cycles than in the standard scenario where sea-level fell well below the shelf-break. Furthermore, as a consequence of the reduced role of erosion, there is less separation of the grain-size classes (Fig. 3.10b). This emphasises the significance of differential preservation as a mechanism for basin-scale grain-size sorting in the development of passive margin stratigraphy.

Scenario with increased precipitation

The third alternative scenario differs from the standard one by having a wetter climate on the continental margin. The exposed shelf has a considerable surface area that also acts as a drainage basin. However, because of the relatively permeable shelf subsurface and low gradients, in the real world groundwater-flow plays an important role in the water cycle, as well as vegetation. Therefore, the model precipitation value must be considered the effective amount of surface

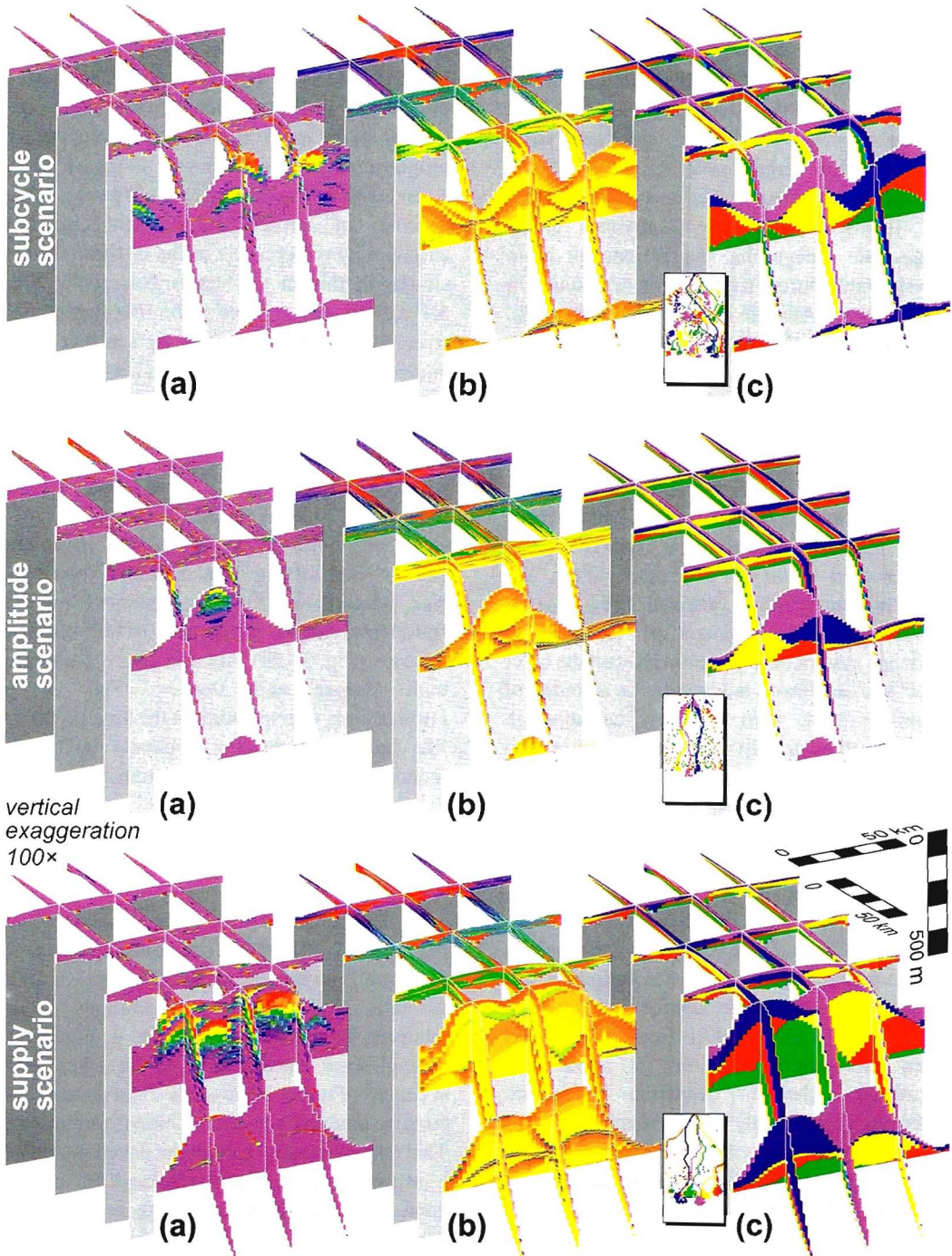


Fig. 3.11 — Lithostratigraphies of examples of model experiments run with various scenarios. Strata represent intervals of 1 kyr. a) Grain-size fraction (relative abundance of the coarse grain-size class) of sediment. b) Time of deposition within a 100-kyr cycle. c) Glacial–interglacial cycle in which deposition occurred. Inset: map view of coarse bodies thicker than 1 m. Colour scales are as in Fig. 3.8.

water. Moreover, in the model, the contribution of rainwater to the main hinterland-fed river system is limited, as these rivers tend to build a (weakly) convex delta-topography around them during regression, thereby directing local rainwater flow largely away (Schumm, 1993). Unless fault structures (Coleman *et al.*, 1983) or exposed submarine canyons create large-scale topographic depressions, or basin physiography forces rivers to join (e.g. southern North Sea, Adriatic (Mulder & Syvitski, 1996)), accumulated rainwater is in reality likely to form a separate, secondary drainage system or is added to sediment-poor streams from small, proximal basins (Schumm, 1993). Channel belts that were abandoned when a competing river branch captured the water discharge at the transfer-valley outlet (i.e., when drainage connection was established (Ch. 2) remained active as ‘overfitted valleys’ for the little runoff they received. Because of lower discharge, incisions of the rain-fed drainage system occurred primarily on the outer shelf and shallowed landward. As a source of sediment, they were relatively unimportant. However, they greatly influenced the formation of unconformities.

Scenario with increased supply during glacials

The effect of climate change in the hinterland on water discharge and sediment yield from the drainage basin during transitions between glacial and interglacial periods is still unclear (Leeder, 1997; Leeder *et al.*, 1998; Goodbred & Kuehl, 2000). Even when a shift from one climate regime to another is identified, chaotic behaviour precludes inference of the supply development. Modified by local vegetation, a cooler and/or wetter climate can lead to both an increase and a decrease of supply (e.g. Walling & Webb, 1983; Schumm, 1993; Leeder *et al.*, 1998). Whether the supply signal changes gradually, abruptly or in pulses, needs to be determined from the sedimentary record. Therefore, sediment budgeting of continental margin

stratigraphy is essential for resolving the control of climate on sediment transport. Pending such empirical datasets, water discharge, sediment load and grain-size fraction in the fourth model variant scenario are proportional to sea level and in phase (Fig. 3.2b). Despite the different supply patterns, the volume of preserved sediment in the stratigraphy with respect to the in-flux value is similar to that in the standard scenario (Fig. 3.10a). However, since in both scenarios the river profile was controlled by sea level, the amount of cannibalized material was reduced in relation to the river load. Therefore, it had less influence on river dynamics and basin-scale grain-size sorting. Moreover, the coarse sediment influx was less during interglacial times, resulting in inner shelf sequences with a lower coarse sediment content (Fig. 3.10d). Hence, there is relatively less enrichment of coarse sediment on the continental slope at the expense of falling-stage deposits (Fig. 3.10b). Incised river valleys are both deeper and steeper (Fig. 3.11). Furthermore, coarse bodies at the base of valley fills have a decreasing thickness landward, reducing the chances of connection.

Concluding remarks

The model presented here is a conceptual one, and the applied scenarios are but a selection from the vast array of natural forcing variables and spatial configurations. To interpret the model results in a particular setting, local factors have to be taken into account. Future basin-scale field studies of passive margins can act as model-prototypes. This may eventually lead to the development of a sequence stratigraphic concept of clastic continental margin systems with grain calibre incorporated as a parameter, similar to the approach of Orton and Reading (1993).

A bipartite sedimentary architecture with a proximal highstand system and a distal lowstand system coupled by a long-distance

regressive shelfal system is a distinctive feature of many Quaternary passive continental margins. This dual character is clearly reflected in the modelled development of volume and grain-size distribution in the stratigraphy. Concentrations of coarse-grained material are found on the innermost shelf and beyond the shelf-break, with sediments finer than average in between.

In the model, small-scale grain-size sorting is controlled by deltaic processes, through the build-up of coarsening-up sequences during normal and forced progradation, and by fluvial/estuarine processes, resulting in onlapping fining-up valley fills during sea-level rise and transgression. However, basin-scale, long-term grain-size sorting is closely related to the formation of an unconformity on the exposed shelf and in the fluvial transfer-valley. Coarse paralic strata and fine-grained prodelta sediments have a different preservation potential; erosion during lowstand preferentially affects coarse falling-stage deposits and subsequently enriches shelf-edge successions with coarse material. This is the

main mechanism for basin-scale sorting.

In the modelled stratigraphy, large coarse bodies are found on the upper continental slope and across the shelf at the base of incised river-valleys. The individual coarse river channel-belts are connected within the complex of highstand deltas, but rarely make contact on the rest of the shelf. Shelf-edge bodies are nearly completely encapsulated by fine material delivered during falling sea-level stage and during early rise, and therefore poorly or not connected to each other. However, they are usually connected to the transgressive valley fills of the same interglacial–glacial cycle.

When relating the model results to real-world situations, a reservation has to be made with regard to the activity of processes not incorporated into the model that have the ability to modify the local interconnectedness of coarse-grained deposits, such as turbidite currents and wave/tidal ravinement. However, from the model it is evident that interconnectedness of major coarse bodies is very unpredictable owing to the large variability of landscape, and thus stratigraphic, development.

Modelling the preservation of sedimentary deposits on passive continental margins during glacial–interglacial cycles

Abstract

The preservation potential of sedimentary deposits is a measure of the chance of a stratigraphic level to escape reworking. In this chapter, the preservation of strata on passive continental margins during glacial–interglacial cycles is investigated by means of a three-dimensional, dynamic numerical model. The reworking of sediment is primarily driven by glacio-eustatic base-level changes, and varies across the shelf. Although local topography and the present drainage pattern influence the occurrence of erosion, statistically the coastal wedge (highstand delta), the adjacent inner shelf and the shelf edge are most vulnerable. The differential preservation, especially of shelf and upper continental slope deposits, is also manifested in the chronostratigraphy, leading to a considerable deviation in the volume distribution from the sediment supply signal. The formation of a subaerial erosional unconformity commences during falling sea-level stage and continues until early rise, and greatly affects paralic deposits. In addition, various scenarios of sea-level change, different gradient contrasts between coastal prism and shelf, and sediment supply and discharge have been investigated.

Introduction

Much of the geological time in sedimentary successions is taken up by hiatuses. Reworking and remobilization are basic aspects of sedimentary processes, and are especially associated with recurrent events over various time scales. During the Quaternary, glacial–interglacial sea-level and climate changes have been important cyclic driving forces on a relatively long time-scale of 40–100 kyr. Basin margins have been particularly affected by the large, glacio-eustatically driven base-level changes, which led to periodic emergence and submergence of continental shelves. As a result of subaerial erosion, fluvial incision and wave ravinement, some deposits are better preserved than others. A measure of the chance of a stratigraphic level to escape reworking is termed its ‘preservation potential’.

The actual preservation of ancient sediments after a certain time-interval following initial deposition gives a quantitative

assessment of the preservation potential of similar, modern deposits. For example, remnant highstand deposits from a previous glacial cycle indicate how much may remain of the Holocene coastal-plain deposits after the next ice age. However, it is difficult to estimate the survival of sedimentary deposits from previous glacial cycles, since the exact volume of the original strata can usually not be reconstructed. Dynamic sediment transport models, on the other hand, are able to record the history of depositional and erosional stages, and thus can assist in evaluating the preservation potential of different sedimentary facies deposited during glacial–interglacial cycles.

Here, a stratigraphic model is used to investigate the preservation of deposits on a general passive continental margin during Quaternary glacial–interglacial cycles. In anticipation of three-dimensional, volumetric data sets of passive margins, the model is applied here as a conceptual tool to study the dynamics of the sedimentary system. The

effects of various scenarios of boundary conditions are examined, including eustatic sea-level change, contrast in gradients of coastal prism and continental shelf, and river discharge and sediment load.

The model used is a cellular model, in which fluxes of water and sediment over a topographic surface from one grid cell to neighbouring cells are defined by a number of straightforward transport rules. The rules describe time-averaged sediment transport in several depositional environments, defined by bathymetric zones, as a function of local conditions such as slope and discharge. There are two transport algorithms: one for short-range, slope-dependent transport and another for long-range, slope and discharge-dependent river transport. Wave action is not modelled explicitly, apart from increased transport capability in the shallow subaqueous environment. Deposition, erosion, and tectonic subsidence change the surface elevation. Feedback through the relationships between topography and transport results in an intricate process-response system, driven by the boundary conditions set by sea-level change, tectonics, precipitation, and the supply of sediment and discharge. The model produces a morphological (palaeogeographical) evolution and builds a

three-dimensional lithostratigraphy and chronostratigraphy by recording the amount and properties (for instance, age, provenance and grain size) of deposited sediment and the presence of hiatuses. See Chapter 2 for a detailed description of the model and its calibration.

Model procedure

The set-up of the model is outlined in Fig. 4.1. Combinations of variables acting as boundary conditions (Fig. 4.2) that are applied to the model are referred to as ‘scenarios’. The scenarios used in this chapter are listed in Table 4.2. For the benefit of statistical analysis, each model scenario was run 50 times, each time with a different white-noise pattern superimposed on the initial topographic surface. This enables the results of different scenarios to be compared.

From the model stratigraphy, the volume of sediment between two ‘stratigraphic levels’ (i.e., the total volume of deposits between certain age limits) is summed for the entire area of interest, for a specific site, or for a depositional environment, and recorded. Subsequently, in order to determine the preservation of a particular stratigraphic interval, the decrease of this initial amount through time owing to erosion is registered. A

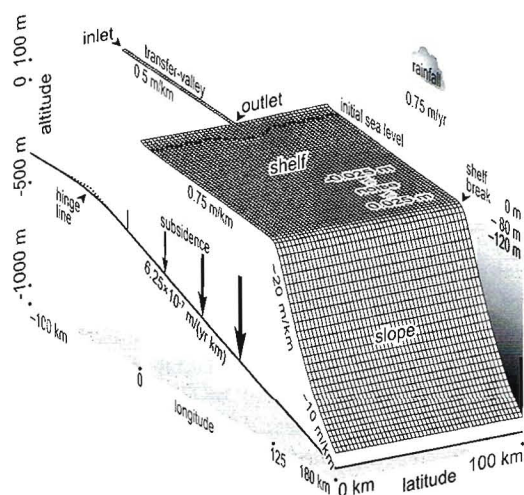


Fig. 4.1 — Overview of the grid set-up of the model. The initial topography outlines a transfer-valley emanating from the drainage basin, an initial highstand delta, a continental shelf and slope. The scale of the passive continental margin system is 280 × 100 km.

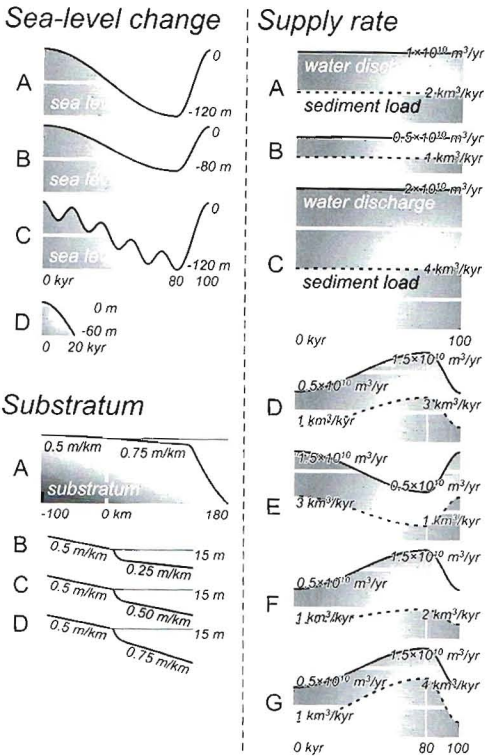


Fig. 4.2 — Variants of applied model variables sea-level change (A–D), initial topography (A–D), and discharge and sediment supply rate (A–G). Table 4.2 lists the combination in which they are used in the different scenarios. For the sea level (except D) and supply variables, only single glacial–interglacial cycles of 100 kyr are depicted. Model runs cover five identical cycles, where the preservation of the second cycle is the object of study.

model run covers five glacial–interglacial cycles, each with a duration of 100 kyr (with

the exception of the gradient scenarios). The first cycle is a preparatory one; the second cycle is the main object of study. Preservation of deposits from the second cycle is monitored both during and after this cycle.

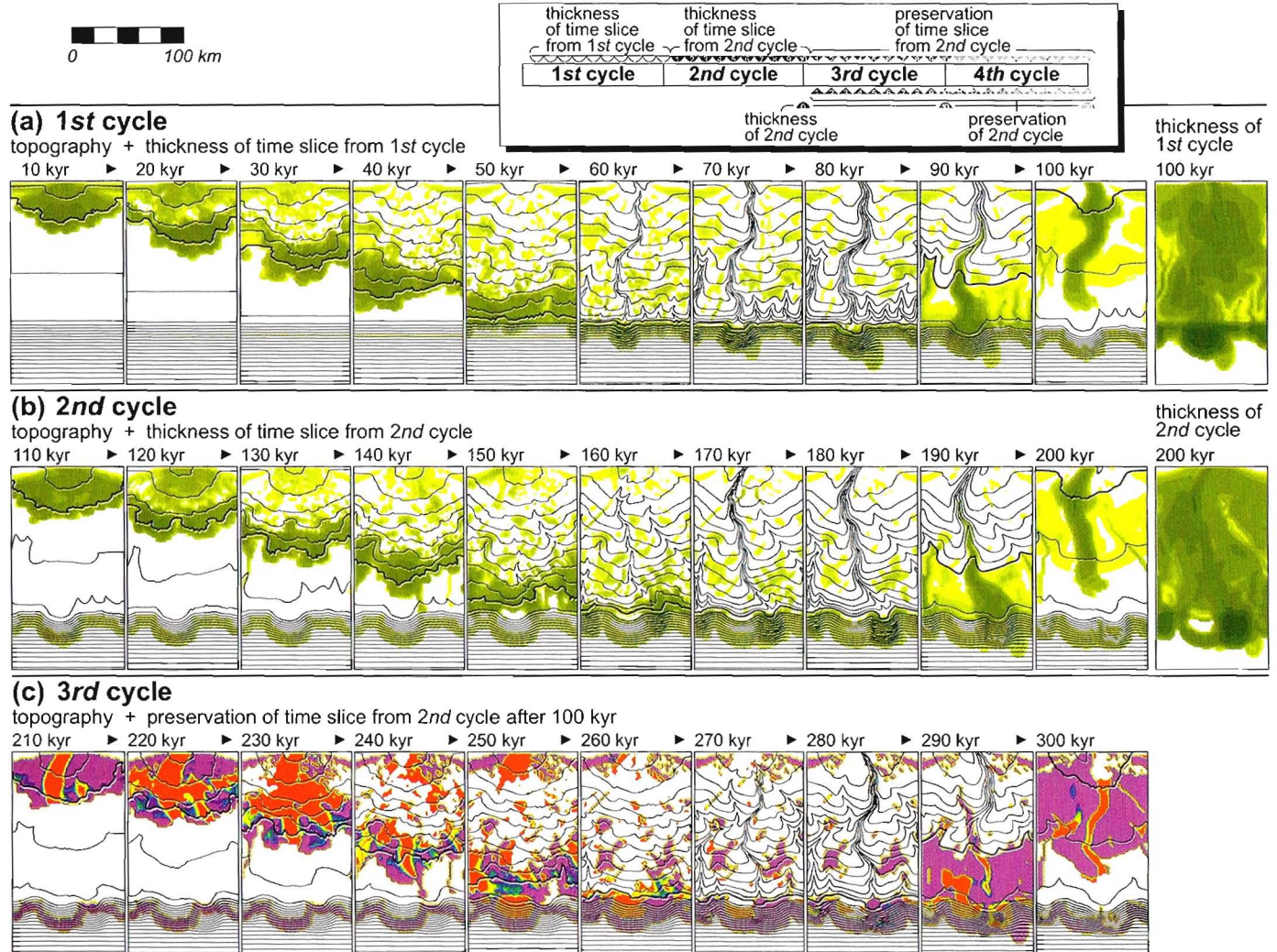
Results and Discussion

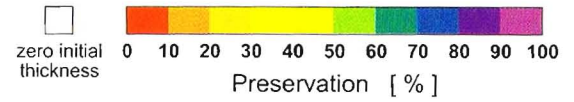
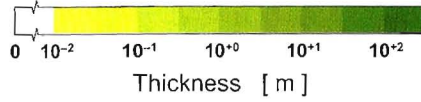
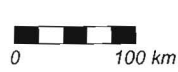
Geomorphology and preservation

Before analysing the preservation of deposits laid down on a passive margin during a glacial–interglacial cycle, the general character of geomorphologic evolution and the associated sediment distribution are first briefly described on the basis of an arbitrary model run. In Figs 4.3a and b, the topographical development of this example for the first two cycles is depicted at 10-kyr intervals, as well as the net sedimentation that has occurred during the preceding 10 kyr.

The model evolution starts during an interglacial with a submerged shelf and a shelf delta. During highstand, river sediment is deposited subaerially and on the inner shelf (Figs 4.3a and b, at ~10 and ~110 kyr). Aggradation on the highstand delta decreases as accommodation decreases under the influence of falling sea level. Avulsions on the delta-plain are initially frequent, but decrease in number. Forced regression (Posamentier *et al.*, 1992) leads to rapid progradation of the coastline over the continental shelf (at ~20–50 and ~120–150 kyr). Relatively shallow

Fig. 4.3 (next two pages) — Maps of the palaeogeographical evolution, sediment thickness and preservation during four glacial–interglacial cycles. Topographic contour interval above sea level is 10 m; below sea level 50 m. The shoreline is indicated by a thick line. Preservation is defined as the sediment thickness relative to the initial thickness. The inset provides an overview of the various types of maps in the figure. a) The first cycle (0–100 kyr) depicted in intervals of 10 kyr. In each frame, the surface topography at the end of a 10-kyr interval and the final thickness of deposits accumulated during the preceding 10 kyr ‘time slice’ are shown. On the far right, the thickness of deposits of the entire first cycle measured at the end of the first cycle is given. b) The second cycle (100–200 kyr), the preservation of which is monitored in subsequent cycles. Shown are topographies and thicknesses of time slices similar to those in a). c) The third cycle (200–300 kyr) with in each frame the surface topography at the end of a 10-kyr interval as well as the preservation of sediments of the time slice from one cycle ago (i.e., those depicted in b). d) The third cycle, with the preservation of sediments of the entire second cycle since the end of the second cycle. On the far right, the preserved thickness of deposits of the entire second cycle. e) The fourth cycle (300–400 kyr), similar to c) but now with the preservation of sediments of time slices from two cycles before (i.e., again those in b). f) The fourth cycle, similar to d).

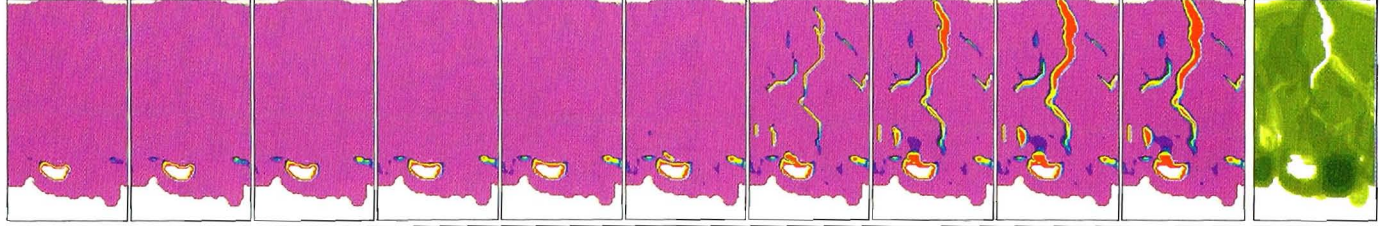




(d) 3rd cycle

preservation of 2nd cycle

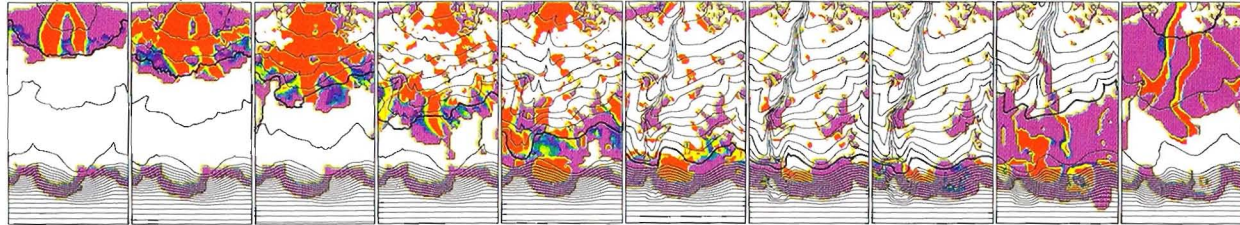
210 kyr ▶ 220 kyr ▶ 230 kyr ▶ 240 kyr ▶ 250 kyr ▶ 260 kyr ▶ 270 kyr ▶ 280 kyr ▶ 290 kyr ▶ 300 kyr



(e) 4th cycle

topography + preservation of time slice from 2nd cycle after 200 kyr

310 kyr ▶ 320 kyr ▶ 330 kyr ▶ 340 kyr ▶ 350 kyr ▶ 360 kyr ▶ 370 kyr ▶ 380 kyr ▶ 390 kyr ▶ 400 kyr



(f) 4th cycle

preservation of 2nd cycle

310 kyr ▶ 320 kyr ▶ 330 kyr ▶ 340 kyr ▶ 350 kyr ▶ 360 kyr ▶ 370 kyr ▶ 380 kyr ▶ 390 kyr ▶ 400 kyr

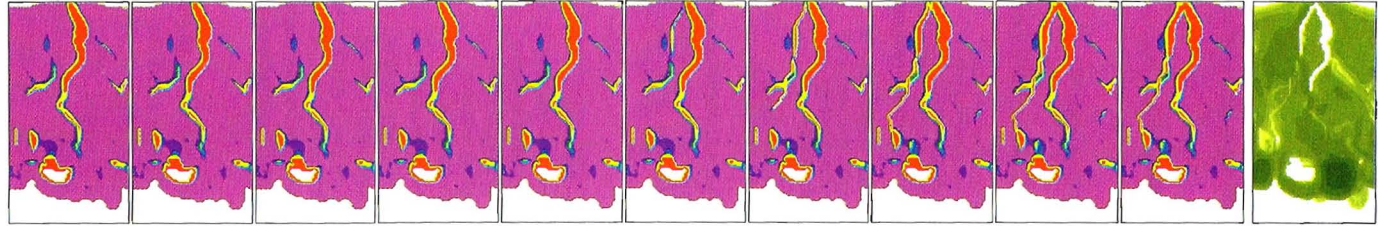


Table 4.1: Values of parameters applied in the model runs. See Chapter 2 for explanation of the parameters and the accompanying equations.

Parameter	Symbol	Environment	Value	Unit
diffusive transport power	U		1.0	–
diffusive transport coefficient	K_D	terrestrial	0.30	$\text{km}^3 \text{kyr}^{-1}$
		coastal	0.40	$\text{km}^3 \text{kyr}^{-1}$
		marine	0.40	$\text{km}^3 \text{kyr}^{-1}$
		deep marine	0.32	$\text{km}^3 \text{kyr}^{-1}$
threshold slope	S_{thr}	terrestrial	0.0005	–
		coastal	0.0040	–
		marine	0.0200	–
		deep marine	0.0200	–
transition depth w.r.t. sea level		terrestrial – coastal	0	m
		coastal – marine	25	m
		marine – deep marine	100	m
discharge distribution threshold	k	terrestrial	0.75	–
		non-terrestrial	0.00	–
stream transport power	V		1.0	–
stream transport power	W		1.0	–
discharge threshold	Q_{thr}		2.0×10^8	$\text{m}^3 \text{yr}^{-1}$
stream transport coefficient	K_S		0.40	–
stream attenuation constant	L_S	at overcapacity	10	–
		at undercapacity	50	–
incision criterion power	v		1.00	–
incision criterion power	ω		0.25	–
incision threshold	P_{thr}		0.224	$(\text{m}^3 \text{yr}^{-1})^{0.25}$
grid cell size			2000	m
time step			10	yr
white-noise range			0.05	m

Table 4.2: Model scenarios used in this chapter. The sea-level curves, initial topographies and supply curves referred to in the table are depicted in Fig. 4.2.

Scenario	Variables Sea-level curve	Initial topography	Supply curve
Standard scenario	A	A	A
Sea-level scenarios			
‘amplitude scenario’	B	A	A
‘subcycle scenario’	C	A	A
Gradient scenarios			
all permutations	D	B, C, D	A, B, C
Supply scenarios			
‘low supply scenario’	A	A	B
‘high supply scenario’	A	A	C
‘high glacial-supply scenario’	A	A	D
‘low glacial-supply scenario’	A	A	E
‘low glacial-load scenario’	A	A	F
‘high glacial-load scenario’	A	A	G

incisions occur in convex delta morphologies, in particular in the front of the coastal prism (Posamentier *et al.*, 1992; Talling, 1998) that has emerged. Thus, river belts become locally embedded in shallow valleys in some reaches. Although upstream avulsion events occur sporadically, the main locus of avulsions shifts basinward along with the active deltas. Delta-lobe switching produces a complex of stacked delta bodies on the shelf, forming a

forced regressive wedge. Deposition is largely limited to the coastal region. As the shoreline approaches the shelf break, accommodation space increases dramatically and the progradation rate diminishes (at ~50 and ~150 kyr). Incipient shelf-edge deltas are formed on the upper continental slope. A continuously falling base level results in the formation of upstream migrating knickpoints in the river belts, and the exposed shelf is incised. Headward erosion produces a diachronous subaerial erosional unconformity across the shelf. As the knickpoints migrate upstream, one of the competing river belts connects to the outlet of the hinterland, capturing all discharge from the drainage basin, and focussing deposition in a major delta along the shelf edge. During the glacial period, this shelf-edge delta remains the main depocentre on the basin margin. Avulsions are restricted to this delta system. At lowstand, as relative sea-level begins to rise, deposition occurs near river mouths in relatively shallow water (at ~80 and ~180 kyr). This submarine aggradation gradually passes into retrogradational coastal and fluvial onlap (at ~90 and ~190 kyr).

Sedimentation is initially confined in incised valleys with limited space for avulsions. As sea-level rise decelerates, a new coastal prism is built with frequent avulsions on the highstand delta (at ~100 and ~200 kyr).

Figure 4.3c shows the topographic evolution during the third glacial–interglacial cycle. In addition, the preservation of the deposits of the 10-kyr time slices of the second cycle (cf. Fig. 4.3b) are depicted after 100 kyr. The preservation at a particular time is defined as the ratio of the stratal thickness at that time to the original thickness.

A 100 kyr after its formation, the highstand delta has been bisected by the incised valley connected to the drainage basin outlet that formed before the sea-level lowstand of the second cycle (Fig. 4.3c, at ~210 kyr). Similarly, the forced regressive wedge on the shelf has been partitioned as a result of several incisions (at ~220–250 kyr). River incision during late falling stage and lowstand of the third cycle (at ~270–280 kyr) again erodes ‘recent’ forced-regressive deposits, but does not greatly affect the preservation of the 100-ka old deposits. This is because the little sediment of this period of the second cycle that was deposited on the shelf has been long since reworked or buried. Deposits that are affected by third-cycle river incision are the highstand delta and early regressive wedge (the result of which can be seen in Fig. 4.3e, at ~310 and ~320 kyr), and the transgressive strata (Fig. 4.3c, at ~280 and ~290 kyr). The preservation of the latter does not only decrease owing to river incision before lowstand, but also by erosion of aggradational strata on top of the shelf-edge deltas. This shelf-edge degradation is slow when the shelf is submerged, and intensified during emergence. Transgressive shelf strata are probably less preserved in the real world than shown here, because of wave ravinement during sea-level rise. Likewise, reworking during falling sea level is likely to play a role in the preservation of shelf sediments (Plint, 1988; Posamentier *et al.*,

1992; Plint & Nummedal, 2000; Posamentier & Morris, 2000). The model results therefore indicate an upper limit to preservation and are applicable especially for natural situations with an absent or mild wave regime.

Instead of looking at time slices of a cycle, we can also determine what deposits are present after a full cycle (Fig. 4.3, right), and see how they survive the next glacial–interglacial cycles. The preservation of the deposits of the entire second cycle can be followed with respect to the stratigraphic thickness at the end of the second cycle, shown in Figs 4.3d and f. Fluvial incision and shelf-edge degradation are the main causes of reworking; subaerial erosion is limited to valley walls and the shelf edge. The effects of incision are especially apparent on the inner shelf, where rivers cut into the former highstand coastal prism. With the burial by younger sediments under the influence of basin subsidence, the intensity of reworking decreases with every new cycle, just as erosion is less vigorous than it had been during the second cycle itself.

Erosion and remobilization of sediment can be quantified in the model by measuring the time between entrance from the drainage basin into the system and eventual deposition (i.e., the actual age of the deposit found in the stratigraphy). In Fig. 4.4b the stratigraphy after five glacial–interglacial cycles is depicted with this difference in ‘grain age’ and stratal age. The closer to the red side of the colour spectrum, the older the sediment that is incorporated into the deposit relative to the age of the stratigraphic level. This property can be related to the maturity of the grains. Figure 4.4b shows that material on the shelf was deposited relatively shortly after it left the drainage basin, whereas markedly more cannibalized sediment is found on the upper continental slope. Moreover, the differential age is low at the base of a shelf-edge delta sequence and increases upward as progressively more cannibalized sediment was supplied from the shelf during the formation of

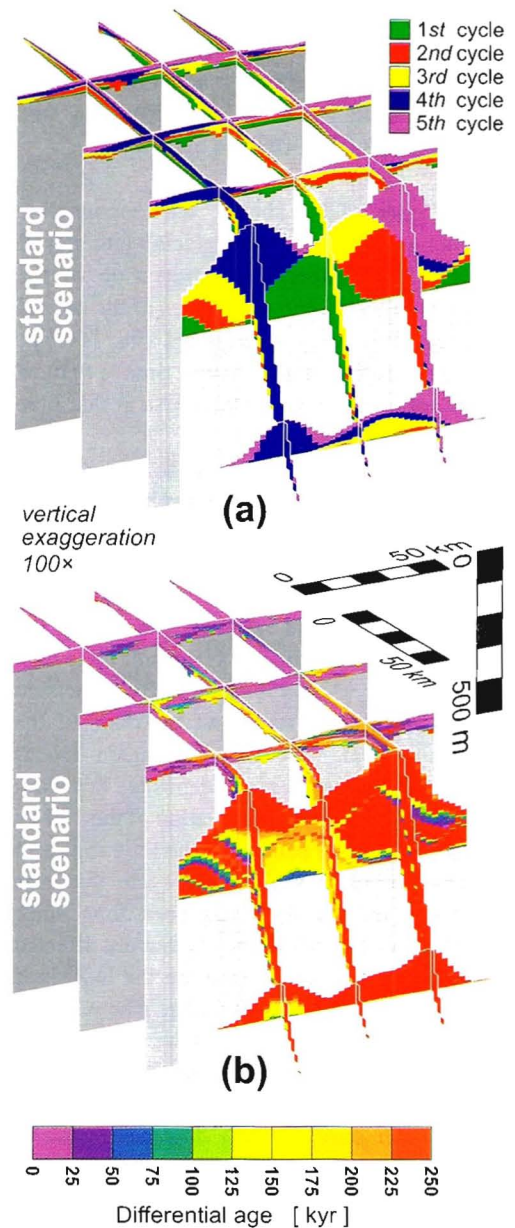
Fig. 4.4—Lithostratigraphy of an example of a model experiment run with the standard scenario. a) The glacial–interglacial cycle in which deposition occurred. b) The ‘differential age’ of deposits, i.e., the difference between the time the sediment entered the system from the hinterland and the time it was incorporated into the deposit in the final stratigraphy. This property indicates cannibalization and remobilization of sediment and is a rough measure of the maturity of the sediment. Note the difference is differential age between shelf and shelf-edge strata.

a subaerial erosional unconformity. Reworked sediment also ends up in fills of incised valleys, since cannibalization continues upstream during fluvial and coastal onlap.

Stratigraphy and preservation

In addition to the spatial distribution of erosion discussed in the previous section, we can also consider preservation from the perspective of the chronostratigraphy of the entire system. The mean of 50 model runs with the same standard scenario, but with different random noise on the initial topography, is determined to examine the trends in preservation.

Figure 4.5 shows how the cumulative volume of the whole study area and the volume relative to the initial amount (indicated on the vertical axes), of deposits of a certain age (indicated on the horizontal axis) decreases with time (the succession of bands from dark to light grey). On the basis of their time of deposition, strata are allocated to stratigraphic intervals with a duration of 1 kyr. Highstand deposits from the beginning of the second cycle initially endure, as erosion is usually limited to minor incision into the front of the highstand delta during the early part of forced regression. The immediate reworking of freshly deposited, forced regressive material increases as the rate of sea-level fall increases. However, after the shelf break emerges above sea level, a subaerial erosional unconformity is formed and erosion in the system accelerates (Schlager, 1993; Posamentier & Morris, 2000). Headward incising rivers start to affect the inner shelf from around 160 kyr, and highstand deposits



are rapidly cannibalized. Close to 40% of the sediments dating from the first half of the second cycle are eroded before the end of the cycle (cf. Figueiredo & Nittrouer, 1995). Deposition after ~150 kyr occurs on the upper continental slope. The depocentres are situated in deep water and rapid burial increases the preservation potential considerably (Fig. 4.5).

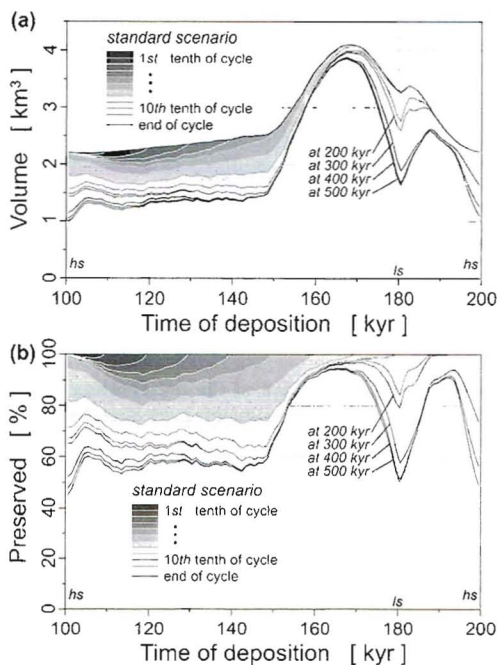


Fig. 4.5 — The volume and preservation of strata of the second glacial–interglacial cycle deposited in intervals of 1 kyr through time. The graphs are constructed as follows: at 1-kyr intervals during the model run, the volume of all deposits of 1 ka and younger is determined and recorded. (E.g. at 140 kyr, deposits laid down between 139 to 140 kyr were found with a total volume of 2.43 km³.) At certain times, during the second cycle at 110, 120, ..., 190 and 200 kyr, and after the second cycle at 300, 400 and 500 kyr, the volumes of sediments in the same, but aged, 1-kyr stratigraphic intervals are re-measured, yielding lower values in case erosion has occurred and corresponding decreased values of preservation. (For the above example, at 170 kyr the volume of the 139–140-kyr stratigraphic interval is 1.83 km³, or 75% of the initial volume; at 500 kyr it is 1.37 km³, or 56%.) Note that the upper boundaries of the volume and preservation graphs are diachronous. The graphs are means of 50 runs with the standard scenario. Also indicated in light grey is the shape of the sea-level curve.

Deposits laid down around lowstand are mostly shallow, aggradational shelf-edge strata, which are relatively badly preserved. In the absence of ravinement, transgressive strata are not eroded until late in the next cycle (~260–280 kyr), after having been covered by regressive sediments.

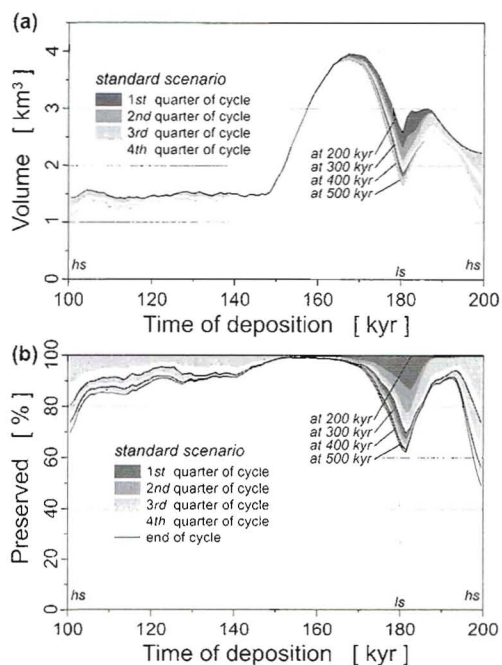


Fig. 4.6 — The volume and preservation of strata of the second glacial–interglacial cycle deposited in intervals of 1 kyr through time. Preservation at a given time is defined as the volume at that time relative to the initial volume. The graphs are similar to those in Fig. 4.5, except the ‘initial’ reference volumes are determined at the end of the second cycle, instead of directly after the creation of the stratigraphic intervals. The graphs are means of 50 runs with the standard scenario. Also indicated in light grey is the shape of the sea-level curve.

Figure 4.6 shows the preservation of the stratigraphic volume that is left at the end of the second glacial–interglacial cycle. As a consequence of previous geomorphic work and burial, reworking is generally not as intense as during the second cycle itself. This is particularly the case for forced-regressive (shelf) deposits. They are only affected during the second halves of following cycles, related to major shelf incision. Strata laid down around lowstand (shelf-edge deposits) and during rising sea level (valley fills and highstand delta), on the other hand, are relatively severely reworked in later glacial–interglacial cycles. The coastal prism that is built up mainly during rise is vulnerable

to incision. Because of its confinement, the transfer-valley is greatly affected by fluvial erosion, although in the real world additional traces of previous cycles will remain in terraces, which are below the resolution of the model. Lowstand shelf-edge deposits are eroded both subaerially and submarine during the entire cycle (Figs 4.6 and 4.7). The bad preservation of these deposits leads to a marked depression in the chronostratigraphic volume around the time of lowstand, which should not be interpreted as a decrease in hinterland supply around that time.

The preserved volume of sediment of the second glacial–interglacial cycle decreases variably with time (Fig. 4.8). Note the relatively slow and steady decrease of

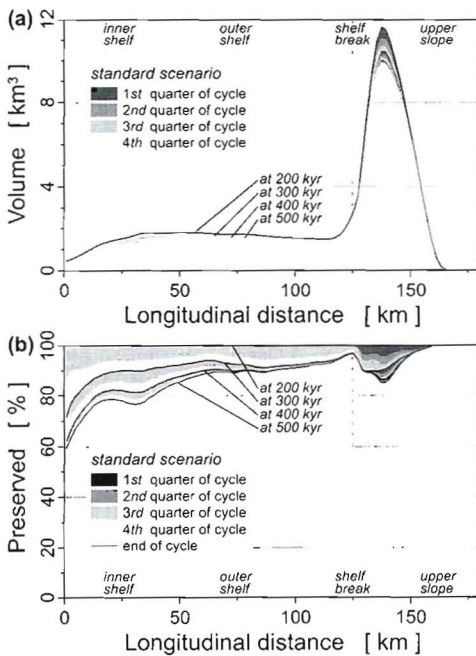


Fig. 4.7 — The volume and preservation of strata of the second glacial–interglacial cycle deposited at a longitudinal distance through time. Preservation at a given time is defined as the volume at that time relative to the initial volume. The graphs are similar to those in Fig. 4.6, except the independent variable is longitudinal distance, instead of the stratigraphic interval. The graphs are means of 50 runs with the standard scenario.

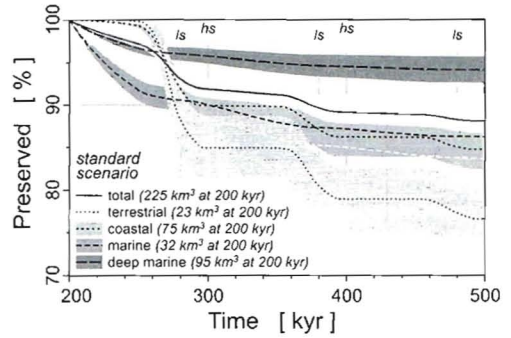


Fig. 4.8 — The evolution of the preservation of the volume of second-cycle sediments present at the end of the second cycle, in total as well as subdivided by depositional environment. Shown are the means and 2σ-confidence intervals of 50 runs with the standard scenario.

preservation during the first halves of the cycles, followed by high rates of decrease during the second halves when the continental shelf was subaerially exposed. There is also a considerable contrast in preservation of sediments of the different depositional environments. Especially terrestrial deposits, and coastal ones to a lesser extent, suffer great losses in volume during shelf emergence. Deep marine sediments on the continental slope, however, seem unaffected directly by the sea-level fluctuations. Erosion is less every next glacial cycle and eventually asymptotic.

Other scenarios

Sea level scenarios

Glacio-eustasy has a great influence on the preservation of deposits on passive continental margins, as it drastically modifies base level and may result in subaerial exposure of the shelf. There is, however, a marked difference between systems where sea level drops below the shelf break and systems where it does not. The ‘amplitude scenario’ (Table 4.2), with a lowstand sea level of only 80 m, is an example of the latter situation. The lower rate of sea-level fall results in sustained fluvial and deltaic aggradation on the inner shelf for ~40 kyr from the start of the cycle. Because there is more accommodation space on the

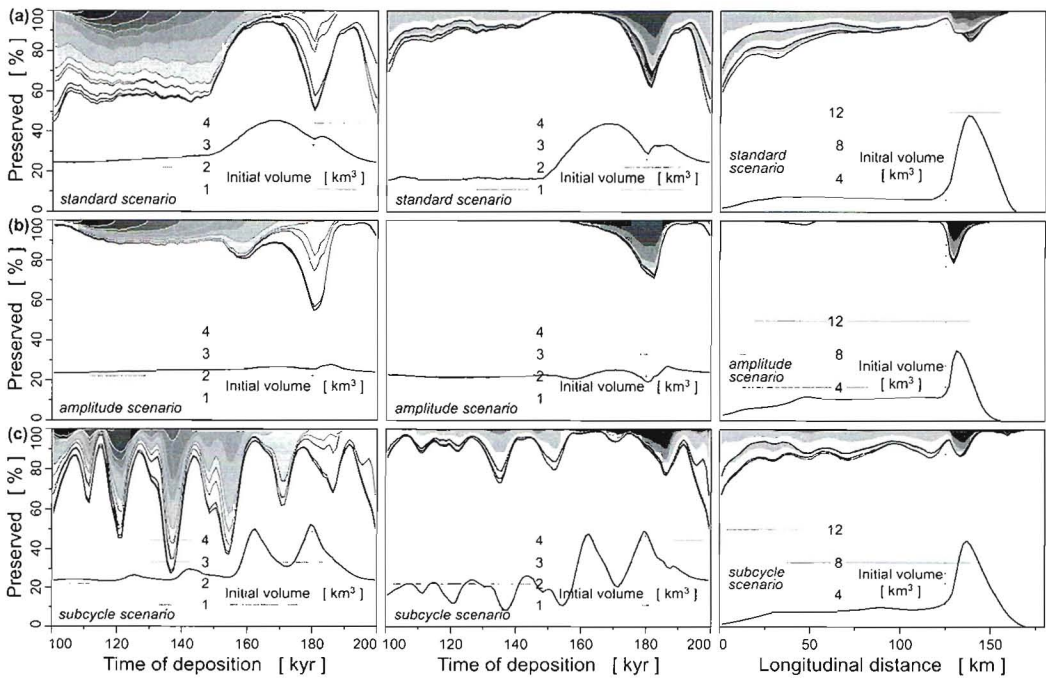


Fig. 4.9 — The volume and preservation of strata of the second glacial–interglacial cycle through time for the standard and sea-level scenarios (Table 4.2). The graphs on the left are similar to Fig. 4.5, those in the middle to Fig. 4.6, and the ones on the right to Fig. 4.7. Also indicated in light grey are the shapes of the respective sea-level curves. a) The standard scenario. b) The ‘amplitude scenario’. c) The ‘subcycle scenario’.

shelf than in the standard scenario, progradation is slower, and shelf-edge deltas are not formed until about 60 kyr into the cycle. Little subaerial erosion occurs since not much relief was built during sea-level fall (cf. Figs 4.9a and b), and the subaerial unconformity represents a smaller hiatus than in the standard scenario. Incision occurs mostly on the outermost shelf (resulting in a decreased preservation of strata from around 160 kyr shown in Fig. 4.9b), but is rarely deep enough to cut through deposits underlying the forced regressive wedge. In the absence of deep river valleys, sedimentation is not confined during sea-level rise, which results in widespread sheet-like transgressive strata. In subsequent cycles, sediment of the second cycle is almost fully preserved owing to burial, with the exception of the shelf edge that is degrading with decreasing intensity (Figs 4.9b, right and 4.10b).

Contrasting with the previous is the ‘subcycle scenario’ (Table 4.2), in which higher-order sea-level fluctuations lead to a pronounced, stepped topography on the shelf (Posamentier & Morris, 2000). The combination of the formation of topography and base-level change results in marked differential preservation of successive deposits (Fig. 4.9c). For instance, deposits laid down around 107 kyr are relatively well preserved because they were buried by a sub-highstand delta from ~118 kyr, in contrast to ~111 kyr sub-lowstand strata that are exposed (Fig. 4.9c, left). Later in the cycle, erosion particularly affects sub-transgressive and sub-highstand strata whenever sea level falls. Large-scale shelf erosion after emergence of the shelf break is interrupted by a short transgression (~164–172 kyr) with onlap in the incised valleys. During the subsequent sea-level fall, the river belts still occupy the same valleys and

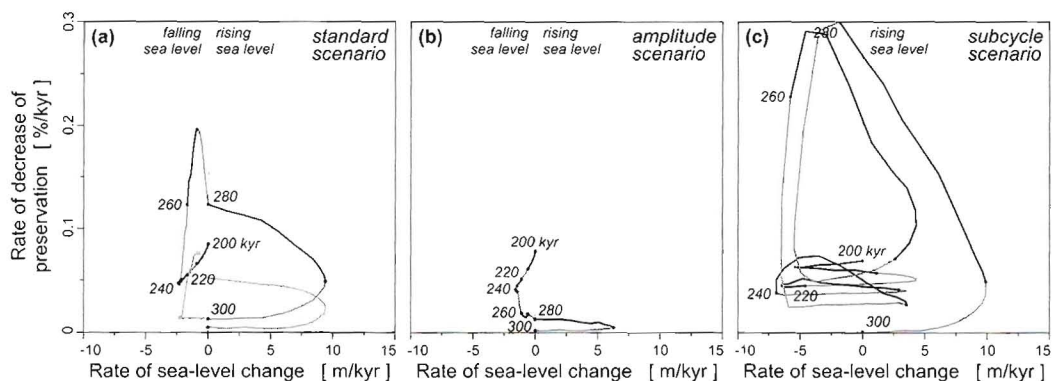


Fig. 4.10 — The relation between the rate of sea-level change and the rate of change of preservation of sediment from the second glacial–interglacial cycle for the standard and the sea-level scenarios (Table 4.2). The graphs are means of 50 runs. a) The standard scenario. b) The ‘amplitude scenario’. c) The ‘subcycle scenario’.

completely flush out the valley fills, resulting in low overall preservation. In contrast to the standard scenario, the rate of decrease of preservation is high at ultimate lowstand (Fig. 4.10c). The chronostratigraphic distribution of volume is greatly modified after the second cycle (Fig. 4.9c, middle).

Gradient scenarios

The difference in gradient between the river profile and the submerged shelf profile has often been put forward as a governing factor in the preservation of the inner shelf when sea level falls (Miall, 1991; Posamentier *et al.*, 1992; Schumm, 1993; Wescott, 1993). However, in that portrayal, the coastal prism is oversimplified by omitting the presence of a steeper shoreface (Törnqvist *et al.*, 2000) and the morphological development takes no account of submarine deposition in the coastal area. In fact, the trajectory of coastline and the ensuing longitudinal river profile is much more complex, especially in three dimensions. Figure 4.11 exemplifies this by means of a number of model runs with varying gradient contrast (vertical) and varying sediment supply (horizontal). Indeed, erosion is dependent on the gradient contrast between coastal prism and shelf, but the amount of sediment supply appears to be more important (Table 4.3). With increasing shelf gradient, fluvial aggradation

on the highstand delta becomes less prominent and incision into the highstand delta rim and the forced regressive deposits right in front of it becomes more common for a given sediment supply. For increasing sediment supply, subaerial exposure of the highstand delta plain and front decreases because they are buried more extensively (Fig. 4.11). Increasing supply improves initial topography preservation, despite the accompanying increase in erosive power of rivers, because deposition inhibits the development of steep slopes. Therefore, incision is more likely with increasing shelf gradient relative to the gradient of the coastal prism and with decreasing sediment supply.

When in the course of sea-level fall, a second convexity in the margin profile basinward of the coastal prism is exposed, be it a shelf break or a curved shelf, a second phase

Table 4.3: The amount of erosion of the initial topography expressed as a percentage of the reference case, which is the underlined mean value, for varying sediment supplies and differences between the gradient of the coastal prism and the shelf.

		Sediment supply			
		Low 1 km ³ kyr ⁻¹	Moderate 2 km ³ kyr ⁻¹	High 4 km ³ kyr ⁻¹	
Gradient contrast	Shallower shelf	0.25 m km ⁻¹	174 ± 14	99 ± 9	56 ± 4
	Equally steep	0.50 m km ⁻¹	180 ± 26	<u>100</u> ± 9	55 ± 4
	Steeper shelf	0.75 m km ⁻¹	199 ± 39	115 ± 29	78 ± 35

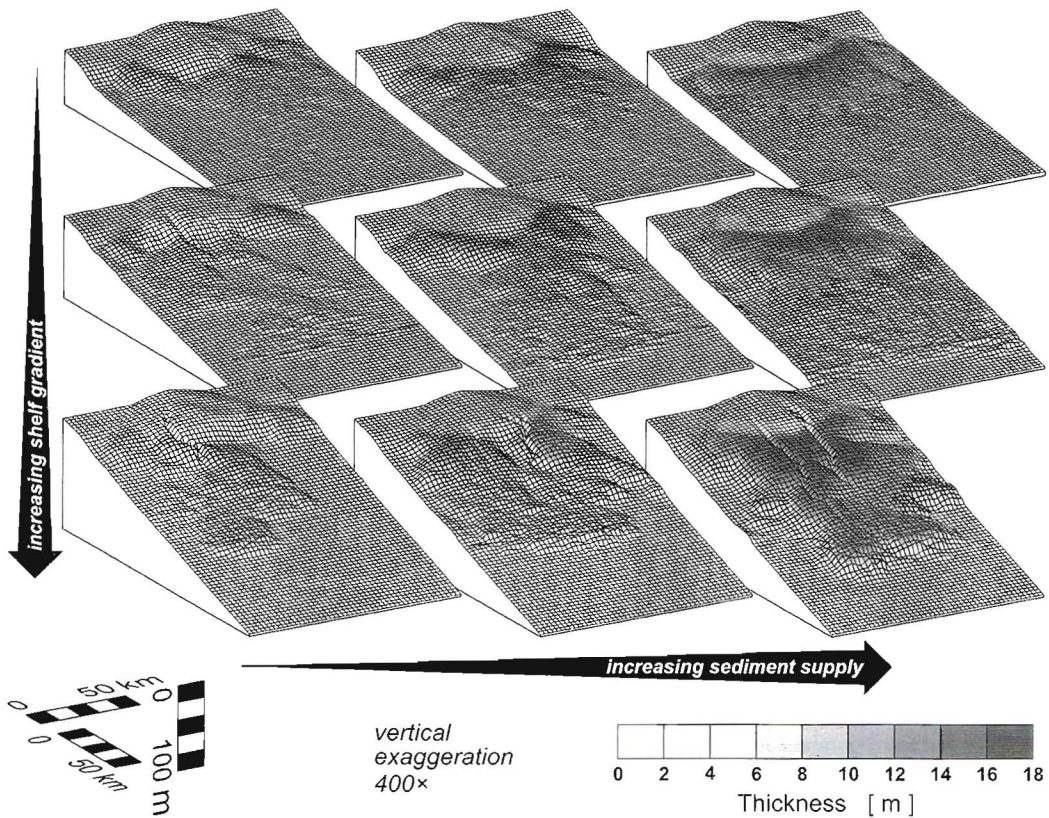


Fig. 4.11 — Surface plots of the coastal prism and shelf produced with the gradient scenarios (Table 4.2), illustrating the relation between preservation of the coastal prism and the shelf gradient following sea-level fall, and how this relation is modified by varying sediment supply. The shelf gradient is less steep, equally steep or steeper than the coastal prism, respectively from top to bottom. The coastline is indicated with a thick line. The depth of incision decreases landward and basinward of the highstand delta rim (Posamentier *et al.*, 1992; Talling, 1998; Törnqvist *et al.*, 2000). The maximum depth of incision increases with increasing shelf gradient and with decreasing sediment supply.

of incision may occur that is more widespread, and which will decrease preservation further. Only in situations where the shelf break is relatively deep or the shelf exceptionally wide, do major cross-shelf incision fail to occur and the formation of large hiatuses is restricted to the inner shelf and coastal prism (Talling, 1998; Wallinga, 2001 ch. 10). An additional influence on the preservation of the coastal prism which is likely to occur is river erosion owing to changes in the palaeohydrology as a result of climate change in the drainage basin (Blum & Price, 1998; Blum & Törnqvist, 2000).

Supply scenarios

Sea level may be the most important driving force in coastal areas (Posamentier & James, 1993; Blum & Törnqvist, 2000), the amount of sediment supply can modify its effect on the formation and preservation of stratigraphy (Schlager, 1993; Posamentier & Allen, 1993). In this section, the model results of a number of scenarios of discharge and sediment load are discussed in terms of morphological development and processes that control preservation, that are distinct from the standard scenario.

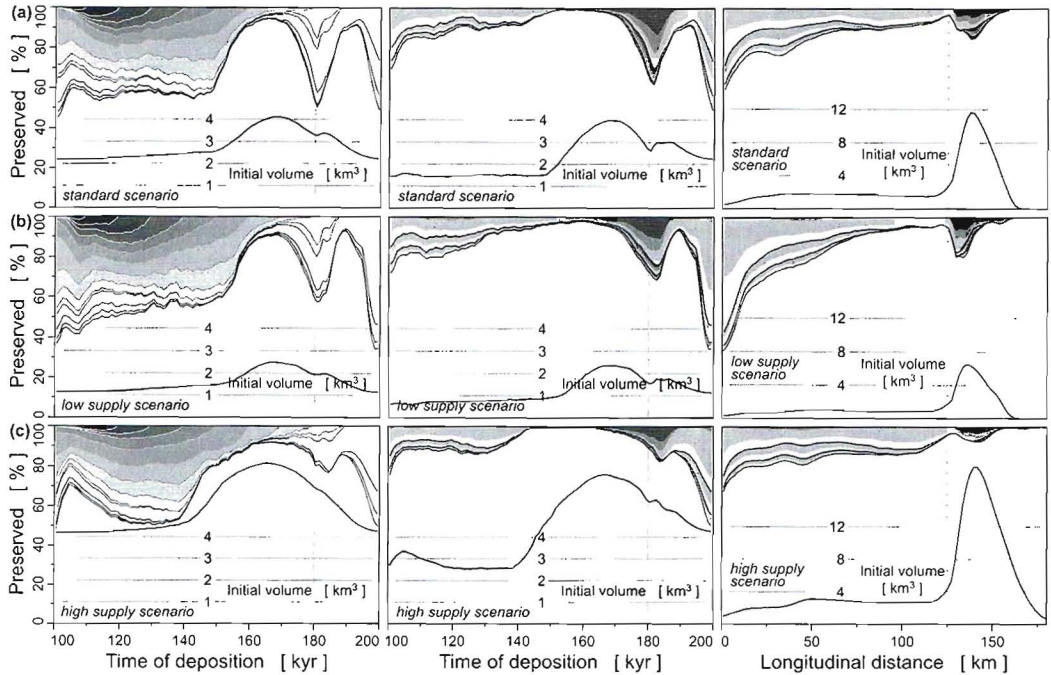


Fig. 4.12 — The volume and preservation of strata of the second glacial–interglacial cycle through time for the standard and two supply scenarios (Table 4.2). The graphs on the left are similar to Fig. 4.5, those in the middle to Fig. 4.6, and the ones on the right to Fig. 4.7. Also indicated in light grey are the shapes of the respective supply curves. a) The standard scenario. b) The ‘low supply scenario’. c) The ‘high supply scenario’.

In the ‘low supply scenario’ (Table 4.2), sediment load and discharge are halved with respect to the standard scenario. As a consequence of low supply, there is less progradation and aggradation at initial highstand. Furthermore, because of slow deltaic deposition, relatively steep gradients arise on the inner shelf as the sea-level fall forces the coastline to migrate basinward, which promotes (small-scale) incision despite the low discharge. The thin forced regressive wedge, as well as underlying deposits from earlier glacial–interglacial cycles, is greatly affected by river incision (Posamentier & Morris, 2000) (Fig. 4.12b). The local, rain-fed drainage system on the shelf plays a more important role relative to the discharge from the hinterland. The system is not able to reverse retrogradation and start progradation before the end of the cycle, and there is a funnel-shaped river mouth at final highstand (Talling, 1998).

Also fluvial onlap does not reach as far up the river as in the standard scenario, and downward profile adjustment still continues during the early part of the following cycle. Because the incised valleys are not filled completely during transgression, there is a greater influence of antecedent topography on the development of forced regressive deposits during the subsequent sea-level fall. When the supply is double the standard value, as in the ‘high supply scenario’ (Table 4.2), rapid, forced progradation occurs that is not as strongly dictated by sea-level fall. Protruding delta lobes reach the shelf edge as soon as ~40 kyr into the cycle, resulting in increased preservation of subsequent upper continental slope deposits (Fig. 4.12c, left). The high erosive capacity of rivers causes relatively prominent incision before the shelf break emerges. The thickness of the forced regressive wedge is considerably more than in

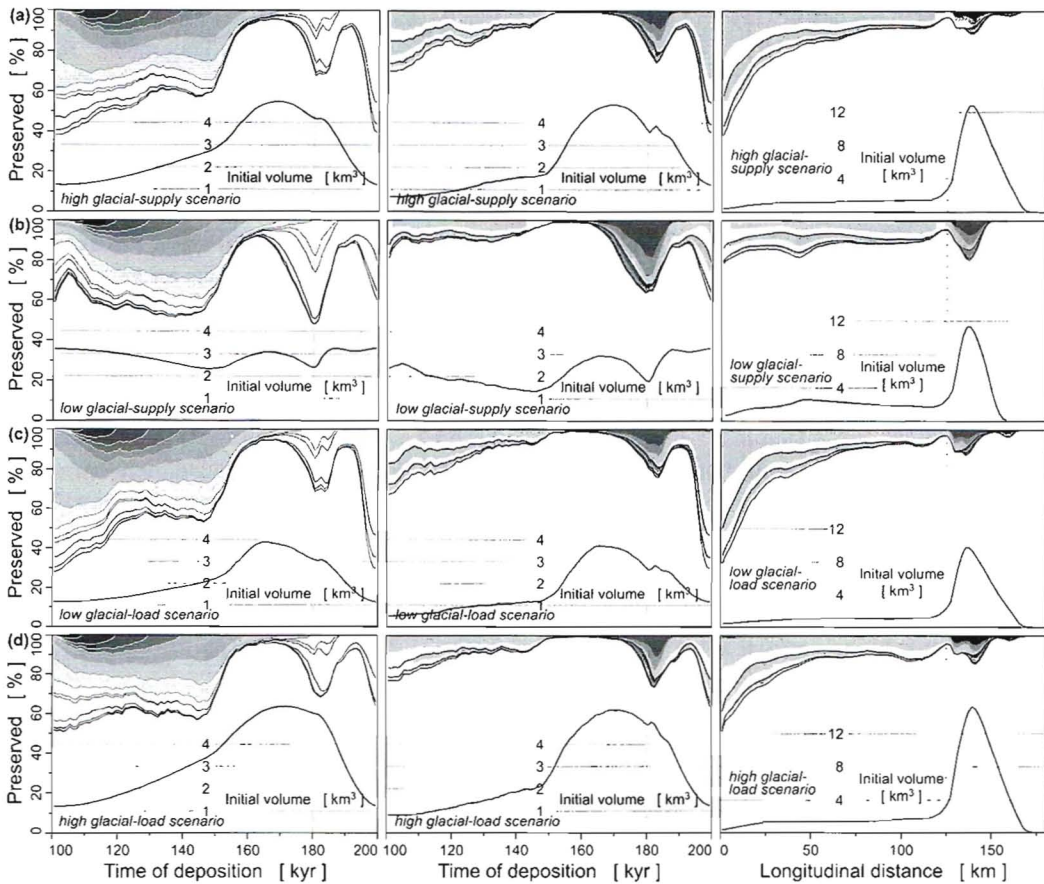


Fig. 4.13 — The volume and preservation of strata of the second glacial–interglacial cycle through time for four supply scenarios (Table 4.2). The graphs on the left are similar to Fig. 4.5, those in the middle to Fig. 4.6, and the ones on the right to Fig. 4.7. Also indicated in light grey are the shapes of the respective supply curves. a) The ‘high glacial-supply scenario’. b) The ‘low glacial-supply scenario’. c) The ‘low glacial-load scenario’. d) The ‘high glacial-load scenario’

the ‘low supply scenario’, which leads to deep river erosion. Fast fluvial onlap and highstand progradation produce a voluminous coastal prism (Talling, 1998).

The ‘high glacial-supply scenario’ (Table 4.2) has a sinusoidally increasing sediment load and discharge from the hinterland. The model results combine features of the ‘low supply scenario’ during interglacial periods and the ‘high supply scenario’ during glacials. The opposite is the case for the ‘low glacial-supply scenario’ (Table 4.2), which has a decreased supply during glacial times. The relatively low rate of sedimentation during initial highstand in

the former scenario results in low preservation of inner shelf strata (Fig. 4.13a). In both scenarios the supplied discharge and sediment load were changed proportionally, keeping carrying capacity and river load balanced, except for changes en route to the river mouth. However, in the ‘low glacial-load scenario’ (Table 4.2), the discharge increases more than the drainage basin yield, resulting in a tendency for rivers to pick up sediment and lower their gradient. Moderate incision occurs steadily during sea-level fall in response to the increasing undercapacity, and subsequent major incision after emergence of the shelf

break results in a relatively low preservation of inner shelf deposits (Fig. 4.13c). In contrast, in the 'high glacial-load scenario' (Table 4.2), the increased yield in proportion to the water discharge leads to overcapacity of the rivers. Rivers are less inclined to incise, and even show local aggradation during forced regression, making mid-shelf river avulsions, as opposed to avulsions on the downstream active delta, more likely to occur. Knickpoint migration from the shelf edge landward is slow and since the achieved equilibrium gradient is steeper than in the standard scenario, knickpoints do not reach as far upstream. Because of this tardy connection, deposits in the transfer-valley are relatively well preserved and more shelf-edge deltas remain active during lowstand. In this scenario, there is an overall greater preservation of deposits on the shelf (Fig. 4.13d).

Concluding remarks

The nature of Quaternary glacio-eustasy favours the formation of depositional units with a relatively low preservation potential, despite the fact that the sediment accumulates on a constantly subsiding basin margin. Because positions of coastlines are repeatedly reoccupied during a succession of

glacial–interglacial cycles, strata must regularly endure cannibalization. The model results show that preservation of deposits from a glacial–interglacial cycle varies both spatially and in time, dependent on the palaeohydrology (discharge and sediment supply), sea-level change and its relation to the surface morphology. There is a marked difference in preservation between deposits on the shelf and the continental slope, which has consequences for basin-scale grain-size sorting (see Ch. 3).

The model results presented here are largely conceptual. In the future, data sets will become available that allow further elaboration of the model and that will lend more empirical support. Given the importance of lateral and temporal variability illustrated in this chapter, these data sets will need to be three-dimensional (i.e., it should be able to yield volumetric data), covering the coastal plain, continental shelf and continental slope, and have good age constraints.

Unravelling the history of deposition on a basin margin is not a straightforward task, especially for Quaternary deposits generated under the influence of drastic base-level fluctuations and shoreline shifts. However, eventually, this research may aid in interpreting the stratigraphy of passive continental margins in terms of sediment yield from the hinterland, which then can be related to climate changes.

Conclusions

Synthesis

A three-dimensional numerical model has been constructed to study passive margin development under conditions that were prevalent during the Quaternary. In this thesis, it was used to examine the dynamics of the sedimentary system and its effect on the formation of stratigraphic successions. By incorporating only a few simple rules of sediment transport, the model unites many principle features of the sequence stratigraphic framework and puts forward other, less well-known characteristics. Awaiting empirical volumetric sediment budgets, the model has been used mainly as a heuristic tool. The solution space has been explored by running various model scenarios described in the previous chapters, and many more. The following is a synthesis of the results of the research of this thesis.

After initially being underappreciated (e.g. Miall, 1991; Wescott, 1993; Schumm, 1993), the role of continental processes in the development of passive margin stratigraphy has now been acknowledged, and fluvial strata have been assimilated into the sequence stratigraphic framework (Wright & Marriott, 1993; Zaitlin *et al.*, 1994; Shanley & McCabe, 1994; Quirk, 1996). The notion that both relative sea level and the effects of climate change in the hinterland play a role in the evolution of passive margins is widely recognized. Furthermore, the fact that river dynamics are an integral part of the sedimentary system of basin margins implies that the fluvial and marine environments should be studied as a whole. Naming the allogenic force that governs the system is complicated by such a comprehensive

approach, however, as it varies in space and through time. Therefore, a number of considerations have to be made when discussing whether the development of sedimentary systems during Quaternary glacial cycles has been dominated by relative sea-level change or whether climatic factors had ascendance over sea level. Firstly, what stage of the system's development is examined (e.g. at what stage of a cycle)? Secondly, what is the location within the system's geography (e.g. in which reach of the river or proximity of the coast)? And thirdly, at what temporal and spatial scales is the system evaluated?

At the large scale of the entire system modelled in this thesis over an entire glacial–interglacial cycle, relative sea level is without a doubt dominant. A good argument of the dominance for the sea today is that the greater part of passive margins are presently covered by tens of metres of seawater. During rise, the sea extends its influence upstream by inducing valley fill and the construction of a coastal wedge. During shelf emergence, on the other hand, river belts adapt their longitudinal profiles to a lowering base level, creating relief on the shelf that incites further erosion and sediment transport. Thus, the effect of sea-level fall moves inland until it dissipates.

The effect of palaeohydrology (discharge and sediment yield), the hinterland response to climate, is discernible in the model by modifications of the process activity, such as the persistence of aggradation and onset of incision, the avulsion frequency, achievement of drainage connection, and the timing of the reversal from lowstand progradation to retrogradation, and vice versa during highstand (Ch. 3 and 4). These variations are by no means negligible. However, seeing that the object of the research in this thesis was to study

the large-scale characteristics of passive continental margins, they are subordinate to the overall trend of development which is dictated by sea-level change. Supply and subsidence are eclipsed by the very high rates of Quaternary sea-level fluctuation most of the time. Nevertheless, someone interested in constituent systems on passive margins on a smaller spatial scale than the entire margin, e.g. river profiles or coasts, will find that palaeohydrology has an essential role in their development. Similarly, someone who studies lowlands over a short time-scale, e.g. during the Holocene, will not be inclined to consider the shelf as part of his area of interest and thus will make a different evaluation of the importance of sea-level change.

Finally, besides the scale and focus of the observation, the relative influence of a sea-level change is also determined by the morphology of the basin margin. Whether or not the shelf break emerges above sea level is a pivotal threshold in the system development. For instance, when an alternative sea-level curve with lower amplitude was applied (Ch. 3 and 4), the system responded quite differently. Similarly, the control of sea-level change will extend less far upstream for basin margin configurations with steep shelves and in exceptional cases such as the low-gradient but extremely wide North Sea shelf (Wallinga, 2001 ch. 10).

The evolution of landscape morphology and stratigraphy along passive continental margins under Quaternary glacio-eustatic conditions is very dynamic. It is a three-dimensional problem, and the fates of the non-marine and marine realms are closely linked. Therefore, when modelling such a system, fluvial and paralic processes should be given particular notice. For the benefit of the incorporation of realistic river dynamics into future models more study of the lower reach of rivers over long ($> 10^3$ yr) time scales is desirable.

The evolution of the drainage pattern

during falling sea level is largely determined by avulsion behaviour. The occurrence of avulsions is correlated to local aggradation rate, which decreases overall when sea-level fall accelerates (Ch. 2). Active deltas become the main areas where avulsions take place. They lead to the formation of distributaries and occasionally cause delta-lobe switching. Avulsion is kept in check by the formation of incisions, restraining channel belts within their valleys. Rivers are inclined to incise because their longitudinal profiles steepen when convex topographic features emerge during fall, starting with the coastal prism, followed by delta lobes on the shelf and finally, dependent on the depth of the shelf break relative to the lowstand sea level, the shelf edge. Forced regressive deposition will reduce the gradient in front of an emerging delta structure, and hence the need for rivers to incise (Ch. 4). Moreover, many researchers have argued that rivers can respond to changes in conditions, such as the emergence of the shelf with a different regional gradient, by processes other than incision (e.g. Schumm, 1993; Wescott, 1993; Leeder & Stewart, 1996). Adapting the characteristics of the river can accommodate changes as well. In order to take this notion into account, a geomorphic threshold on incision, dependent on water discharge and slope, has been incorporated into the model (Ch. 2). It limits river erosion to relatively minor incision in the coastal prism with decreasing depth upstream and downstream, and shallow valleys in discontinuous reaches on the exposed shelf, for a long time during falling sea-level stage. Major incision is postponed until sea level falls below the shelf break. Then, the emergence of the steep upper continental slope compels rivers to cut down into the shelf, resulting in a rejuvenation of the drainage network that propagates upstream. A succession of knickpoints arises at the coastline at the shelf edge under the influence of continuing relative sea-level fall and shelf-delta activity. The train of knickpoints migrates upstream and results in surges of

erosion in the channel belts alternating with phases of non-deposition which may turn to deposition and subsequent local terrace formation in response to palaeohydrological (climate-related) changes. Finally, drainage connection (Ch. 2) prompts the definitive cessation of avulsion activity on the shelf, at least until sea-level rise. The time lag between the formation of the first knickpoint and the achievement of drainage connection is too long (in the order of 10^4 yr, depending on the dimensions of the system) to be considered instantaneous on the scale of glacial–interglacial cycles.

During forced regression, the trajectory of the coastline for the applied margin configuration is such that it allows no widespread aggradation despite progradation. Little sedimentation occurs on the shelf after emergence; sediment is primarily deposited subaqueously in the frontal parts of the deltas. Therefore, the hiatus between falling stage and transgressive deposits is at least comparable to the time of exposure which increases from the shelf edge landwards. However, the interval is increased where a subaerial erosional unconformity has formed and will be increased further by transgressive wave ravinement. Topographic gradients on the shelf are relatively low except at the shelf edge and adjacent to incised valleys. Therefore, the formation of the subaerial erosional unconformity away from the shelf edge is governed by fluvial incision, either by the main drainage system or by secondary, rain-fed tributaries. The depth of incision decreases upstream and channel belts can be abandoned after drainage connection. Furthermore, erosion of the valley walls continues when fluvial onlap occurs on the valley floor in response to relative sea-level rise. The combination of the above features results in great lateral variation in the diachroneity of the unconformity.

The formation of a subaerial erosional unconformity is also, together with degradation

of the shelf edge, an important phenomenon that determines the preservation potential of deposits on passive continental margins (Ch. 4). Preservation of shelf strata is related to the proximity to the drainage network and the depth of incision. Since the presence of a channel belt is certain and the convex shape of the coastal prism encourages incision, highstand delta-complexes are likely to be subject to reworking. In general, the preservation potential increases with burial depth. The deposits laid down on the shelf during forced regression are deltaic, coarsening-up successions (Ch. 3). When these deposits are eroded, the coarse delta-topsets are more predisposed to cannibalization than the fine foresets. The sediment is carried by rivers to the shelf edge which enriches the shelf-edge deposits with coarse material and reduces the coarse sediment content on the shelf. In this manner, the formation of a subaerial erosional unconformity is a driving mechanism in basin-scale grain-size sorting (Ch. 3).

Understanding the evolution of the drainage pattern during a glacial–interglacial cycle is not only important to describe the development of the terrestrial environment. The drainage pattern also determines the location of sediment supply to the coastline. Thus, it controls for a large part the stratigraphic architecture, and more specifically, the presence of coarse-grained bodies in transgressive valley-fills and shelf-edge deltas, and their interconnectedness (Ch. 3). Therefore, especially in three dimensions, river dynamics are crucial for predictive modelling of reservoir rock.

Modelling in three spatial dimensions, instead of only two, involves a dramatic increase of the system complexity: the additional degree of freedom accentuates non-linear behaviour. The sensitive dependence on initial conditions entails that a relatively small-scale event may be sufficient to let a sedimentary system evolve differently

under the same circumstances with the same forcing factors. For instance, a single upstream avulsion event is enough to shift the depocentre over tens of kilometres, resulting in a different stratigraphic architecture than if the avulsion would not have occurred. In the studies performed in this thesis, random noise on the initial topography was used to demonstrate non-linear behaviour (Ch. 2). Geologists are aware that antecedent topography that has contributed to a system's development is never accurately known and that it is more often completely unknown. Beside small differences in topography, there are also other conditions, for example of a tectonic, meteorological or biological nature, which can induce similar chaotic effects in a sedimentary system. Since models of chaotic systems can not make detailed predictions (or 'postdictions') in a deterministic sense, they should be used to gain insight into the system by using a statistical approach. Therefore, the emphasis in this thesis was on the statistics of a large number of model runs, such as the mean response and its variance. Statistical analyses, supported by statistical field data, provide generic knowledge on how a sedimentary system works and show the probability of system development.

Concluding remarks

The development of passive continental margins outlined in the three studies in this thesis has some characteristics that are

inextricably bound up with the conditions during Quaternary glacial–interglacial cycles, and glacio-eustasy in particular. The sequence stratigraphic concept was never intended to be a template, but should rather be applied as a tool or approach (Posamentier & James, 1993). It consists of basic principles, which need to be modified to suit local factors. Still, Quaternary glacial–interglacial cycles represent an assemblage of circumstances that are markedly different from those during non-glacially driven ('third order') cycles covering a few million years. Although it is generally bad practice to exchange a general concept for several restrictive schemes, it may be useful to have an adapted subsidiary version for use in Quaternary basin margin stratigraphy. Because the Quaternary is in the recent geological past, it receives relatively much attention and offers the best chance to reliably reconstruct the intensity of the driving forces from sources independent of stratigraphy. Promising initiatives to gather comprehensive data sets, like the Strataform projects and the MARGINS Source-to-Sink program, are currently being undertaken and will be very beneficial for the advance of numerical modelling. It may be practical to compare empirical Quaternary prototypes with a detailed Quaternary concept that is already in the proper context. In such a model, more attention could be given to sedimentological processes (e.g. river avulsion and autocyclicity) and sedimentological characteristics (e.g. grain size) in the evolution of the sedimentary system.

References

- Ainsworth, R. B., Bosscher, H. & Newall, M. J. (2000) Forward stratigraphic modelling of forced regressions: evidence for the genesis of attached and detached lowstand systems. In: *Sedimentary Responses to Forced Regressions* (Ed. by D. Hunt and R. L. Gawthorpe), *Geol. Soc. Spec. Publ.*, **172**, 163-176.
- Anderson, J. B., Abdulah, K., Sarzalejo, S., Siringan, F. & Thomas, M. A. (1996) Late Quaternary sedimentation and high-resolution sequence stratigraphy of the east Texas shelf. In: *Geology of Siliciclastic Shelf Seas* (Ed. by M. De Batist and P. Jacobs), *Geol. Soc. Spec. Publ.*, **117**, 95-124.
- Angevine, C. L., Heller, P. L. & Paola, C. (1990) Quantitative sedimentary basin modeling. *AAPG Continuing Education Course Note Series*, **32**.
- Aslan, A. & Blum, M. D. (1999) Contrasting styles of Holocene avulsion, Texas Gulf Coastal Plain, USA. In: *Fluvial Sedimentology VI* (Ed. by N. D. Smith and J. Rogers), *Spec. Publ. Int. Assoc. Sedim.*, **28**, 193-209.
- Berger, W. H., Yasuda, M. K., Bickert, T., Wefer, G. & Takayama, T. (1994) Quaternary time scale for the Ontong Java Plateau: Milankovitch template for Ocean Drilling Program Site 806. *Geology*, **22**, 463-467.
- Bitzer, K. & Harbaugh, J. W. (1987) DEPOSIM: a Macintosh computer model for two-dimensional simulation of transport, deposition, erosion, and compaction of clastic sediments. *Comput. Geosci.*, **13**, 611-637.
- Bledsoe, B. P. & Watson, C. C. (2001) Logistic analysis of channel pattern thresholds: meandering, braiding, and incising. *Geomorphology*, **38**, 281-300.
- Blum, M. D. & Price, D. M. (1998) Quaternary alluvial plain construction in response to glacio-eustatic and climatic controls, Texas Gulf Coastal Plain. In: *Relative Role of Eustasy, Climate, and Tectonism in Continental Rocks* (Ed. by K. W. Shanley and P. J. McCabe), *Spec. Publ. Soc. Econ. Paleont. Miner.*, **59**, 31-48.
- Blum, M. D. & Törnqvist, T. E. (2000) Fluvial responses to climate and sea-level change: a review and look forward. *Sedimentology*, **47**, 2-48.
- Bridge, J. S. (1993) The interaction between channel geometry, water flows, sediment transport and deposition in braided rivers. In: *Braided Rivers* (Ed. by J. L. Best and C. S. Bristow), *Geol. Soc. Spec. Publ.*, **75**, 13-71.
- Bryant, M., Falk, P. & Paola, C. (1995) Experimental study of avulsion frequency and rate of deposition. *Geology*, **23**, 365-368.
- Burgess, P. M. & Allen, P. A. (1996) A forward-modelling analysis of the controls on sequence stratigraphical geometries. In: *Sequence Stratigraphy in British Geology* (Ed. by S. P. Hesselbo and D. N. Parkinson), *Geol. Soc. Spec. Publ.*, **103**, 9-24.
- Burgess, P. M. & Hovius, N. (1998) Rates of delta progradation during highstands: consequences for timing of deposition in deep-marine systems. *J. Geol. Soc. London*, **155**, 217-222.
- Butcher, S. W. (1990) The nickpoint concept and its implications regarding onlap to the stratigraphic record. In: *Quantitative Dynamic Stratigraphy* (Ed. by T. A. Cross), 375-385.
- Coleman, J. M. (1976) *Deltas: processes of deposition & models for exploration*. Continuing Education Publication Company, Champaign, 102 pp.
- Coleman, J. M., Prior, D. B. & Lindsay, J. F. (1983) Deltaic influences on shelfedge instability processes. In: *The shelfbreak: critical interface on continental margins* (Ed. by D. J. Stanley and G. T. Moore), *SEPM Spec. Publ.*, **33**, 121-137.
- Crave, A. & Davy, P. (2001) A stochastic "precipiton" model for simulating erosion/sedimentation dynamics. *Comp. & Geosci.*, **27**, 815-827.
- Den Bezemer, T., Kooi, H., Kranenborg, J. & Cloetingh, S. (2000) Modelling grain-size distributions. A comparison of two models and their numerical solution. *Tectonophysics*, **320**, 347-373.
- Emery, D. & Myers, K. J. (1996) *Sequence Stratigraphy*. Blackwell Science, Oxford, 297 pp.
- Ethridge, F. G., Wood, L. J. & Schumm, S. A. (1998) Cyclic variables controlling fluvial sequence development: problems and perspectives. In: *Relative Role of Eustasy, Climate, and Tectonism in Continental Rocks* (Ed. by K. W. Shanley and P. J. McCabe), *Spec. Publ. Soc. Econ. Paleont. Miner.*, **59**, 17-29.
- Figueiredo, A. G., Jr. & Nittrouer, C. A. (1995) New insights to high-resolution stratigraphy on the Amazon continental shelf. *Marine Geol.*, **125**, 393-399.

- Freeman, T. G. (1991) Calculating catchment area with divergent flow based on a regular grid. *Comp. & Geosci.*, **17**, 413-422.
- Galloway, W. E. (1989) Genetic stratigraphic sequences in basin analysis I: architecture and genesis of flooding-surface bounded depositional units. *AAPG Bull.*, **73**, 125-142.
- Gensous, B. & Tesson, M. (1996) Sequence stratigraphy, seismic profiles, and cores of Pleistocene deposits on the Rhône continental shelf. *Sedim. Geol.*, **105**, 183-190.
- Goodbred, S. L. & Kuehl, S. A. (2000) Enormous Ganges-Brahmaputra sediment discharge during strengthened early Holocene monsoon. *Geology*, **28**, 1083-1086.
- Granjeon, D. & Joseph, P. (1999) Concepts and applications of a 3-D multiple lithology, diffusive model in stratigraphic modeling. In: *Numerical Experiments in Stratigraphy: Recent Advances in Stratigraphic and Sedimentologic Computer Simulations* (Ed. by J. W. Harbaugh, W. L. Watney, E. C. Rankey, R. Slingerland, R. H. Goldstein and E. K. Franseen), *SEPM Spec. Publ.*, **62**, 197-210.
- Heckel, P. H. (1986) Sea-level curve for Pennsylvanian eustatic marine transgressive-regressive depositional cycles along midcontinent outcrop belt, North America. *Geology*, **14**, 330-334.
- Heller, P. L., Burns, B. A. & Marzo, M. (1993) Stratigraphic solution sets for determining the roles of sediment supply, subsidence, and sea level on transgressions and regressions. *Geology*, **21**, 747-750.
- Hernández-Molina, F. J., Somoza, L. & Lobo, F. (2000) Seismic stratigraphy of the Gulf of Cádiz continental shelf: a model for Late Quaternary very high-resolution sequence stratigraphy and response to sea-level fall. In: *Sedimentary Responses to Forced Regressions* (Ed. by D. Hunt and R. L. Gawthorpe), *Geol. Soc. Spec. Publ.*, **172**, 329-362.
- Hodell, D. A., Elmstrom, K. M. & Kennett, J. P. (1986) Latest Miocene benthic $\delta^{18}\text{O}$ changes, global ice volume, sea level and the 'Messinian salinity crisis'. *Nature*, **320**, 411-414.
- Jones, L. S. & Schumm, S. A. (1999) Causes of avulsion: an overview. In: *Fluvial Sedimentology VI* (Ed. by N. D. Smith and J. Rogers), *Spec. Publ. Int. Assoc. Sedim.*, **28**, 171-178.
- Kooi, H. & Beaumont, C. (1996) Large-scale geomorphology: classical concepts reconciled and integrated with contemporary ideas via a surface processes model. *J. Geophys. Res.*, **101**, 3361-3386.
- Koss, J. E., Ethridge, F. G. & Schumm, S. A. (1994) An experimental study of the effects of base-level change on fluvial, coastal plain and shelf systems. *J. Sedim. Res.*, **B64**, 90-98.
- Leeder, M. R. (1997) Sedimentary basins: tectonic recorders of sediment discharge from drainage catchments. *Earth Surf. Proc. Land.*, **22**, 229-237.
- Leeder, M. R., Harris, T. & Kirkby, M. J. (1998) Sediment supply and climate change: implications for basin stratigraphy. *Basin Res.*, **10**, 7-18.
- Leeder, M. R. & Stewart, M. D. (1996) Fluvial incision and sequence stratigraphy: alluvial responses to relative sea-level fall and their detection in the geological record. In: *Sequence Stratigraphy in British Geology* (Ed. by S. P. Hesselbo and D. N. Parkinson), *Geol. Soc. Spec. Publ.*, **103**, 25-39.
- Lorenz, E. N. (1993a) Chaos and limitations to prediction. *Abstracts with Programs - Geol. Soc. Am.*, **25**, 251.
- Lorenz, E. N. (1993b) *The Essence of Chaos*. UCL Press, London, 227 pp.
- Maynard, J. R. & Leeder, M. R. (1992) On the periodicity and magnitude of Late Carboniferous glacio-eustatic sea-level changes. *J. Geol. Soc.*, **149**, 303-311.
- Miall, A. D. (1991) Stratigraphic sequences and their chronostatigraphic correlation. *J. Sedim. Petrol.*, **61**, 497-505.
- Miall, A. D. (1995) Whither stratigraphy? *Sed. Geol.*, **100**, 5-20.
- Mulder, T. & Syvitski, J. P. M. (1996) Climatic and morphologic relationships of rivers: implications of sea-level fluctuations on river loads. *J. Geol.*, **104**, 509-523.
- Nummedal, D., Riley, G. W. & Templet, P. L. (1993) High-resolution sequence architecture: a chronostratigraphic model based on equilibrium profile studies. In: *Sequence Stratigraphy and Facies Association* (Ed. by H. W. Posamentier, C. P. Summerhayes, B. U. Haq and G. P. Allen), *Spec. Publ. Int. Assoc. Sedim.*, **18**, 55-68.
- Orton, G. J. & Reading, H. G. (1993) Variability of deltaic processes in terms of sediment supply, with particular emphasis on grain size. *Sedimentology*, **40**, 475-512.
- Paola, C. (2000) Quantitative models of sedimentary basin filling. *Sedimentology*, **47**, 121-178.
- Paola, C., Heller, P. L. & Angevine, C. L. (1992) The large-scale dynamics of grain-size variation in alluvial basins, 1: theory. *Basin Res.*, **4**, 73-90.
- Pillans, B., Chappell, J. & Naish, T. R. (1998) A review of the Milankovitch climatic beat: template for Plio-Pleistocene sea-level changes and sequence stratigraphy. *Sedim. Geol.*, **122**, 5-21.

- Plint, A. G. (1988) Sharp-based shoreface sequences and 'offshore bars' in the Cardium formation of Alberta: their relationship to relative changes in sea level. In: *Sea-level changes: an integrated approach* (Ed. by C. K. Wilgus, B. S. Hastings, C. G. S. C. St Kendall, H. W. Posamentier, C. A. Ross and J. C. Van Wagoner), *Society of Economic Paleontologists and Mineralogists Special Publication*, **42**, 357-370.
- Plint, A. G. & Nummedal, D. (2000) The falling stage systems tract: recognition and importance in sequence stratigraphic analysis. In: *Sedimentary Responses to Forced Regressions* (Ed. by D. Hunt and R. L. Gawthorpe), *Geol. Soc., London Spec. Publ.*, **172**, 1-17.
- Posamentier, H. W. & Allen, G. P. (1993) Variability of the sequence stratigraphic model: effects of local basin factors. *Sed. Geol.*, **86**, 91-109.
- Posamentier, H. W., Allen, G. P., James, D. P. & Tesson, M. (1992) Forced regressions in a sequence stratigraphic framework: concepts, examples, and exploration significance. *Am. Assoc. Petrol. Geol. Bull.*, **76**, 1687-1709.
- Posamentier, H. W. & James, D. P. (1993) An overview of sequence-stratigraphic concepts: uses and abuses. In: *Sequence Stratigraphy and Facies Associations* (Ed. by H. W. Posamentier, C. P. Summerhayes, B. U. Haq and G. P. Allen), *Spec. Publ. Int. Assoc. Sedim.*, **18**, 3-18.
- Posamentier, H. W., Jervey, M. T. & Vail, P. R. (1988) Eustatic controls on clastic deposition I: conceptual framework. In: *Sea-level Changes: An Integrated Approach* (Ed. by C. K. Wilgus, B. S. Hastings, C. G. S. C. St Kendall, H. W. Posamentier, C. A. Ross and J. C. Van Wagoner), *Spec. Publ. Soc. Econ. Paleont. Miner.*, **42**, 109-124.
- Posamentier, H. W. & Morris, W. R. (2000) Aspects of the stratal architecture of forced regressive deposits. In: *Sedimentary Responses to Forced Regressions* (Ed. by D. Hunt and R. L. Gawthorpe), *Geol. Soc. Spec. Publ.*, **172**, 19-46.
- Posamentier, H. W. & Vail, P. R. (1988) Eustatic controls on clastic deposition II: sequence and systems tract models. In: *Sea-level Changes: An Integrated Approach* (Ed. by C. K. Wilgus, B. S. Hastings, C. G. S. C. St Kendall, H. W. Posamentier, C. A. Ross and J. C. Van Wagoner), *Spec. Publ. Soc. Econ. Paleont. Miner.*, **42**, 125-154.
- Quirk, D. G. (1996) Base profile: a unifying concept in alluvial sequence stratigraphy. In: *High Resolution Sequence Stratigraphy: Innovations and Applications* (Ed. by J. A. Howell and J. F. Aitken), *Geol. Soc. Spec. Publ.*, **104**, 37-49.
- Ritchie, B. D., Hardy, S. & Gawthorpe, R. L. (1999) Three-dimensional numerical modeling of coarse-grained clastic deposition in sedimentary basins. *J. Geophys. Res.*, **104**, 17759-17780.
- Rivenæs, J. C. (1992) Application of a dual-lithology, depth-dependent diffusion equation in stratigraphic simulation. *Basin Res.*, **4**, 133-146.
- Salter, T. (1993) Fluvial scour and incision: models for their influence on the development of realistic reservoir geometries. In: *Characterization of Fluvial and Aeolian Reservoirs* (Ed. by C. P. North and D. J. Prosser), *Geol. Soc. Spec. Publ.*, **73**, 33-51.
- Schlager, W. (1993) Accommodation and supply - a dual control on stratigraphic sequences. *Sedimentary Geology*, **86**, 111-136.
- Schoorl, J. M., Sonneveld, M. P. W. & Veldkamp, A. (2000) Three-dimensional landscape process modelling: the effect of DEM resolution. *Earth Surf. Proc. Land.*, **25**, 1025-1034.
- Schumm, S. A. (1981) Evolution and response of the fluvial system, sedimentologic implications. In: *Recent and Ancient Nonmarine Depositional Environments: Models for Exploration* (Ed. by F. G. Ethridge and R. M. Flores), *Spec. Publ. Soc. Econ. Paleont. Miner.*, **31**, 19-29.
- Schumm, S. A. (1977) *The Fluvial System*. John Wiley & Sons, New York, 338 pp.
- Schumm, S. A. (1993) River response to baselevel change: implications for sequence stratigraphy. *J. Geol.*, **101**, 279-294.
- Schumm, S. A. (1998) *To Interpret the Earth: Ten Ways to be Wrong*. Cambridge University Press, Cambridge, 133 pp.
- Schumm, S. A., Mosley, M. P. & Weaver, W. E. (1987) *Experimental Fluvial Geomorphology*. John Wiley, New York.
- Schumm, S. A. & Parker, R. S. (1973) Implications of complex response of drainage systems for Quaternary alluvial stratigraphy. *Nature*, **243**, 99-100.
- Shanley, K. W. & McCabe, P. J. (1994) Perspectives on the sequence stratigraphy of continental strata. *Am. Ass. Petrol. Geol. Bull.*, **78**, 544-568.

- Slingerland, R. (1990) Predictability and chaos in quantitative dynamic stratigraphy. In: *Quantitative Dynamic Stratigraphy* (Ed. by T. A. Cross), 45-53.
- Smith, D. G. (1994) Cyclicity or chaos? Orbital forcing versus non-linear dynamics. In: *Orbital Forcing and Cyclic Sequences* (Ed. by P. L. De Boer and D. G. Smith), *Spec. Publ. Int. Assoc. Sedim.*, **19**, 531-544.
- Smith, P. (1998) *Explaining Chaos*. Cambridge University Press, Cambridge, 193 pp.
- Syvitski, J. P. M. & Daughney, S. (1992) Delta2: delta progradation and basin filling. *Comp. & Geosci.*, **18**, 839-897.
- Syvitski, J. P. M. & Hutton, E. W. H. (2001) 2D SEDFLUX 1.0C: an advanced process-response numerical model for the fill of marine sedimentary basins. *Comput. Geosci.*, **27**, 731-753.
- Talling, P. J. (1998) How and where do incised valleys form if sea level remains above the shelf edge? *Geology*, **26**, 87-90.
- Talling, P. J. & Sowter, M. J. (1998) Erosion, deposition and basin-wide variations in stream power and bed shear stress. *Basin Res.*, **10**, 87-108.
- Tebbens, L. A., Veldkamp, A., Van Dijke, J. J. & Schoorl, J. M. (2000) Modeling longitudinal-profile development in response to Late Quaternary tectonics, climate and sea-level changes: the River Meuse. *Global Planet. Change*, **27**, 165-186.
- Tetzlaff, D. M. (1990) Limits to the predictive ability of dynamic models that simulate clastic sedimentation. In: *Quantitative Dynamic Stratigraphy* (Ed. by T. A. Cross), 55-65.
- Tetzlaff, D. M. & Harbaugh, J. W. (1989) *Simulating Clastic Sedimentation*. Van Nostrand Reinhold, New York, 202 pp.
- Thomas, M. A. & Anderson, J. B. (1994) Sea-level controls on the facies architecture of the Trinity/Sabine incised-valley system, Texas continental shelf. In: *Incised-valley Systems: Origin and Sedimentary Sequences* (Ed. by R. W. Dalrymple, R. Boyd and B. A. Zaitlin), *Spec. Publ. Soc. Econ. Paleont. Miner.*, **51**, 63-82.
- Törnqvist, T. E., Wallinga, J., Murray, A. S., De Wolf, H., Cleveringa, P. & De Gans, W. (2000) Response of the Rhine-Meuse system (west-central Netherlands) to the last Quaternary glacio-eustatic cycles: a first assessment. *Global Planet. Change*, **27**, 89-111.
- Van den Berg, J. H. (1995) Prediction of alluvial channel pattern of perennial rivers. *Geomorphology*, **12**, 259-279.
- Van Heijst, M. W. I. M. & Postma, G. (2001) Fluvial response to sea-level changes: a quantitative analogue, experimental approach. *Basin Res.*, **13**, 269-292.
- Van Heijst, M. W. I. M., Postma, G., Meijer, X. D., Snow, J. N. & Anderson, J. B. (2001) Quantitative analogue flume-model study of river-shelf systems: principles and verification exemplified by the Late Quaternary Colorado river-delta evolution. *Basin Res.*, **13**, 243-268.
- Vanney, J. R. & Stanley, D. J. (1983) Shelfbreak physiography: an overview. In: *The shelfbreak: critical interface on continental margins* (Ed. by D. J. Stanley and G. T. Moore), *SEPM Spec. Publ.*, **33**, 1-24.
- Walling, D. E. & Webb, B. W. (1983) Patterns of sediment yield. In: *Background to Palaeohydrology* (Ed. by K. J. Gregory), pp. 69-100. John Wiley & Sons, Chichester.
- Wallinga, J. (2001) The Rhine-Meuse system in a new light: optically stimulated luminescence dating and its application to fluvial deposits. PhD Thesis, Utrecht University, Utrecht, 180 pp.
- Wescott, W. A. (1993) Geomorphic thresholds and complex response of fluvial systems – some implications for sequence stratigraphy. *Am. Assoc. Petrol. Geol. Bull.*, **77**, 1208-1218.
- Wood, L. J., Ethridge, F. G. & Schumm, S. A. (1993) The effects of rate of base-level fluctuation on coastal-plain, shelf and slope depositional systems: an experimental approach. In: *Sequence Stratigraphy and Facies Associations* (Ed. by H. W. Posamentier, C. P. Summerhayes, B. U. Haq and G. P. Allen), *Spec. Publ. Int. Assoc. Sedim.*, **18**, 43-53.
- Wright, V. P. & Marriott, S. B. (1993) The sequence stratigraphy of fluvial depositional systems: the role of floodplain sediment storage. *Sed. Geol.*, **86**, 203-210.
- Zaitlin, B. A., Dalrymple, R. W. & Boyd, R. (1994) The stratigraphic organization of incised-valley systems associated with relative sea-level change. In: *Incised-valley Systems: Origin and Sedimentary Sequences* (Ed. by R. W. Dalrymple, R. Boyd and B. A. Zaitlin), *SEPM Spec. Publ.*, **51**, 45-60.

Samenvatting

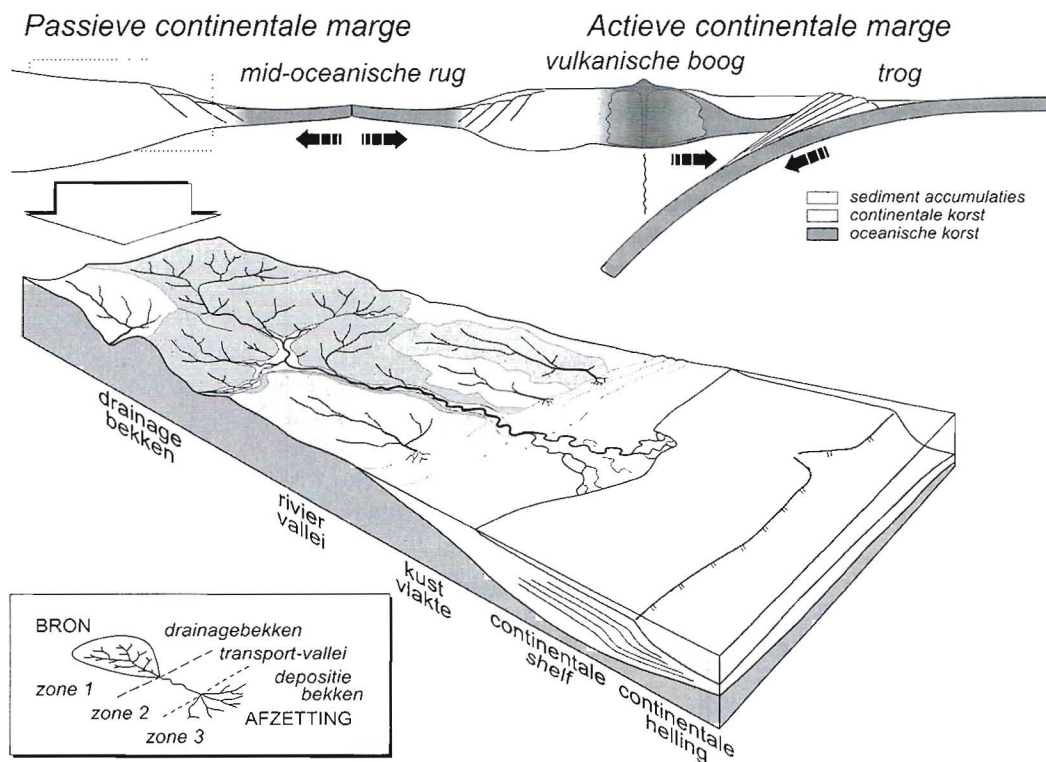
Algemene introductie

Als gevolg van continentverschuiving zijn de oceanen van de wereld omzoomd door enkele typen continentale marges met duidelijk verschillende korst configuraties. Eén van die oceanische bekkenrand-typen wordt gevormd na het opbreken van tektonische platen and spreiding van de zeebodem. Hierdoor ontstaan passieve continentale marges (Figuur 1), zogenoemd naar aanleiding van de relatieve afwezigheid van aardbevingen en vulkanische activiteit. Dit in tegenstelling tot actieve continentale marges die grenzen aan botsende plaatranden. Passieve marges worden gekenmerkt door enige initiële opheffing tijdens het opbreken gevolgd door hoofdzakelijk bekkendaling. Deze daling neemt bekkenwaarts toe vanaf een scharnierlijn en wordt minder in the loop van de tijd. Onder deze omstandigheden accumuleren sedimentopvolgingen tot enkele kilometers dikte over perioden van miljoenen jaren, waardoor de grootte van de continenten toeneemt.

Het Kwartair wordt gekenmerkt door de uitbreiding van permanente continentale ijsmassa's die reeds in het Tertair aanwezig waren. Het maakte grote variaties in het polaire ijsvolume en een afwisseling van oprukkend en terugwijkend ijs in Europa en Noord Amerika door. Dit resulteerde in grote zeespiegelveranderingen en een opeenvolging van intervallen met glaciële en interglaciële condities. De indeling van de Kwartaire stratigrafie is gebaseerd op deze fluctuaties. Wereldwijde klimaatveranderingen en 'glacio-eustasy', de wereldwijde verandering van zeeniveau als gevolg van de volumeverandering van continentale ijsmassa's en de gemiddelde zeewatertemperatuur, zijn op

een ingewikkelde manier gekoppeld en zijn gerelateerd aan Milankovitch insolatiecycli (bijv. Berger *et al.*, 1994). Zeespiegelschommelingen vinden plaats met een hoge frequentie, aanvankelijk met een periode van ~41 kyr, geassocieerd met het ritme van de variatie van de hoek van de aardas, totdat in het midden van het Pleistoceen de ~100 kyr cyclus, veroorzaakt door verandering van de excentriciteit van de aardbaan, dominant werd. Het verloop van zeespiegelverandering is gewoonlijk asymmetrisch, met een langzame daling tijdens de aangroei van de ijskappen en een snelle stijging tijdens het smelten. De amplitude ervan is groot, met een bereik van ~120 m tussen zeespiegelhoogstand en -laagstand. Van dergelijke glaciële episoden gedreven door astronomische cycli wordt verondersteld dat zij ook eerder in het Phanerozoicum hebben plaatsgevonden, zoals in het Permo-Carboon (bijv. Heckel, 1986; Maynard & Leeder, 1992) en het Neogeen (bijv. Hodell *et al.*, 1986; Pillans *et al.*, 1998).

De effecten van glaciële–interglaciële zeespiegel- en klimaatverandering op de morfologie van passieve continentale marges resulteren, wat de accommodatieruimte betreft, in een dynamisch sedimentair systeem. Door zeespiegelveranderingen vallen de laaglanden die bekend staan als het continentaal plat (*shelf*) herhaaldelijk droog en verdrinken vervolgens weer. Dit gaat gepaard met regressies en transgressies waarbij kustlijnen zich over grote afstanden respectievelijk zeewaarts en landwaarts verplaatsen over deze zogenaamde *shelves*. Dit gaat gepaard met verschuivingen van de plaats van depositie van riviersediment. De evolutie van een passieve marge die zeespiegelverandering ondergaat wordt ruwweg gekarakteriseerd door de transitie van een zeespiegelhoogstand situatie



Figuur 1 — Bovenaan, een overzicht van divergente en convergente plaatgrenzen en de respectievelijk passieve en actieve continentale marges die daaraan grenzen. In grote lijnen heeft een passieve marge een over het algemeen grote rivier die sediment uit een vaak ver gelegen drainagebekken naar de kust vervoert, waarbij onderweg sediment geërodeerd of afgezet wordt. De positie van de kustlijn wordt beïnvloed door zeespiegelveranderingen. Hier afgebeeld is een interglaciale situatie met een hoge zeespiegelstand, waarbij een delta wordt opgebouwd op een ondergelopen *shelf* (naar Van Heijst *et al.*, 2001). Tijdens glaciële perioden met een lagere zeespiegelstand ligt de kustlijn meer bekkenwaarts of zelfs langs de *shelf*-rand. De inzet linksonder toont een vereenvoudigde schets van een systeem van sediment productie, transport en depositie (naar Schumm, 1977). In dit proefschrift worden alleen zone 2 en in het bijzonder zone 3 behandeld.

waarbij depositie beperkt blijft tot hellingopwaartse gebieden en waarbij sediment nagenoeg geheel aan de verdronken continentale *shelf* en helling wordt onthouden, naar een situatie rond zeespiegellaagstand waarbij *shelf*-erosie en sedimentdoorvoer naar de *shelf*-rand mogelijk is — en weer terug. Dit zijn de grondbeginselen van het concept van de sequentie stratigrafie (Posamentier *et al.*, 1988; Galloway, 1989), die aangepast dienen te worden aan de specifieke omstandigheden van de glacio-eustatische cycli van het Kwartair.

Het doel van Sedimentologie is onder meer het verkrijgen van begrip van de rol van

sedimentaire processen in de ontwikkeling van stratigrafische opeenvolgingen. De twee complementaire aspecten van sedimentatie, proces en product, zijn daarbij belangrijk. Het doel van sequentie stratigrafie is het ontrafelen van de oorzakelijke verbanden tussen de evolutie van een sedimentair systeem en de drijvende krachten, zoals zeespiegelverandering, bekkendaling en sedimentaanvoer, om zodoende de geologische opeenvolging van facies (procesgerelateerde assemblages van sedimentaire eigenschappen) en sequenties (opeenvolgende afzettingsspakketten met vergelijkbare eigenschappen) te interpreteren. Ondanks de

problemen waarmee we geconfronteerd worden bij het volbrengen van deze opgave voor Kwartaire passieve continentale marges is er veel vooruitgang geboekt in de afgelopen decennia (Emery & Myers, 1996, ch. 1; Miall, 1995). De te nemen hindernissen zijn tweeledig.

Ten eerste, het samenstellen van een compleet en gedetailleerd beeld van de stratigrafische architectuur van een bekkenrand is moeilijk vanwege de grote oppervlakte en de laterale variabiliteit van het te bestuderen gebied. Daar komt bij dat het gebied bij de huidige zeespiegelstand bijna volledig onder water ligt. Dat bemoeilijkt het vergaren van velddata, maakt het buitengewoon kostbaar en legt derhalve beperkingen op wat betreft de hoeveelheid en het type informatie dat kan worden verzameld. Op dit moment zijn uitgebreide, driedimensionale stratigrafische datasets met goede leeftijdsbepalingen nauwelijks voorhanden. Bovendien, de intensiteit van processen in het verleden verschilt waarschijnlijk van die welke heden ten dage worden gemeten en bepaalde geomorfologische drempels worden onder huidige omstandigheden niet overschreden. Holocene fluxen zijn niet representatief voor een gehele glaciale–interglaciale cyclus, laat staan voor het gehele Kwartair. Omdat glaciale cycli wereldwijde gebeurtenissen zijn, is de substitutie van tijd en plaats niet van toepassing en zijn moderne analogen moeilijk of helemaal niet te vinden.

De tweede complicatie is een incompleet begrip van de mechanismen van sediment erosie, transport en depositie, en de moeilijkheid ze op te schalen naar lange tijd- en grote ruimtelijke schaal. De complexiteit is overweldigend door het enorme aantal variabelen dat in het spel is, bestaande uit fysische, chemische en biologische elementen, in een ruim assortiment van afzettingmilieus. Verder bemoeilijkt equifinaliteit, het begrip dat verschillende processen soortgelijke resultaten kunnen produceren (Schumm, 1998, p. 58; Heller *et al.*, 1993), het herkennen van

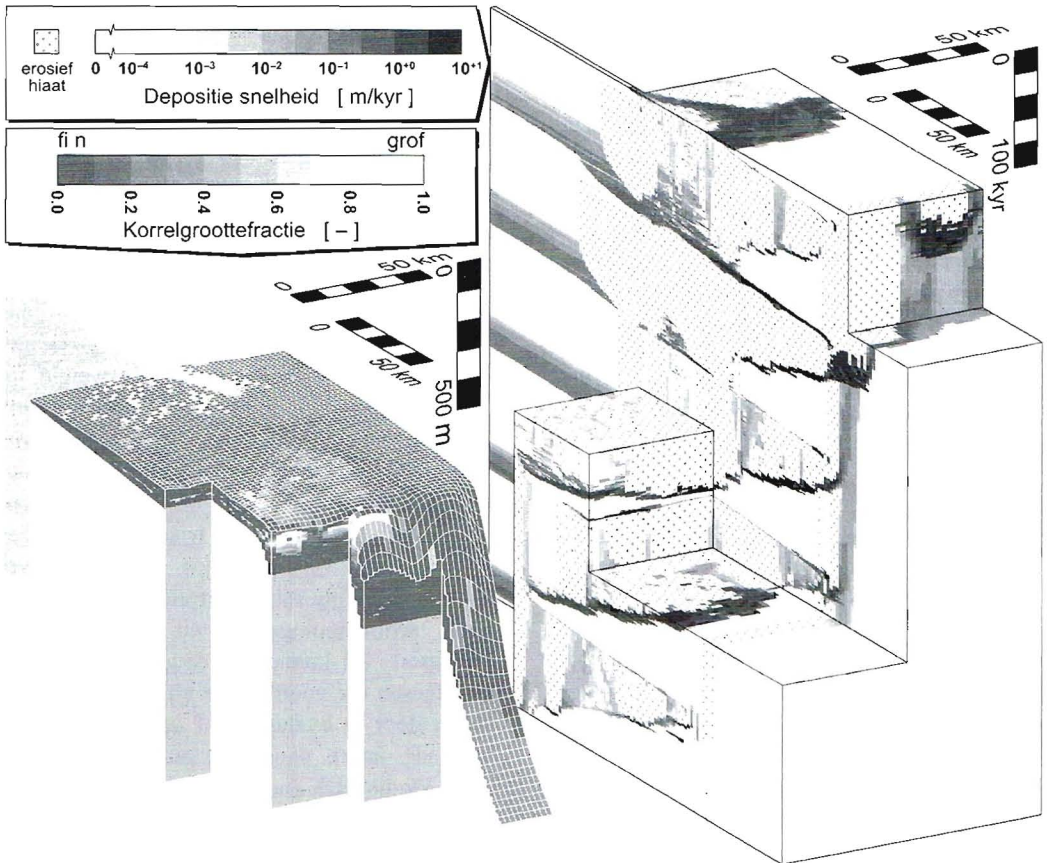
oorzakelijke verbanden. Ten slotte, de evolutie van sedimentaire systemen vertoont chaotisch, niet-lineair gedrag, met andere woorden gedrag met een sterke afhankelijkheid van initiële omstandigheden, zodat minieme afwijkingen in de initiële condities aanleiding kunnen zijn tot grote verschillen in product (Lorenz, 1993b; Smith, 1998). De interactie tussen drijvende en afremmende deelprocessen is zo ingewikkeld en vergeven van terugkoppelingen dat het onderscheid tussen oorzaak en gevolg verloren gaat (Slingerland, 1990; Smith, 1994) en de ontwikkelingen die zich voordoen slechts in beperkte mate voorspelbaar zijn. Dergelijke chaotische processen komen veel voor in de natuur (Tetzlaff, 1990; Lorenz, 1993a) en zeker in sedimentaire systemen.

Modellering is een bruikbare ondersteuning bij het onderzoek van sedimentaire systemen op passieve continentale marges (Emery & Myers, 1996, ch. 12; Paola, 2000). Aanvankelijk was de aard van de Sedimentologie voornamelijk beschrijvend. Zoals in alle natuurwetenschappen was de eerste prioriteit van Sedimentologen een grondige inventarisatie en catalogus van de wereld te maken. Sindsdien is het zwaartepunt echter gestadig verschoven van kwalitatief naar kwantitatief onderzoek, een trend die zich in de toekomst zal voortzetten. Modellen zijn een additioneel instrument naast empirische studies, en bieden een kwantitatieve aaneenschakeling van algemeen geaccepteerde, losse sedimentologische en stratigrafische principes. Zij kunnen de deugdelijkheid van hypothesen die voortkomen uit veldonderzoek testen door te evalueren of deze hypothesen haalbaar, intern consistent en waarschijnlijk zijn. Methodisch onderzoek over een volledig bereik van variabelen kan hiaten in de kennis aantonen en kan verdere vergaring van gegevens sturen. De voorspellende verdienste van grootschalige en lange termijn modellen van passieve marge sequentie stratigrafie, is in principe de interpretatie van de huidige

lithologie en stratigrafische architectuur (Posamentier & James, 1993), het product van de evolutie in het verleden, en niet de toekomstige ontwikkeling. Bijvoorbeeld, een voorspelling van hetgeen zal gebeuren met continentale *shelves* in de komende 100 000 jaar heeft geen prioriteit, in tegenstelling tot voorspellingen van korte termijn ontwikkelingen op basis van (rivier-, kust- of delta) modellen.

Wetenschappelijk onderzoek wordt in de eerste plaats gedaan om een volledig begrip van de natuur te verkrijgen; met andere woorden, om onze 'wetenschappelijke nieuwsgierigheid'

te bevredigen. In dit geval willen we weten hoe een bepaald sedimentair systeem zich gedraagt om daarmee veldobservaties te verklaren en ze te voorspellen waar ze ontbreken. Echter, deze academische benadering sluit praktische toepassingen van het onderzoek geenzins uit. Zo is er bijvoorbeeld een aanzienlijk economisch belang vanwege de aanwezigheid van reservoirs van koolwaterstoffen (olie en gas) en zoetwaterreserves in afzettingen langs passieve continentale marges. Het doel van de bekkenrandstudies gepresenteerd in dit proefschrift is om zowel de zuiver wetenschappelijke als de toegepaste aspecten



Figuur 2 — Een voorbeeld van een lithostratigrafie en een bijbehorende chronostratigrafie gemaakt met het model dat in dit proefschrift wordt gepresenteerd. De lithostratigrafie (links) laat de korrelgroottefractie (het relatieve voorkomen van de grove korrelgrootteklasse; zie Hoofdstuk 3) van het sediment zien, en de chronostratigrafie (rechts) geeft de snelheid van depositie weer.

van onderzoek aan te spreken. Recentelijk zijn gerelateerde onderwerpen geadresseerd in experimentele stroomgoot studies (Wood *et al.*, 1993; Koss *et al.*, 1994; Van Heijst *et al.*, 2001; Van Heijst & Postma, 2001) en numeriek modelleerwerk (bijv. Syvitski & Daughney, 1992; Burgess & Allen, 1996; Ritchie *et al.*, 1999; Granjeon & Joseph, 1999; Ainsworth *et al.*, 2000; Tebbens *et al.*, 2000; Syvitski & Hutton, 2001).

Een studie van de sedimentaire ontwikkeling van passieve bekkenranden is het onderwerp van dit proefschrift. De resultaten zijn gebaseerd op een hiervoor nieuw ontwikkeld numeriek model. Het is driedimensionaal, dynamisch en van toepassing op lange tijd (enkele 100-den kyr) en ruimtelijke ($\sim 100 \times 300$ km) schaal. De opzet van het model is met opzet eenvoudig om de rekensnelheid te bevorderen. Dit maakt een statistisch significant aantal model *runs* in een redelijke tijdsbestek en een korte cyclus van opstellen en testen van hypothesen mogelijk. Tijdgemiddelde sediment fluxen in het model zijn gebaseerd op een stel regels voor materiaal (sediment en water) transport over een cellulaire (rooster) voorstelling van een passieve bekkenmarge. Onderlinge interactie tussen naast elkaar gelegen roostercellen beschreven door deze relatief simpele regels resulteert in een complex, niet-lineair proces-respons systeem. De expliciete overdracht van sediment van cel naar cel maakt het bijhouden van zijn eigenschappen zoals korrelgrootte, herkomst en leeftijd mogelijk. Deze informatie kan vervolgens worden opgeslagen in de modelstratigrafie bij afzetting en blijft beschikbaar wanneer het sediment wordt geërodeerd en opnieuw getransporteerd. Kortom, het model dat hier wordt gepresenteerd, is in staat de evolutie van de geomorfologie en ook de lithostratigrafie en chronostratigrafie van een bekkenmarge weer te geven (Figuur 2).

Vanwege de enorme natuurlijke variatie tussen passieve marges in de wereld, beperkt

deze studie zich tot systemen met enkel siliciclastisch sediment, dat wil zeggen zonder biogene sedimenten (carbonaten), die bovendien niet worden beïnvloed door gletsjer activiteit. Standaard voor alle model *runs* is een basis configuratie bestaande uit een rivier uit het achterland, een deltakust, een continentale *shelf* en het bovendee van een continentale helling op een rijpe passieve marge. De randvoorwaarden zijn eustatische zeespiegelbewegingen en de invloed van klimaat in het achterland die tot uiting komt in de opbrengst van het drainagebekken, dat wil zeggen het waterdebiet en de sedimentaanvoer. Tektonische bekkendaling is van minder belang aangezien deze veel geringer is in vergelijking met typische snelheden van Kwartaire zeespiegelschommelingen en krijgt daarom minder aandacht.

Het model wordt hier gebruikt als een heuristisch gereedschap om het effect van alternatieve scenario's van drijvende krachten te testen, en is daarom generiek in plaats van toegesneden op een specifieke veldcasus. Het doel is algemene uitspraken over de sedimentaire systeemontwikkeling te toetsen en eerste orde trends die naar voren komen te herkennen. Bepaalde sequentie stratigrafische terminologie, zoals sequentiegrens en *systems tracts*, wordt vermeden waar mogelijk, omdat er geen consensus is over de toepassing van alternatieve sequentie stratigrafische paradigma's zoals het gebruik van 'depositionele' (Posamentier *et al.*, 1988; Posamentier & James, 1993) of 'genetische' (Galloway, 1989) sequenties en bijvoorbeeld de inlijving van een *falling stage systems tract* in het concept (bijv. Plint & Nummedal, 2000).

Drie facetten van passieve continentale marge evolutie tijdens Kwartaire glaciale–interglaciale cycli zijn onderzocht. Eerst de ontwikkeling van palaeogeografie en drainagepatronen, gevolgd door een analyse van de stratigrafische architectuur en korrelgroottesortering op bekkenschaal, en tenslotte de stratigrafische ontwikkeling vanuit het perspectief van preservatie.

Synopsis

Hoofdstuk 2 — Modelling the drainage evolution of a river–shelf system forced by Quaternary glacio-eustasy

In Hoofdstuk 2 wordt het model geïntroduceerd. De opzet, de onderliggende aannamen en de algoritmen van het model worden uiteengezet. Vervolgens wordt een uitgebreide beschrijving gegeven van de modelevolutie van de accommodatieruimte, depocentrumverschuiving, palaeogeografie en drainagepatroon op een passieve continentale marge tijdens één enkele glacio-eustatische cyclus. Getoond wordt dat rivieravulsie, deltalob *switching*, incisie en knikpuntmigratie belangrijke processen zijn bij de ontwikkeling van het systeem. Met name van belang is ‘drainage connectie’, een gebeurtenis waarbij een directe en onlosmakelijke verbinding tussen het drainagebekken en het depocentrum op de *shelf*-rand tot stand wordt gebracht, waarbij de droogliggende *shelf* door de rivier wordt gepasseerd. Het experiment is vele malen herhaald met verschillende ruis op de initiële topografie, hetgeen leidde tot telkens andere model realisaties. Dit toont aan dat initiële condities grote invloed kunnen hebben in niet-lineaire systemen. Door een groot aantal model *runs* te verzamelen, verschijnt een beeld van de drainage-evolutie dat verborgen blijft in individuele *runs*, hetgeen pleit voor een uitgebreider gebruik van statistiek in modelstudies om inzichten in systeemgedrag te verbeteren.

Hoofdstuk 3 — Grain-size sorting of river–shelf–slope sediments during glacial–interglacial cycles: modelling grain-size distribution and interconnectedness

Hoofdstuk 3 gaat over korrelgroottesortering op bekkenschaal. Tijdens zeespiegelhoogstand en -daling, worden opwaarts grover wordende paralische successies afgezet op de continentale *shelf*,

doordat grof materiaal dichtbij de riviermonding wordt afgezet en fijn materiaal de prodelta opbouwt. Wanneer de *shelf* droogvalt, maken de grove bovenlagen van de delta meer kans geërodeerd te worden dan de fijne sedimenten in de tenen van de delta. Dit hoofdstuk beschrijft hoe dit verschil in preservatie potentiaal van afzettingen op de *shelf* resulteert in verrijking van de rivierlast met grof materiaal tijdens de vorming van een subaerische erosieve *unconformity*. Dit verarmt de *shelf* aan grof materiaal en verrijkt de *shelf*-rand afzettingen ermee. De distributie van sediment volume en korrelgrootte in de stratigrafie na verschillende glaciale–interglaciale cycli wordt besproken, alsmede het voorkomen van grofkorrelige lichamen in de stratigrafische architectuur. Belangrijke grove lichamen zijn te vinden in *shelf*-rand delta’s die gevormd zijn in tijden van laag zeeniveau en aan de basis van transgressieve opvullingen in ingesneden valleien. De interconnectiviteit van dergelijke lichamen hangt sterk samen met de ontwikkeling van de palaeogeografie van het systeem.

Hoofdstuk 4 — Modelling the preservation of sedimentary deposits on passive continental margins during glacial–interglacial cycles

De preservatie van afzettingen, de variatie ervan in ruimte en tijd en de relatie tot de ontwikkeling van de palaeogeografie wordt onderzocht in Hoofdstuk 4. De deltawig en binnenste *shelf*, en de *shelf*-rand, allen convexe morfologieën op passieve continentale marges, zijn het meest getroffen door rivierinsnijding en gradientafhankelijke transport processen. Sedimenten die zijn afgezet op de *shelf*, hebben een grotere kans om geremaniëerd te worden dan die aan de continentale helling. Vandaar dat blijkt dat de afzettingen van ruwweg de eerste helft van een glaciale–interglaciale cyclus minder gepreserveerd zijn dan die van de tweede helft.

Voorts worden verscheidene scenario's van zeespiegelverandering, waterdebiet en sedimentaanvoer vergeleken, en wordt ingegaan op de preservatie van zeespiegelhoogstand topografieën als functie van het verschil in gradient tussen de deltawig en de *shelf*, en de sedimentaanvoer.

Hoofdstuk 5 — Conclusions

In Hoofdstuk 5 wordt een synthese van de resultaten in Hoofdstukken 2, 3 en 4 gepresenteerd. De rol van relatieve

zeespiegelverandering en klimaat-gerelateerde palaeohydrologie in de evolutie van passieve marge systemen worden besproken. Het relatieve gewicht van deze belangrijkste drijvende krachten is afhankelijk van de plaats, tijd en schaal die bestudeerd wordt. Voorts wordt de relatie tussen palaeogeografische ontwikkeling, stratigrafische architectuur, korrelgrootteverdeling en preservatiepotentiaal samengevat. Tenslotte wordt betoogd dat een statistische benadering vereist is voor het driedimensionaal dynamisch modelleren van sedimentaire systemen.

Dankwoord

Velen hebben op één of andere wijze een bijdrage hebben geleverd aan de totstandkoming van dit proefschrift. Enkelen daarvan wil ik hier kort, maar welgemeend bedanken voor hun aandeel (in alfabetische, chronologische of volstrekt willekeurige volgorde).

Om te beginnen wil ik promotoren Poppe de Boer (Faculteit Aardwetenschappen) en Peter Burrough (Faculteit Ruimtelijke Wetenschappen) en co-promotor George Postma (Faculteit Aardwetenschappen) bedanken voor de samenwerking. Zij boden mij de vrijheid die ik nodig had om dit onderzoek tot een goed einde te brengen.

Ik ben de leden van de dissertatiecommissie R.D. van Hilst (MIT/UU), S. Kroonenberg (TUD), A. Veldkamp (LUW), Th.E. Wong (TNO-NITG/UU), C.J. van der Zwan (SIEP) zeer erkentelijk voor hun werk.

Veel steun heb ik gehad aan de promovendi van de afdeling Sedimentologie die mij voorgingen en volgden: Maarten Prins, Max van Heijst, Jelmer Cleveringa, Jan-Berend Stuu, Bastian van Dijck, Quintijn Clevis, Wessel van Kesteren, Sjoukje de Vries, Aart-Peter van den Berg van Saparoea. Dankzij hun kameraadschap heb ik de afgelopen vier jaar kunnen doorstaan.

Ook dank ik de promovendi van de afdelingen Stratigrafie/Palaeontologie (Faculteit Aardwetenschappen) en Fysische Geografie (Faculteit Ruimtelijke Wetenschappen) voor gedachtewisselingen over het onderzoek of anderszins. Met name de discussies met Gert Jan Weltje (TUD) en kamergenoten Max van Heijst en Quintijn Clevis waren aangenaam en waardevol. Mijn vrienden Ernst-Jan Noordhuis en Erik Snel wil ik bedanken voor de broodnodige afleiding van mijn werk waar zij voor zorgden.

Marnella van der Tol, Marjolein Boonstra, Paul Anten en Marjan Reith hebben een onmisbare rol gespeeld in de dagelijkse ondersteuning aan de afdeling Sedimentologie.

Voor hun steun en geduld bedank ik tenslotte mijn ouders, die zich, net als ik, de afgelopen jaren afvroegen wat ik toch in vredesnaam daarginds in Utrecht uitvoerde. Hopelijk beantwoordt dit boekje eindelijk hun vragen.

Curriculum Vitae

Xander Dagmar Meijer werd geboren op 22 september 1973 te Nijmegen. In 1991 behaalde hij het diploma VWO aan het Isendoorn College te Wamsveld. Het doctoraalexamen Geologie werd behaald in 1997 aan de Faculteit Aardwetenschappen van de Universiteit Utrecht. Van 15 september 1998 tot 15 september 2002 was hij werkzaam als Onderzoeker in Opleiding bij de Faculteiten Aardwetenschappen en Ruimtelijke Wetenschappen.

